

EFFECTS OF CHANGES IN SOIL MOISTURE ON COMPOSITION AND
ACTIVITY OF SOIL MICROBIAL COMMUNITIES CONTROLLING
GREENHOUSE GAS CYCLING IN SOILS

A Dissertation

Presented to the Faculty of the Graduate School
of Cornell University

In Partial Fulfillment of the Requirements for the Degree of
Doctor of Philosophy

by

Cristina Paola Fernandez-Baca

December 2018

© 2018 Cristina Paola Fernandez-Baca

Effects of changes in soil moisture on composition and activity of soil microbial communities controlling greenhouse gas cycling

Cristina Paola Fernandez-Baca Ph. D.

Cornell University 2018

Onsite wastewater treatment systems service more than 1 in 5 households in the U.S. In spite of their prevalence, the subsurface soil-dispersal component of these systems (e.g. septic tank leach fields) is understudied in terms of its air and water quality impacts. Treatment performance of these systems is seldom monitored, particularly with regards to greenhouse gas (GHG) emissions such as methane (CH₄), nitrous oxide (N₂O), and carbon dioxide (CO₂). Additionally, microbial controls on GHG cycling in these soil-based treatment systems are poorly understood. This work aimed to elucidate the link between atmospheric GHG emissions from leach field and control lawns, and distribution and activity of microbial populations directly involved in GHG cycling. In particular, we examined the effect of soil volumetric water content (VWC), both by sustained flooding and a precipitation event, on surface GHG fluxes, subsurface production, and distribution and activity of GHG cycling microbial populations in leach field and control lawns. Functional genes for production and consumption of CH₄ (*mcrA* and *pmoA*, respectively) and N₂O (*cnorB* and *nosZ*, respectively) were used to quantify *in situ* presence and activity of these key GHG cycling populations. In the first study, leach field and control lawn GHG emissions, soil VWC, and microbial community presence and distribution (with a focus on CH₄ cycling populations) were measured at nine sites in central New York. Results from this study suggested microbial communities did not differ between control and leach field lawns except under flooded conditions. High soil VWC drove CH₄ emissions and

gene abundances of *mcrA* and *pmoA* but was not a significant driver of N₂O fluxes or biomarker genes. In the second study we aimed to explore the relationship between flooding and GHG cycling in leach field soils. Leach field soil columns were constructed in lab to monitor performance of these systems under either well-maintained or failing-by-flooding conditions. The columns were compared in their surface CH₄ flux, subsurface CH₄ production, distribution, presence, and activity of microbial communities involved in CH₄ cycling, and nutrient (nitrogen and phosphorus) and chemical oxygen demand (COD) removal. Results indicated flooding significantly increases CH₄ production in leach field soils and decreases both COD removal and diversity of soil microbial communities. The final study examined the effect of rainfall on GHG fluxes and subsurface profiles in soils above an active leach field system. GHG measurements were coupled to quantification of biomarker abundances for CH₄ and N₂O cycling populations. This study revealed that all GHG fluxes increase after a rain event but trends vary by compound. Additionally, transcript abundances were not reliable indicators of increases in atmospheric GHG fluxes after a rain event.

BIOGRAPHICAL SKETCH

I was born in Ames, IA, the child of immigrants from Peru. I have one brother who I was very close with growing up. Throughout our childhood, our parents took us to spend summers in Peru. There we learned how to speak Spanish fluently, but were also exposed to how different life is outside of the U.S. In particular, visiting Peru gave me a strong sense of how important clean water is for life. Not just clean drinking water but also surface waters, rivers, lakes and oceans.

My parents met at UNAM, both pursuing degrees in Mexico City, due to the political instability of Peru in the late 70s and early 80s. They were both in their late teens and had left their families and their home country to study abroad. Through their, and their families', sacrifices I was lucky enough to be born in a country full of opportunities. I've always been taught that education is fundamental to success, and I believe that today. I pursued my PhD not only because I care about water quality and wastewater treatment, but also because I know my parents sacrificed and came to this country to give me the opportunity to have a good education and to be successful.

I came to Cornell, wanting to pursue research in sustainable wastewater treatment, however my research path changed and developed throughout my time here. I became an IGERT member and had the chance to develop skills and knowledge in areas I'd never before considered. I feel that I've learned many valuable skills and I'm happy to have spent 6 wonderful, sometimes challenging, years in Ithaca and at Cornell. I look forward to continuing doing science that increases our understanding of the world we live in as well as furthering science that will lead to solutions for pressing environmental issues globally.

To my family.

ACKNOWLEDGMENTS

Thank you to Ruth, who gave me the amazing opportunity to study at Cornell. Your passion for increasing opportunities and support for women in science and academia is inspiring. I would also like to thank my minor committee members Jim Gossett, Todd Walter, and Brian Rahm. Each of you has provided valuable guidance for my work and has always been willing to help me throughout my time at Cornell.

I would like to thank my family and friends who have supported me throughout grad school and in all of my pursuits. I'm grateful to my mother, who always pushed me to be better, to study harder, and to give back to my community, and who has always had my back. To my father and his father who both inspired me to pursue a graduate degree. I'm thankful to be able to follow in your footsteps. To both my parents for giving me the opportunity to spend time in Peru and build a strong connection with my family and culture, I am forever grateful. Thanks to my brother, Daniel, and his amazing daughter, Elena. My brother has always been a steady source of love, support, great advice, and bad jokes.

I am forever in debt to my wonderful husband, Peter who put up with countless night and weekends of me working. He is a wonderful cook who always kept me fed, even when I was "too busy" to cook. He is my closest friend and is the only person in the world who can make me laugh with just a look. I love you to infinity and beyond. Thank you also to his family, who supported us when we moved halfway across the country so I could pursue my PhD.

Thanks to my friends both old and new. I'm grateful to SKOCKY who have been my friends for over 15 years, I feel at home with you all. I'm incredibly thankful for my lab mate Annie who always lent an ear when things were difficult, but who also knew how to let go of work and have fun, you are a lifelong friend. Thank you to my friends Erin, Natalie, Will and Nick, who became close friends during my time in

Ithaca. Thank you to my friend Heather. It was amazing to work together during these last few days of writing.

Finally, thank you to the undergraduates and lab mates I've had the pleasure of working with. Thank you to Egidio and Andrew who are talented scientists and who I've learned a lot from. I'm very grateful for the wonderful undergraduates I've worked with including Walker, Erica, Justin, and Amir. Special thanks to Amir for his dedication in lab and always filling in on my soccer team when we needed him.

TABLE OF CONTENTS

Chapter 1	16
Introduction	16
1.1 Background on soil-based onsite wastewater treatment	16
1.2 Soil microbial communities controlling greenhouse gas cycling	18
1.3 Overview of research chapters	24
References	26
Chapter 2	32
Methane and nitrous oxide cycling microbial communities in soils above septic leach fields: abundances with depth and correlations with net surface emissions	32
Abstract	32
2.1 Introduction	34
2.2 Materials and methods	37
2.2.1 Site descriptions.....	37
2.2.2 Flux measurements and analysis	37
2.2.3 Environmental parameters	38
2.2.4 Soil sampling	38
2.2.5 DNA extraction.....	38
2.2.6 Quantitative PCR	39
2.2.7 Atypical nosZ denitrifiers and anaerobic methanotroph 16S rRNA analyses.....	42
2.2.8 Amplicon library sequencing.....	43
2.2.9 Microbial community analysis	43
2.2.10 Statistical analyses	45
2.3. Results	46
2.3.1 Abundance of GHG cycling genes in leach field soils.....	46
2.3.2 Modeling of GHG cycling gene abundances.....	48
2.3.3 Biomarker abundances as drivers of GHG fluxes from leach field soils	50
2.3.4 Characterizing functional microbial communities in leach field soils	53
2.4 Discussion	60
2.4.1 Quantification of functional biomarkers in leach field soils	61
2.4.2 Modeling functional biomarker quantity in leach field soils.....	61
2.4.3 Drivers of GHG fluxes from leach field soils.....	62
2.4.4 Presence of anaerobic methanotrophs and atypical denitrifiers	64
2.4.5 16S rRNA and functional gene characterization of GHG cycling microbial communities.....	65
2.5 Conclusions	67
References	69
Chapter 2: Supplemental Information	80
Chapter 3	84
Microbial communities controlling methane and nutrient cycling in leach field soils	84
Abstract.....	84

3.2 Methods	88
3.2.1 Soil column construction	88
3.2.2 Soil column operation.....	89
3.2.3. Surface methane flux measurements	91
3.2.4 Influent, effluent, and pore water sampling.....	92
3.2.5 Soil sampling, nucleic acid extractions, and qPCR.....	93
3.2.6 Illumina sequencing of 16S rRNA, mcrA and pmoA libraries	94
3.2.7 Analyses of 16S rRNA, mcrA, and pmoA amplicon libraries	95
3.3 Results	96
3.3.1 Soil volumetric water content.....	96
3.3.2 Atmospheric CH ₄ flux measurements	97
3.3.3 Subsurface CH ₄ concentration profiles.....	98
3.3.4 mcrA, pmoA, and 16S rRNA gene and transcript abundances	99
3.3.5 16S rRNA, mcrA, and pmoA amplicon library sequencing.....	102
3.3.6 Nutrient and COD removal.....	105
3.4 Discussion	106
3.4.1 CH ₄ cycling in leach field soil columns	106
3.4.2 CH ₄ cycling community composition.....	108
3.4.3 Microbial community composition in leach field soils	109
3.4.4 Nitrogen, phosphorus, and COD removal	112
3.5 Conclusions	113
References	115
Chapter 3: Supplemental Information	123
Chapter 4	128
Varied trends in CH₄, N₂O, and CO₂ fluxes stimulated by rain events in well-drained soils above leach fields	128
Abstract	128
4.1 Introduction	130
4.2 Materials and Methods	134
4.2.1 Study site description.....	134
4.2.2 Surface soil gas flux measurements.....	134
4.2.3 Subsurface soil gas probe installation and measurements.....	134
4.2.4 Baseline gas flux and depth measurements	135
4.2.5 Rain event study	136
4.2.6 Soil temperature and volumetric water content measurements	137
4.2.7 Soil Sampling	137
4.2.8 Nucleic acid extractions and qPCR assays	138
4.3 Results	140
4.3.2 Baseline greenhouse gas flux measurements.....	140
4.3.3 Baseline subsurface gas measurements	142
4.3.4 Preliminary rain event data (2016)	144
4.3.5 Rain event simulation	144
4.3.5.1 Soil volumetric water content and temperature.....	144
4.3.5.2 Rain event gas flux measurements	146
4.3.5.3 Rain event subsurface gas concentrations	148
4.3.5.4 CH ₄ and N ₂ O cycling genes and transcript abundances	151
4.4 Discussion.....	154
4.4.1 Baseline gas flux and subsurface concentrations	154

4.4.2 Precipitation driven trends in greenhouse gas emissions and subsurface concentrations from leach field and lawn-covered soils	157
4.4.2.1 CH ₄ emissions.....	157
4.4.2.2 N ₂ O emissions	158
4.4.2.3 CO ₂ emissions.....	159
4.4.2.4 Presence and activity of greenhouse gas cycling organisms	161
4.5 Conclusions	164
References	166
Chapter 5.....	177
Conclusions	177
5.1 Quantifying greenhouse gas emissions from lawn and leach field soils.....	177
5.3 Advancing the understanding of soil microbial communities controlling CH ₄ and N ₂ O cycling in soils.....	180
5.3 Limitations	183
5.4 Future Directions	186
References	189
Appendix	191

LIST OF FIGURES

Figure 1.1. Greenhouse gas cycling in soils above leach field systems. Relevant biomarker genes used in this work are shown in italics.	19
Figure 1.2. Methanogenesis pathway for acetoclastic and hydrogenotrophic methanogens. Both types of methanogens use MCR in the final step reduction of methyl-S-CoM to methane. Figure adapted from Lambie et al. (2015).	20
Figure 1.3. Methane oxidation pathway of aerobic methanotrophs showing both versions of methane monooxygenase (pMMO and sMMO) responsible for the first oxidation step of methane to methanol. Figure adapted from Murrell et al. (2000).	21
Figure 1.5. Enzymes involved in bacterial denitrification of nitrate to nitrogen gas. Figure adapted from Shapleigh (2006).	24
Figure 2.1. Surface soil gene abundances in copies per gram soil for <i>mcrA</i> (A), <i>pmoA</i> (B), <i>cnorB</i> (C), and <i>nosZ</i> (D) by treatment type (Control, Leach Field, and Sand Filter) for sites 1 through 9.	47
Figure 2.2. Comparison of log ₁₀ gene abundances for surface samples and subsurface samples by site of <i>mcrA</i> (circle), <i>pmoA</i> (cross), <i>cnorB</i> (triangle), and <i>nosZ</i> (square). Dotted line indicates a 1-to-1 relationship. The majority of sites had greater biomarker gene abundances in the surface sample.	48
Figure 2.3. CH ₄ fluxes (mg m ⁻² day ⁻¹) versus ratio of <i>mcrA</i> : <i>pmoA</i> gene abundances by treatment. Treatments are indicated by shape and color: Control (black circle), Leach Field (grey triangle), Sand Filter (light grey square). Inset shows data excluding site 9. The dotted line indicates zero net CH ₄ emissions.	51
Figure 2.4. N ₂ O flux (mg m ⁻² day ⁻¹) versus ratio of <i>cnorB</i> : <i>nosZ</i> gene abundances. Treatments are indicated by shape and color: Control (black circle), Leach Field (grey triangle), Sand Filter (light grey square). The dotted line indicates no net N ₂ O emissions.	52
Figure 2.5. Microbial community structure in 9 septic system soils showing all treatment types (control (circle), leach field (triangle), and sand filter (square)) and depths (surface and subsurface). PCoA plot based on the pairwise weighted UniFrac distance matrix (A). Constrained dbRDA of soil microbial communities with environmental parameters CH ₄ flux, VWC, and N ₂ O flux best explaining variation in microbial community structure (B).	55
Figure 2.6. Phylogenetic tree based on 16S rRNA reads for families within the Euryarchaeota phylum. Read abundance is indicated by the size of the marker, and treatment is shown by shape: control (black circle), leach field (dark grey triangle), and sand filter (light grey square). Tree tips are labeled at the family level. Brackets ([]) indicate a predicted family. Blank tips indicate taxonomic information was not available at the family level from the Greengenes database.	57
Figure 2.7. Phylogenetic tree based on 16S rRNA sequence reads of aerobic methanotrophs of the Gamma- and Alpha-proteobacteria as well as anaerobic methanotrophs of the NC10 phylum. Read abundance is indicated by the size of the marker, and treatment is shown by shape: control (black circle), leach field	

(dark grey triangle), and sand filter (light grey square). Tree tips are labeled at the family level. Blank tips indicate taxonomic information was not available at the family level from the Greengenes database.....	58
Figure 2.8. Relative abundance of <i>mcrA</i> reads assigned at the family level grouped by treatment. All 1,268,909 <i>mcrA</i> reads obtained from all 84 samples (control: n = 40, leach field: n = 30, sand filter: n=14).	60
Figure 3.1. Experimental lab column set-up constructed using soil from an active leach field system. Figure shows flooded vs. well-maintained operation and depths of pore water samplers, soil moisture sensors, and distribution (inlet) pipe. Soil columns were dosed with synthetic wastewater by peristaltic pumps. Effluent wastewater was pumped out from the base of the soil columns and into 1 l Nalgene bottles.	91
Figure 3.2. Soil volumetric water content ($\text{m}^3 \text{m}^{-3}$) measured continuously above the inlet (15 cm below the surface) and below the inlet (64 cm below the surface) in both soil columns. Vertical lines indicate phases of operation.	97
Figure 3.3. Boxplots of flux measurements for three different periods of operation, a) Phase I Column A flooded, Column B well-maintained ($n = 10$); b) Phase II both columns flooded ($n = 16$); c) Phase III Column A flooded, Column B drained ($n = 11$). Significant differences are shown at a 95% confidence interval. Inter-quartile range (IQR) defined between 25% and 75% of data, median shown by black bar. Upper and lower whiskers indicate the highest and lowest data point within 1.5 times the IQR.	98
Figure 3.4. Mean monthly methane depth profiles for Column A and B, a) Phase I Column A flooded, Column B well-maintained; b) Phase II Column A flooded, Column B flooding; c) Phase III Column A flooded, Column B drained.	99
Figure 3.5. Gene copies of 16S rRNA, <i>mcrA</i> , and <i>pmoA</i> per gram of dry soil on three sampling dates for Column A (solid line) and Column B (dashed line). Error bars indicate the standard error between duplicate extractions and triplicate qPCR reactions.....	100
Figure 3.6. Transcript abundances over depth of 16S rRNA, <i>mcrA</i> , and <i>pmoA</i> per gram soil dw for Column A (solid line) and Column B (dashed line) on three sampling dates. Error bars indicate the standard error between duplicate extractions and triplicate qPCR reactions.....	101
Figure 3.7. PCoA (a) and dbRDA (b) constrained by CH ₄ fluxes and soil VWC. Both analyses were based on the weighted UniFrac distance matrix of 16S rRNA sequencing data for DNA samples.	103
Figure 3.8. Functional gene sequencing results for a) <i>mcrA</i> and b) <i>pmoA</i> amplicon libraries. Relative abundances for Column A, Column B and original soils (leach field and control) are shown at the family level. Total number of assigned reads was higher for <i>mcrA</i> (78,258) compared to <i>pmoA</i> (853).	104
Figure 3.9. Influent (solid line) and effluent (dashed line) concentrations of (a) NH ₄ -N and effluent concentrations of NO ₃ -N+NO ₂ -N (dotted line), (b) PO ₄ -P, (c) COD for Column A and B, with vertical lines marking the three phases of operation.	106

Figure 4.1. Experimental set-up for rain event with three flux chamber locations per treatment and all 8-soil gas vapor probe locations shown (not drawn to scale). Subsurface leach field lateral locations are shown with dotted outlines. Soil gas vapor probe depths are the same for leach field and control: Probe 1 – 0.2 m; Probe 2 – 0.5 m, Probe 3 – 0.2 m, and Probe 4 – 0.5 m.	137
Figure 4.2. Surface CH ₄ , N ₂ O, and CO ₂ gas fluxes in g m ⁻² d ⁻¹ for the 4-week baseline measurement period prior to the simulated rain event in both control and leach field soils (<i>n</i> = 4 for each treatment and week). Boxplots show the inter-quartile range (IQR) from quartile 1 at 25% to quartile 3 at 75%. The horizontal black line within the box indicates the median. Upper and lower whiskers indicate the highest and lowest data point within 1.5 times the IQR.	141
Figure 4.3. Subsurface concentrations of CH ₄ , N ₂ O, and CO ₂ at 0.2 m and 0.5 m below the soil surface for both leach field and control soils over four weeks prior to simulated rain event (<i>n</i> = 2 for each sample date, treatment, and depth). Significant differences between depths at a 95% confidence interval are indicated with double asterisks (**), significance at a 90% confidence interval are shown with one asterisk (*). Boxplots show the inter-quartile range (IQR) from quartile 1 at 25% to quartile 3 at 75%. The horizontal black line within the box indicates the median. Upper and lower whiskers indicate the highest and lowest data point within 1.5 times the IQR.	143
Figure 4.4. Soil volumetric water content (VWC) (leach field: triangles, control: circles) and temperature (leach field: solid lines, control: dotted lines) measured within the infiltration ring immediately following the rain event, approximately 10 cm below ground. Legend indicates treatment and wet or dry conditions: control soils wet (C-W), control soils dry (C-D), leach field wet (LF-W), and leach field dry (LF-D); triplicate measurements were taken at each time point.	146
Figure 4.5. Boxplots of CH ₄ , N ₂ O, and CO ₂ flux measurements before and after the rain event in leach field and control soils. Dry (<i>n</i> = 3), 0.5 h 1.5 h, and 3 h Post Rain (<i>n</i> = 2). Lowercase letters represent significant differences (<i>p</i> < 0.05) between sampling times. Boxplots show the inter-quartile range (IQR) from quartile 1 at 25% to quartile 3 at 75%. The horizontal black line within the box indicates the median. Upper and lower whiskers indicate the highest and lowest data point within 1.5 times the IQR.	148
Figure 4.6. Subsurface CH ₄ , N ₂ O and CO ₂ concentrations before rain, 0.5 h, 1.5 h, and 3 h post rain event at 0.2 m (solid line) and 0.5 m (dotted line) in control (C) and leach field (LF) soils. Wetted (W) and dry (D) probes are shown for each treatment.	151
Figure 4.7. Gene abundances in a) control and b) leach field sites in dry soils, 1.5 h and 3 h after rain event for general bacterial 16S rRNA, <i>mcrA</i> , <i>pmoA</i> , <i>cnorB</i> , and “typical” <i>nosZ</i> . Error bars represent errors associated with duplicate DNA extractions and triplicate qPCR reactions.	152
Figure 4.8. Ratios of transcript abundances for a) CH ₄ cycling genes (<i>mcrA:pmoA</i>) and N ₂ O cycling genes (<i>cnorB:nosZ</i>) for dry soils and 1.5 and 3 h after rain event. Error bars represent errors associated with duplicate DNA and RNA extractions and triplicate qPCR reactions for each extract.	153

LIST OF TABLES

Table 2.1. Primers used for qPCR assays for each biomarker gene.	40
Table 2.2. Pure cultures and associated primers used to create qPCR standards. All primers were designed using the PrimerQuest tool from IDT (Rozen and Skaletsky, 2000).	41
Table 2.3. Results for LME models of biomarker gene abundances using site as the random effect. Individual biomarker genes were modeled using the ‘partner’ gene (e.g. <i>mcrA</i> modeled by <i>pmoA</i>), treatment, and soil parameters as effectors. Models for ratios of production to consumption gene abundances (e.g. <i>mcrA:pmoA</i>) with environmental parameters as effectors are also shown. Only models with at least one significant effect are presented. No significant effects were found for N ₂ O cycling genes. N.A. indicates the effector was not part of the model.	49
Table 2.4. Results of LME models for CH ₄ emissions using site as the random effect. Fluxes were modeled using fixed effects of either biomarker gene abundances or the ratio of production:consumption gene abundances and soil environmental parameters. Only significant effectors are shown. No significant effects were found for N ₂ O fluxes.	53

CHAPTER 1

INTRODUCTION

1.1 Background on soil-based onsite wastewater treatment

Septic systems are a common form of onsite wastewater treatment used by more than 1 in 5 homes in the U.S. (US EPA, 2012). These systems are popular in rural and peri-urban areas due to low operating and maintenance costs. They provide a practical and cost-effective alternative for rural homes that would otherwise require extensive and costly sewer system construction to connect remote homes to centralized wastewater treatment plants. Under optimal siting and operating conditions, septic systems also can provide public health and environmental benefits comparable to those provided by the more energy intensive wastewater treatment plants (US EPA, 2002).

Septic systems have two main components: the septic tank and the subsurface soil-dispersal system also known as the leach field. In the septic tank, solids settle out and anaerobic microbial processes reduce organic carbon and nutrient loads, such as nitrogen (N), from the waste stream creating greenhouse gases (GHG) in the process. Effluent from the septic tank is then discharged in soils through leach field laterals installed subsurface in well-drained soils. Leach fields take advantage of native soil microbial communities to further treat septic effluent before it comes in contact with the ground water table (or surface water sources). Together the two components of septic systems, the tank and the leach field, provide physical and microbial (both aerobic and anaerobic) treatment ultimately reducing nitrogen (N), phosphorus (P), and carbon (C) loads from waste streams by leveraging soils, and the native soil microbial communities therein, surrounding leach field laterals.

However, despite their prevalence, treatment performance and efficiency of septic systems go largely unmonitored, especially in comparison to centralized treatment plants, which are required to regularly monitor and document performance. Hence, little is known about septic systems' impacts on both air and water quality. These systems are estimated to be responsible for approximately 65% of domestic wastewater GHG emissions, but account for only 25% of treatment (US EPA, 2012). In particular, the soil dispersal system for the septic tank effluent (i.e. leach field) has been understudied in terms of both air and water quality impacts. Additionally, the ability of associated soil microbial communities to control nutrient and GHG cycling in leach field systems is poorly characterized.

Greenhouse gases such as methane (CH_4), carbon dioxide (CO_2), and nitrous oxide (NO_2) are produced by microorganisms in the anaerobic environment of the septic tank, but the fate of GHGs produced in the tank are poorly understood. Both CH_4 and N_2O are potent greenhouse gases with global warming potentials (GWP) of 21 and 310 times that of CO_2 over a 100-year timespan (US EPA, 2012). Previous studies have quantified greenhouse gas emissions from different components of septic systems including the leach field (Diaz-Valbuena et al., 2011; Truhlar et al., 2016). Truhlar et al. (2016) found that the septic roof vent accounted for the majority of greenhouse gas emissions from septic systems; however, leach fields accounted for almost 19% of the total greenhouse gas emissions septic systems, mostly from N_2O fluxes. Indeed, leach field soils were found to be a significant source of N_2O but not CH_4 or CO_2 as compared to control soils. Additionally, Truhlar et al. (2016) observed a one-to-one relationship between CO_2 emissions from the roof vent and leach field soils whereas CH_4 and N_2O emissions were greater from the roof vent as compare to leach field soils. These results suggest significant GHG mitigation, specifically of CH_4 and N_2O , may be occurring in soils above leach fields with GHG cycling

microorganisms consuming these GHG before they can reach the surface. This dissertation aims to examine whether abundance and activity of key microbial communities involved in greenhouse gas cycling corresponds to observed greenhouse gas fluxes from leach field soils, in particular the effect of soil volumetric water content (VWC) on these processes was studied.

1.2 Soil microbial communities controlling greenhouse gas cycling

Microbial communities in soils above leach field systems have the potential to contribute significantly to GHG cycling. In fact, soil microbial communities are thought to be responsible for approximately 70% of N₂O production and 80% of CH₄ consumption in soils (and around 5% of atmospheric CH₄ consumption) (Conrad, 1996; Conrad and Rothfuss, 1991). However, these estimates of microbial GHG production and consumption do not reflect the dynamic nature of GHG cycling processes, which vary temporally. Additionally, producers and consumers of GHGs in soils are likely differentially impacted by environmental conditions such as soil VWC. Thus, quantifying the presence and activity of these key soil microbial populations responsible for GHG cycling is essential to a better understanding of GHG emissions from soil systems and particularly soils impacted by leach field systems (Figure 1.1).

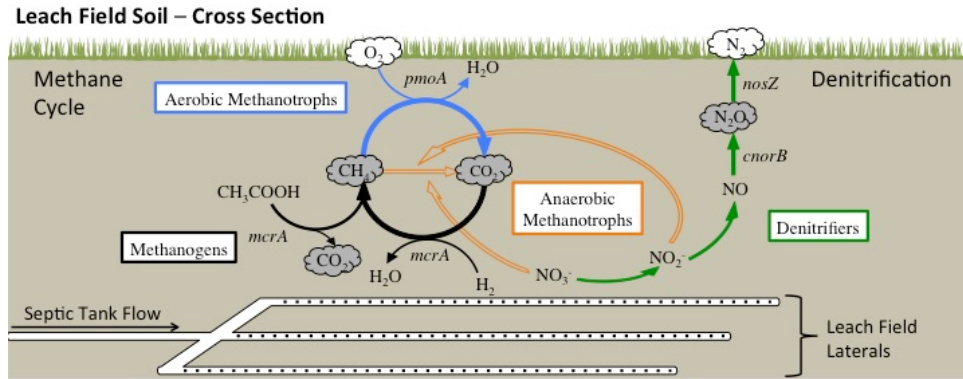


Figure 1.1. Greenhouse gas cycling in soils above leach field systems. Relevant biomarker genes used in this work are shown in italics.

Microbial methane production and consumption are well-studied processes. Methanogenesis is the anaerobic process by which methanogens convert organic substrates and/or hydrogen and carbon dioxide to methane (Figure 1.2). Methyl coenzyme-M reductase (MCR) catalyzes the final reduction step of the methanogenesis pathway, ultimately releasing methane (Thauer, 1998). The gene encoding for the α -subunit of MCR (*mcrA*) is unique to methanogens, with the exception of anaerobic methane oxidizing (ANME) archaea, and is found in all known methanogens both acetoclastic and hydrogenotrophic (Lambie et al., 2015; Luton et al., 2002; Steinberg and Regan, 2008). Because the *mcrA* gene is highly conserved, correlates strongly with phylogeny based on 16S rRNA sequences, and is directly involved in methane production, it is a suitable biomarker for methanogen presence and activity in environmental samples (Luton et al., 2002). *mcrA* has been used to link CH₄ emissions to methanogen activity in a variety of soil environments including peat bogs, landfills, and rice paddies (Freitag and Prosser, 2009; Lee et al., 2014; Luton et al., 2002; Ma et al., 2012).

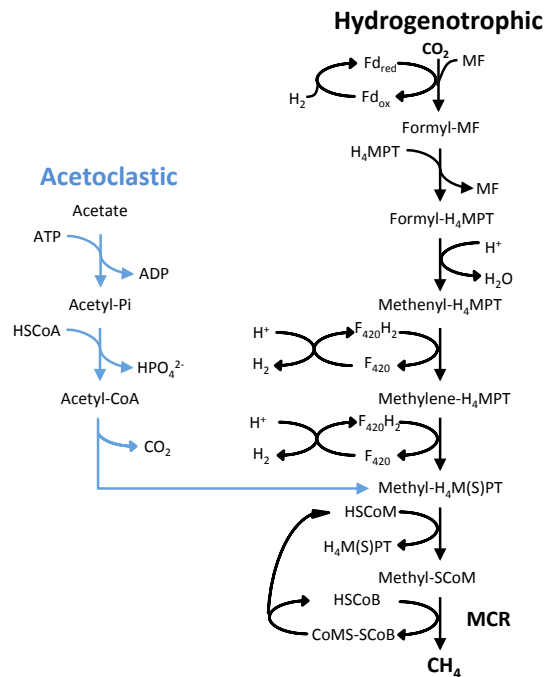


Figure 1.2. Methanogenesis pathway for acetoclastic and hydrogenotrophic methanogens. Both types of methanogens use MCR in the final step reduction of methyl-SCoM to methane. Figure adapted from Lambie et al. (2015).

Similarly, all aerobic methane oxidizing bacteria (MOB) contain methane monooxygenase (MMO), which catalyzes methane conversion to methanol in the first step of methane oxidation to carbon dioxide (Conrad, 2007). Two forms of MMO exist in aerobic methanotrophs, the particulate membrane bound, pMMO, and the soluble version, sMMO, located in the cytoplasm (Figure 1.3) (Murrell et al., 2000). The majority of MOB contain the pMMO version, which is also found in the more recently discovered nitrite-dependent anaerobic methanotrophs of the NC10 phylum. Some methanotrophs contain both pMMO and sMMO, while only a handful contain just the soluble form (Semrau et al., 1995, 2010). Thus, due to its near ubiquity in methanotrophs, the *pmoA* gene, encoding the α -subunit of pMMO, has been used as a functional biomarker gene for methanotrophs in soils as varied as peat bogs, fens, rice paddies, and forest soils (Cheema et al., 2015; Freitag et al., 2010; Kolb et al., 2003;

Seo et al., 2013).

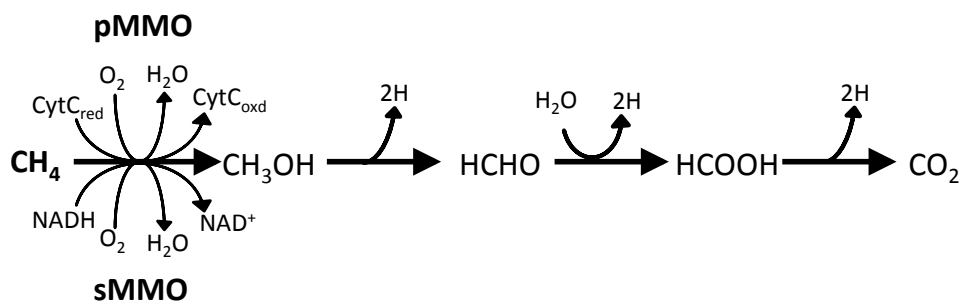


Figure 1.3. Methane oxidation pathway of aerobic methanotrophs showing both versions of methane monooxygenase (pMMO and sMMO) responsible for the first oxidation step of methane to methanol. Figure adapted from Murrell et al. (2000).

Recent discoveries of anaerobic oxidation of methane (AOM) have complicated the picture of biomarkers for the microbial CH_4 cycle. Where previously the methane cycle was thought to be controlled by two populations, aerobic methanotrophs and anaerobic methanogens, newer findings have elucidated the presence and activity of two phylogenetically distinct groups of AOM-performing microorganism: nitrite-dependent anaerobic methane oxidizing bacteria (n-damo) of the NC10 phylum and anaerobic methane oxidizing (ANME) archaea (Figure 1.4). N-damo bacteria couple methane oxidation to nitrite reduction by creating molecular O_2 intracellularly (Ettwig et al., 2012; Welte et al., 2016). Interestingly, these bacteria use the same *pmoA* gene as aerobic methanotrophs, thus the same gene can be used to quantify both aerobic and anaerobic bacterial methanotrophs, provided that qPCR assays are designed to specifically distinguish aerobic *pmoA* sequences from n-damo *pmoA* sequences. Indeed, n-damo populations have *pmoA* sequences distinct from typical aerobic methanotrophs' and have been found in freshwater sediments, rice paddy soils, and wastewater (Haroon et al., 2013; Hu et al., 2015; Luesken et al., 2011; Shen et al., 2015). ANME archaea are proposed to do AOM using a reverse

methanogenesis pathway and are thought to couple methane oxidation to a variety of electron acceptors including sulfate, nitrate, and metals such as iron and manganese (Beal et al., 2009; Haroon et al., 2013; Oni and Friedrich, 2017; Orphan et al., 2001). ‘*Candidatus Methanoperedens nitroreducens*’ is a nitrate-dependent AOM archaea of the ANME-2D clade, that have recently been found in environments such as freshwater sediments and paddy soils where traditionally methane production is high and oxygen availability is low, as well as in enrichment cultures with NC10 type organisms (Ettwig et al., 2009; Haroon et al., 2013; Vaksmaa et al., 2016; Weber et al., 2017). These two distinct groups of anaerobic methanotrophs have the potential contribute significantly to CH₄ cycling, particularly in oxygen-limited environments, and have not previously been studied in leach field soils or other lawn-covered soil systems.

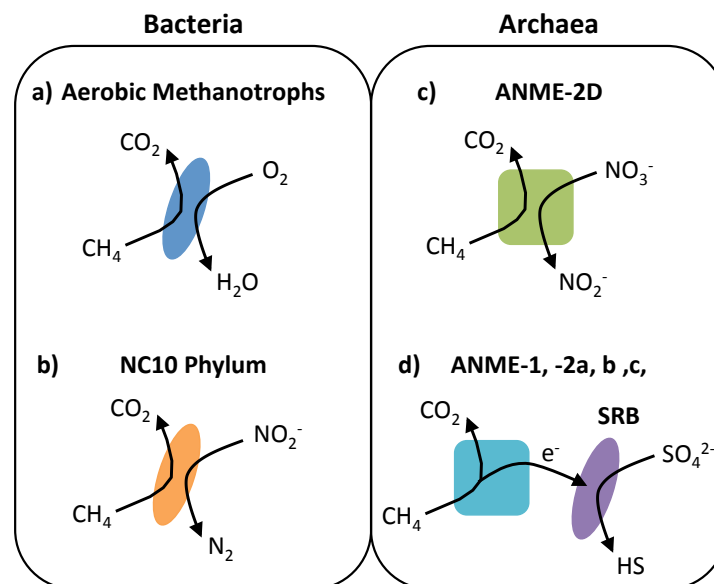


Figure 1.4. Methane oxidation by bacteria, a and b, and archaea, c and d. Including aerobic methanotrophic bacteria (a) and anaerobic bacteria coupled to nitrite reduction (b) and ANME archaea coupling methane oxidation to nitrate (c) or sulfate reduction (d) by sulfate reducing bacteria (SRB). Figure adapted from Oni and Friedrich (2017).

While our understanding of the CH₄ cycle has evolved with recent discoveries of AOM microbial populations, the complexity of the denitrification cycle has long been known. Complete denitrification involves several steps to reduce nitrate (NO₃⁻) to nitrogen gas (N₂). These sequential reduction steps are catalyzed by the enzymes nitrate reductase (Nar), nitrite reductase (Nir), nitric oxide reductase (Nor), and nitrous oxide reductase (Nos) (Figure 1.5) (Philippot, 2002; Shapleigh, 2006). However, the majority of denitrifiers contain only a subset of the denitrification genes required for complete denitrification and thus partial or incomplete biological denitrification is prevalent and can result in significant N₂O emissions (Henry et al., 2006; Sanford et al., 2012). The key enzymes involved in N₂O production and consumption are Nor and Nos, respectively. Previous studies have used these functional genes *cnorB* and *nosZ* to explore the relationship between denitrifier presence and/or activity and N₂O emissions in paddy soils (Seo et al., 2013). However, the genetic diversity found in both Nor and Nos enzymes complicates the use of qPCR assays to monitor the denitrification pathway. Nor has two distinct versions, cNor (cytochrome C as the electron donor) and qNor (quinol electron donor). cNor is specific to denitrifying bacteria whereas qNor is found in some denitrifier strains but has also been found in non-denitrifying populations that use the enzyme to detoxify nitric oxide. Thus *cnorB*, a gene encoding for the cNor enzyme, is favored for use as a biomarker for N₂O production (Braker and Tiedje, 2003; Dandie et al., 2007). NosZ has many atypical variants which cannot all be captured by one primer set, thus the use of any one primer set potentially leads to underestimation of denitrifiers capable of reducing N₂O. However the typical *nosZ* gene has previously been used to quantify N₂O consuming populations in soils with some success (Henry et al., 2006; Sanford et al., 2012; Seo et al., 2013).

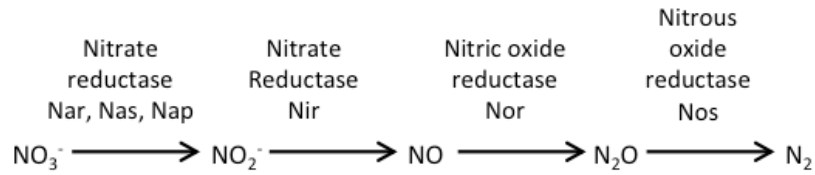


Figure 1.5. Enzymes involved in bacterial denitrification of nitrate to nitrogen gas. Figure adapted from Shapleigh (2006).

1.3 Overview of research chapters

The overall aim of this dissertation was to broaden our understanding of the impacts of onsite soil-based wastewater treatment, specifically septic leach field systems, on air and water quality and examining how those impacts are dynamically controlled by the presence and activity of soil microbial communities involved in greenhouse gas and nutrient cycling in soils above leach field laterals. This dissertation is arranged in three research chapters (Chapters 2 through 4) with a focus on understanding the interplay between soil VWC, soil microbial populations' abundance and activity, and greenhouse gas cycling in septic leach field systems.

The first chapter presents a field study of 9 septic leach field systems in central New York. The goal of the study was to quantify the presence, abundance, and distribution of soil microbial populations involved in greenhouse gas cycling. The study also aimed to elucidate drivers of GHG fluxes from leach field systems as well as drivers of biomarker gene abundances for key genes involved in GHG cycling using linear mixed effects models. Finally, the soil microbial community was profiled using high-throughput sequencing technology on 16S rRNA, *mcrA*, and *pmoA* amplicon libraries to examine the broader soil microbial populations associated with leach field systems as well as to examine methane cycling microbial populations more closely.

The second chapter presents a laboratory study, using soil columns, constructed from excavated soil from an active leach field to do controlled studies.

The goal of these studies was to examine how a leach field system failing due to flooding compares to a functioning, well-maintained system in four key ways: surface CH₄ emissions; subsurface CH₄ concentration profiles; presence, distribution, and activity of microbial populations with a focus on those involved in CH₄ cycling; effectiveness of nutrient (N and P) and chemical oxygen demand (COD) removal. Methane surface flux and subsurface measurements were taken and coupled with soil DNA and RNA extractions to explore the link between measured CH₄ production at depth and the present and active CH₄ cycling populations. Illumina sequencing of DNA and cDNA were further used to examine how soil VWC affected the soil microbial community diversity in the flooded system as compared to the well-maintained system.

The third chapter presents a field-based study to examine how a leach field soil system responds to a precipitation event in terms of greenhouse gas (CH₄, CO₂, and N₂O) emissions and subsurface gas concentrations. The leach field system was monitored for 4 weeks prior to the rain event to quantify the baseline greenhouse gas emissions and subsurface GHG profile of the system. Subsequent to baseline measurements, a rain event was simulated over both leach field and control lawns. CH₄, CO₂, and N₂O fluxes and subsurface concentrations were measured before and after the simulated precipitation event and coupled to soil samples for DNA and RNA analyses. Key biomarker genes for the production and consumption of CH₄ and N₂O were used to quantify relevant microbial populations using qPCR. RNA was reverse transcribed (RT) and subjected to qPCR (RT-qPCR) to monitor gene expression trends. Together, the objective of these studies was to use cross-scales tools to understand microbial controls on greenhouse gas cycling in soils. Additionally, elucidating the dynamic responses of soil microbial populations, and thus GHG fluxes, to changes in soil VWC was a key goal of this work.

References

- Beal, E.J., House, C.H., Orphan, V.J., 2009. Manganese- and iron-dependent marine methane oxidation. *Science* 325, 184–7. <https://doi.org/10.1126/science.1169984>
- Braker, G., Tiedje, J.M., 2003. Nitric oxide reductase (norB) genes from pure cultures and environmental samples. *Appl. Environ. Microbiol.* 69, 3476–83.
- Cheema, S., Zeyer, J., Henneberger, R., 2015. Methanotrophic and Methanogenic Communities in Swiss Alpine Fens Dominated by *Carex rostrata* and *Eriophorum angustifolium*. *Appl. Environ. Microbiol.* 81, 5832–44.
<https://doi.org/10.1128/AEM.01519-15>
- Conrad, R., 2007. Microbial Ecology of Methanogens and Methanotrophs. *Adv. Agron.* 96, 1–63.
- Conrad, R., 1996. Soil microorganisms as controllers of atmospheric trace gases (H₂, CO, CH₄, OCS, N₂O, and NO). *Microbiol. Rev.* 60, 609–40.
- Conrad, R., Rothfuss, F., 1991. Methane oxidation in the soil surface layer of a flooded rice field and the effect of ammonium. *Biol. Fertil. Soils* 12, 28–32.
<https://doi.org/10.1007/BF00369384>
- Dandie, C.E., Miller, M.N., Burton, D.L., Zebarth, B.J., Trevors, J.T., Goyer, C., 2007. Nitric oxide reductase-targeted real-time PCR quantification of denitrifier populations in soil. *Appl. Environ. Microbiol.* 73, 4250–8.
<https://doi.org/10.1128/AEM.00081-07>
- Diaz-Valbuena, L.R., Leverenz, H.L., Cappa, C.D., Tchobanoglous, G., Horwath, W.R., Darby, J.L., 2011. Methane, carbon dioxide, and nitrous oxide emissions from septic tank systems. *Environ. Sci. Technol.* 45, 2741–7.
<https://doi.org/10.1021/es1036095>

- Ettwig, K.F., Speth, D.R., Reimann, J., Wu, M.L., Jetten, M.S.M., Keltjens, J.T., 2012. Bacterial oxygen production in the dark. *Front. Microbiol.* 3, 273. <https://doi.org/10.3389/fmicb.2012.00273>
- Ettwig, K.F., van Alen, T., van de Pas-Schoonen, K.T., Jetten, M.S.M., Strous, M., 2009. Enrichment and molecular detection of denitrifying methanotrophic bacteria of the NC10 phylum. *Appl. Environ. Microbiol.* 75, 3656–62. <https://doi.org/10.1128/AEM.00067-09>
- Freitag, T.E., Prosser, J.I., 2009. Correlation of methane production and functional gene transcriptional activity in a peat soil. *Appl. Environ. Microbiol.* 75, 6679–87. <https://doi.org/10.1128/AEM.01021-09>
- Freitag, T.E., Toet, S., Ineson, P., Prosser, J.I., 2010. Links between methane flux and transcriptional activities of methanogens and methane oxidizers in a blanket peat bog. *FEMS Microbiol. Ecol.* 73, 157–65. <https://doi.org/10.1111/j.1574-6941.2010.00871.x>
- Haroon, M.F., Hu, S., Shi, Y., Imelfort, M., Keller, J., Hugenholtz, P., Yuan, Z., Tyson, G.W., 2013. Anaerobic oxidation of methane coupled to nitrate reduction in a novel archaeal lineage. *Nature* 500, 567–70. <https://doi.org/10.1038/nature12375>
- Henry, S., Bru, D., Stres, B., Hallet, S., Philippot, L., 2006. Quantitative detection of the *nosZ* gene, encoding nitrous oxide reductase, and comparison of the abundances of 16S rRNA, *narG*, *nirK*, and *nosZ* genes in soils. *Appl. Environ. Microbiol.* 72, 5181–9. <https://doi.org/10.1128/AEM.00231-06>
- Hu, S., Zeng, R.J., Haroon, M.F., Keller, J., Lant, P.A., Tyson, G.W., Yuan, Z., 2015. A laboratory investigation of interactions between denitrifying anaerobic methane oxidation (DAMO) and anammox processes in anoxic environments. *Sci. Rep.* 5, 8706. <https://doi.org/10.1038/srep08706>

- Kolb, S., Knief, C., Stubner, S., Conrad, R., 2003. Quantitative Detection of Methanotrophs in Soil by Novel *pmoA*-Targeted Real-Time PCR Assays. *Appl. Environ. Microbiol.* 69, 2423–2429. <https://doi.org/10.1128/AEM.69.5.2423-2429.2003>
- Lambie, S.C., Kelly, W.J., Leahy, S.C., Li, D., Reilly, K., McAllister, T.A., Valle, E.R., Attwood, G.T., Altermann, E., 2015. The complete genome sequence of the rumen methanogen *Methanosarcina barkeri* CM1. *Stand. Genomic Sci.* 10, 57. <https://doi.org/10.1186/s40793-015-0038-5>
- Lee, H.J., Kim, S.Y., Kim, P.J., Madsen, E.L., Jeon, C.O., 2014. Methane emission and dynamics of methanotrophic and methanogenic communities in a flooded rice field ecosystem. *FEMS Microbiol. Ecol.* 88, 195–212. <https://doi.org/10.1111/1574-6941.12282>
- Luesken, F.A., Zhu, B., van Alen, T.A., Butler, M.K., Diaz, M.R., Song, B., Op den Camp, H.J.M., Jetten, M.S.M., Ettwig, K.F., 2011. *pmoA* Primers for detection of anaerobic methanotrophs. *Appl. Environ. Microbiol.* 77, 3877–80. <https://doi.org/10.1128/AEM.02960-10>
- Luton, P.E., Wayne, J.M., Sharp, R.J., Riley, P.W., 2002. The *mcrA* gene as an alternative to 16S rRNA in the phylogenetic analysis of methanogen populations in landfill. *Microbiology* 148, 3521–3530.
- Ma, K., Conrad, R., Lu, Y., 2012. Responses of methanogen *mcrA* genes and their transcripts to an alternate dry/wet cycle of paddy field soil. *Appl. Environ. Microbiol.* 78, 445–54. <https://doi.org/10.1128/AEM.06934-11>
- Murrell, J.C., McDonald, I.R., Gilbert, B., 2000. Regulation of expression of methane monooxygenases by copper ions. *Trends Microbiol.* 8, 221–225. [https://doi.org/10.1016/S0966-842X\(00\)01739-X](https://doi.org/10.1016/S0966-842X(00)01739-X)
- Oni, O.E., Friedrich, M.W., 2017. Metal Oxide Reduction Linked to Anaerobic

- Methane Oxidation. *Trends Microbiol.* 25, 88–90.
<https://doi.org/10.1016/J.TIM.2016.12.001>
- Orphan, V.J., Hinrichs, K.U., Ussler, W., Paull, C.K., Taylor, L.T., Sylva, S.P., Hayes, J.M., Delong, E.F., 2001. Comparative analysis of methane-oxidizing archaea and sulfate-reducing bacteria in anoxic marine sediments. *Appl. Environ. Microbiol.* 67, 1922–34. <https://doi.org/10.1128/AEM.67.4.1922-1934.2001>
- Philippot, L., 2002. Denitrifying genes in bacterial and Archaeal genomes. *Biochim. Biophys. Acta - Gene Struct. Expr.* 1577, 355–376.
[https://doi.org/10.1016/S0167-4781\(02\)00420-7](https://doi.org/10.1016/S0167-4781(02)00420-7)
- Sanford, R.A., Wagner, D.D., Wu, Q., Chee-Sanford, J.C., Thomas, S.H., Cruz-García, C., Rodríguez, G., Massol-Deyá, A., Krishnani, K.K., Ritalahti, K.M., Nissen, S., Konstantinidis, K.T., Löffler, F.E., 2012. Unexpected nondenitrifier nitrous oxide reductase gene diversity and abundance in soils. *Proc. Natl. Acad. Sci. U. S. A.* 109, 19709–14. <https://doi.org/10.1073/pnas.1211238109>
- Semrau, J., Chistoserdov, A., Lebron, J., Costello, A., Davagnino, J., Kenna, E., Holmes, A., Finch, R., Murrell, J., Lidstrom, M., 1995. Particulate methane monooxygenase genes in methanotrophs. *J. Bacteriol.* 177, 3071–3079.
- Semrau, J.D., DiSpirito, A.A., Yoon, S., 2010. Methanotrophs and copper. *FEMS Microbiol. Rev.* 34, 496–531. <https://doi.org/10.1111/j.1574-6976.2010.00212.x>
- Seo, J., Jang, I., Gebauer, G., Kang, H., 2013. Abundance of Methanogens, Methanotrophic Bacteria, and Denitrifiers in Rice Paddy Soils. *Wetlands* 34, 213–223. <https://doi.org/10.1007/s13157-013-0477-y>
- Shapleigh, J.P., 2006. The Denitrifying Prokaryotes Defining the Denitrifiers 769–792.
- Shen, L., Huang, Q., He, Z., Lian, X., Liu, S., He, Y., Lou, L., Xu, X., Zheng, P., Hu, B., 2015. Vertical distribution of nitrite-dependent anaerobic methane-oxidising

- bacteria in natural freshwater wetland soils. *Appl. Microbiol. Biotechnol.* 99, 349–357. <https://doi.org/10.1007/s00253-014-6031-x>
- Steinberg, L.M., Regan, J.M., 2008. Phylogenetic comparison of the methanogenic communities from an acidic, oligotrophic fen and an anaerobic digester treating municipal wastewater sludge. *Appl. Environ. Microbiol.* 74, 6663–71. <https://doi.org/10.1128/AEM.00553-08>
- Thauer, R.K., 1998. Biochemistry of methanogenesis: a tribute to Marjory Stephenson. 1998 Marjory Stephenson Prize Lecture. *Microbiology* 144 (Pt 9, 2377–406.
- Truhlar, A.M., Rahm, B.G., Brooks, R.A., Nadeau, S.A., Makarsky, E.T., Walter, M.T., 2016. Greenhouse Gas Emissions from Septic Systems in New York State. *J. Environ. Qual.* 45, 1153. <https://doi.org/10.2134/jeq2015.09.0478>
- US EPA, 2012. Global Anthropogenic Non-CO2 Greenhouse Gas Emissions: 1990-2030 [WWW Document]. URL http://www.epa.gov/climatechange/Downloads/EPAactivities/EPA_Global_Non_CO2_Projections_Dec2012.pdf (accessed 4.13.15).
- US EPA, 2002. Onsite Wastewater Treatment and Disposal Systems. Washington, D.C.
- Vaksmas, A., Lüke, C., van Alen, T., Valè, G., Lupotto, E., Jetten, M.S.M., Ettwig, K.F., 2016. Distribution and activity of the anaerobic methanotrophic community in a nitrogen-fertilized Italian paddy soil. *FEMS Microbiol. Ecol.* 92, fiw181. <https://doi.org/10.1093/femsec/fiw181>
- Weber, H.S., Habicht, K.S., Thamdrup, B., 2017. Anaerobic Methanotrophic Archaea of the ANME-2d Cluster Are Active in a Low-sulfate, Iron-rich Freshwater Sediment. *Front. Microbiol.* 8, 619. <https://doi.org/10.3389/fmicb.2017.00619>
- Welte, C.U., Rasigraf, O., Vaksmas, A., Versantvoort, W., Arshad, A., Op den Camp,

H.J.M., Jetten, M.S.M., Lüke, C., Reimann, J., 2016. Nitrate- and nitrite-dependent anaerobic oxidation of methane. *Environ. Microbiol. Rep.* 8, 941–955.
<https://doi.org/10.1111/1758-2229.12487>

CHAPTER 2

METHANE AND NITROUS OXIDE CYCLING MICROBIAL COMMUNITIES IN SOILS ABOVE SEPTIC LEACH FIELDS: ABUNDANCES WITH DEPTH AND CORRELATIONS WITH NET SURFACE EMISSIONS¹

Abstract

Onsite septic systems use soil microbial communities to treat wastewater, in the process creating potent greenhouse gases (GHGs): methane (CH₄) and nitrous oxide (N₂O). Subsurface soil dispersal systems of septic tank overflow, known as leach fields, are an important part of wastewater treatment and have the potential to contribute significantly to GHG cycling. This study aimed to characterize soil microbial communities associated with leach field systems and quantify the abundance and distribution of microbial populations involved in CH₄ and N₂O cycling. Functional genes were used to target populations producing and consuming GHGs, specifically methyl coenzyme M reductase (*mcrA*) and particulate methane monooxygenase (*pmoA*) for CH₄ and nitric oxide reductase (*cnorB*) and nitrous oxide reductase (*nosZ*) for N₂O. All biomarker genes were found in all soil samples regardless of treatment (leach field, sand filter, or control) or depth (surface or subsurface). In general, biomarker genes were more abundant in surface soils than subsurface soils suggesting the majority of GHG cycling is occurring in near-surface soils. Ratios of production to consumption gene abundances showed a positive relationship with CH₄ emissions (*mcrA:pmoA*, $p < 0.001$) but not with N₂O emission (*cnorB:nosZ*, $p > 0.05$). Of the three measured soil parameters (volumetric water content (VWC), temperature, and conductivity), only VWC was significantly

¹ Fernández-Baca, C.P., Truhlar, A.M., Omar, A.-E.H., Rahm, B.G., Walter, M.T., Richardson, R.E.,

correlated to a biomarker gene, *mcrA* ($p = 0.0398$), but not *pmoA* or either of the N₂O cycling genes ($p > 0.05$ for *cnorB* and *nosZ*). 16S rRNA amplicon library sequencing results revealed soil VWC, CH₄ flux and N₂O flux together explained 64% of the microbial community diversity between samples. Sequencing of *mcrA* and *pmoA* amplicon libraries revealed treatment had little affect on diversity of CH₄ cycling organisms. Overall, these results suggest GHG cycling occurs in all soils regardless of whether or not they are associated with a leach field system.

2.1 Introduction

Septic systems account for approximately 25% of U.S. wastewater treatment however they are estimated to be responsible for almost 65% of domestic wastewater greenhouse gas (GHG) emissions (US EPA, 2012). Septic systems typically consist of two parts: the septic tank and the subsurface soil dispersal system hereafter referred to as the leach field. Some newer systems have an additional sand filter between the tank and the leach field to improve discharged water quality (USEPA, 2002). Both the septic tank and leach field portions of the system use microbial communities to degrade complex organics in wastewater and mineralize nutrients. Together they provide both *physical* (i.e., solids settling and collection) and *microbial* (anaerobic and aerobic) treatments to effectively reduce organic carbon (C), nitrogen (N) and phosphorus (P) loads.

As a consequence of transforming C and N, microorganisms can produce the potent greenhouse gases methane (CH₄) and nitrous oxide (N₂O) with global warming potentials (GWP) of 20 and 200 times that of CO₂ over a 25-year time span, respectively. Still, only a handful of studies have quantified GHG emissions from septic systems (Diaz-Valbuena et al., 2011; IPCC, 2006; Kinnicutt et al., 1919; Leverenz et al., 2010; Winneberger, 1983). Greenhouse gases from these systems escape primarily through the roof vent, however a portion of these gases can be released through supersaturated septic tank effluent or be produced subsurface in soils surrounding leach field laterals. Truhlar et al. (2016) provided the first measurements of GHG emissions from two key septic system outlets: the roof vent and leach field soils. They found that CO₂ emissions from the roof vent and soils above leach fields were comparable. In contrast, CH₄ and N₂O emissions were significantly greater from the roof vent as compared to the leach field. The discrepancy between roof vent and

leach field emissions suggests that microbial GHG cycling in soils above leach fields is, in part, responsible for mitigating CH₄ and N₂O emissions from leach field systems. This study aims to examine whether the abundance of key GHG cycling microbial populations in leach field soils correlates to measured CH₄ and N₂O emissions from these systems.

For microbial CH₄ production and aerobic consumption, biomarker selection is relatively straightforward. In methanogens, the α -subunit of the methyl-coenzyme M reductase (*mcrA*) enzyme, involved in the final step of methanogenesis, is well conserved across all known methanogens with the exception of anaerobic methane oxidizing (ANME) archaea (Friedrich, 2005; Luton et al., 2002; Steinberg and Regan, 2009). Similarly, all aerobic methane-oxidizing bacteria (MOB) contain the enzyme methane monooxygenase (MMO). MMO catalyzes the first step in CH₄ oxidation and the particulate form (pMMO) of the enzyme is found in the majority of cultivated methanotrophs (Dedysh et al., 2003; Semrau et al., 1995, 2010). The *pmoA* gene, encoding the α -subunit of pMMO, has near universal presence in both aerobic and nitrite-reducing bacterial methanotrophs and has been used as a biomarker for their presence and activity (Freitag and Prosser, 2009; Lee et al., 2014; Seo et al., 2013; Tate, 2015).

Recent discoveries of anaerobic methanotrophs make the CH₄ cycle more complex than previously thought. Nitrite-dependent anaerobic methane oxidizing (n-damo) bacteria of the NC10 phylum and anaerobic methane oxidizing (ANME) archaea - are phylogenetically diverse groups that have the potential to contribute significantly to CH₄ mitigation globally. N-damo processes are carried out by *Candidatus Methyloirabilis oxyfera*-like bacteria, which couple methane oxidation to nitrite reduction. These bacteria have previously been identified and quantified by targeting their *pmoA* or 16S rRNA gene (Ettwig et al., 2009; Luesken et al., 2011).

ANME-2D archaea are thought to couple methane oxidation to nitrate reduction in a reverse methanogenesis pathway and can be studied using the same *mcrA* gene used to for methanogens (Ettwig et al., 2010; Hallam et al., 2004; Haroon et al., 2013; Wu et al., 2011). Both types of anaerobic methanotrophs have been found across a wide variety of soil systems and may be well suited for the leach field soil environment (Beal et al., 2009; Hui et al., 2017; Meng et al., 2016; Orphan et al., 2001; Shen et al., 2015, 2016; Vaksmaa et al., 2016; Wang et al., 2012; Weber et al., 2017).

The N₂O cycle is more complex than the CH₄ cycle and represents only a portion of the full denitrification pathway. Denitrification is the sequential reduction of nitrate to dinitrogen (N₂) gas. Each reduction step is catalyzed by one of four enzymes: nitrate reductase (Nar), nitrite reductase (Nir), nitric oxide reductase (Nor), and nitrous oxide reductase (Nos). Many denitrifying bacteria lack the genes encoding for Nos making partial or incomplete biological denitrification a significant source of N₂O (Henry et al., 2006; Sanford et al., 2012). Quantifying the microbial populations directly involved in production (Nor) and consumption (Nos) of N₂O is therefore key to understanding N₂O cycling in soils (Levy-Booth et al., 2014). Two types of bacterial nitric oxide reductases exist: cNor (cytochrome c electron donor) and qNor (quinol electron donor) (Braker and Tiedje, 2003; Dandie et al., 2007). cNor is specific to denitrifier populations and the *cnorB* gene has previously been used as a biomarker for N₂O production (Braker and Tiedje, 2003; Hendriks et al., 2000). For N₂O consumption, the *nosZ* gene has proven to be a suitable biomarker (Henry et al., 2006; Levy-Booth et al., 2014).

Studying the microbial populations involved in GHG cycling is essential to gaining greater insight into the factors controlling GHG emissions from soil systems. This study provides the first examination of presence, abundance, distribution, and characterization of GHG cycling microbial populations associated with septic system

leach field soils. We quantified four functional gene biomarkers involved in GHG production and consumption in leach field systems: *mcrA* and *pmoA* for CH₄ and *cnorB* and *nosZ* for N₂O. Statistical models were used to investigate whether treatment type or measured soil environmental parameters control the abundance of these GHG cycling microbes. Additional statistical models were created to examine the relationship between functional gene abundances and net GHG fluxes from leach field soils. Furthermore, we examined microbial community composition in these soils by sequencing and analyzing 16S rRNA, *mcrA*, and *pmoA* amplicon libraries.

2.2 Materials and methods

2.2.1 Site descriptions

Nine homes in central New York using septic systems for onsite wastewater treatment volunteered to participate in this study. The characteristics for 8 of the 9 sites are summarized in Truhlar et al. (2016). Site 9, which was previously omitted due to a saturated leach field system, is included in this study and had a leach field area of 168 ft². Gas flux measurements, soil samples, and other relevant environmental parameters were taken between June and August of 2014. Three soil treatments were examined: leach field, sand filter and control soils. Control soils were selected on nearby lawn approximately 15 to 12 feet upslope from the leach field and/or sand filter soils. Seven of the sites had leach field and control soils, one of these seven sites had an additional sand filter between the leach field and control. Two sites had only sand filter and control soils.

2.2.2 Flux measurements and analysis

Gas flux measurement methods were previously reported in Truhlar et al. (2016). Briefly, triplicate static gas flux chambers were used to measure soil gas fluxes

based on a method by Molodovskaya et al. (2011). Headspace gases were sampled at 0, 10, 20 and 30 minutes. Gas analyses were performed via gas chromatography, using a flame ionization detector for CH₄ and an electron capture detector for N₂O (Model 6890N GC/ECD, Agilent Technologies Inc.). Gas fluxes were calculated by fitting a linear regression to gas concentration data and dividing the slope of the line by the soil surface area of the chamber for a per meter squared gas flux.

2.2.3 Environmental parameters

Conductivity, volumetric water content (VWC) and soil temperature were all measured in triplicate immediately adjacent to the static gas flux chambers over a soil depth of 0-4 inches as previously reported in Truhlar et al. (2016).

2.2.4 Soil sampling

Soil samples were taken at each of the 9 locations from all treatment types found at that site (i.e. leach field, sand filter, and control). Samples were taken adjacent to the static flux chambers with a 1-inch diameter sterilized soil corer. Between samples the soil corer was cleaned with deionized water and ethanol. Soil cores were taken to a depth of 8 inches and grouped into two depth ranges: 0 to 4 inches (for surface samples) or 4 to 8 inches (for subsurface samples). Samples were immediately stored in sterile 50 ml centrifuge tubes and placed on ice before returning to lab where samples were stored at -20°C until DNA extraction.

2.2.5 DNA extraction

Soil samples were homogenized manually using a sterile spatula. Soil was then subsampled from the homogenized mixture into sterile 2 ml centrifuge tubes. DNA was extracted within 24 hours of sampling using the PowerSoil DNA Isolation kit

(MoBio Laboratories, Carlsbad, CA). For all soil samples, approximately 0.25 g of wet soil were placed in a 2 ml centrifuge tube and 0.5 g of 0.1 mm Zirconia-Silicate beads (BioSpec Products, Bartlesville, OK) were added. PowerBead solution was pipetted out of the manufacturer's microcentrifuge tubes and added to the soil/bead mixture. Following this brief modification, the extraction was carried out according to manufacturer's instructions. A comparison of DNA yields from both the manufacturer's method and the modified method was done and it was determined that DNA yields were higher using the modified extraction method (data not shown). DNA was quantified using the Quant-iT PicoGreen dsDNA assay (Molecular Probes, Eugene, OR) on a Tecan Infinite Fluorimeter and quality was checked with a NanoDrop spectrophotometer (Nanodrop ND-1000, ThermoScientific, Waltham, MA). DNA was stored at -20°C until further analysis.

2.2.6 Quantitative PCR

2.2.6.1 Primer selection and standard curves

Quantification of microbial communities involved in GHG cycling was assessed via quantitative PCR (qPCR) targeting biomarker genes *mcrA*, *pmoA*, *nosZ*, and *cnorB*. Previously published degenerate primers *mlsF/mcrA*-rev were used for quantifying *mcrA* gene copies in soil samples (Luton et al., 2002; Steinberg and Regan, 2008). *pmoA* was quantified to target aerobic methanotrophs using the primer set A189F/mb661R (Costello and Lidstrom, 1999). This primer set has been shown to recover a greater diversity of methanotrophs than other *pmoA*-targeted primer sets while not amplifying the homologous ammonia monooxygenase (*amoA*) gene (Bourne et al., 2001).

To quantify denitrifier populations involved directly in production and destruction of N₂O we selected genes encoding for the Nor and Nos enzymes. For

Nor, the *cnorB2F/cnorB6R* primer set was used to target the *cnorB* gene, encoding the cytochrome b-subunit of cNor (Braker and Tiedje, 2003; Hendriks et al., 2000). The *nosaZ1F/nosZ1R* primer set was selected to quantify denitrifying microbial populations responsible for the final reduction of N₂O to N₂ (Henry et al., 2006). Atypical versions of the *nosZ* gene were not quantified but endpoint PCR was used to examine their presence (see section 2.7 Atypical *nosZ* denitrifiers and anaerobic methanotroph 16S rRNA analyses). All degenerate primers used for quantification of the selected biomarkers are listed in Table 2.1.

Table 2.1. Primers used for qPCR assays for each biomarker gene.

Target		Primer			Amplicon	
Microbial Community	Gene	Primer	Length (bp)	Sequence (5'-3')	Length (bp) ^a	Reference(s)
Methanogens	<i>mcrA</i>	mlasF	23	GGTGGTGTMGDDTTCACMCART	490	Steinberg & Regan, 2009; Luton et al., 2002
		mcrA	24	CGTTCATBGCCTAGTTVGGRTAG		
		rev		T		
Methanotrophs	<i>pmoA</i>	A189F	18	GGNGACTGGGACTTCTGG	508	Costello & Lidstrom, 1999
		mb661R	19	CCGGMGCAACGTCYTTACC		
Denitrifiers	<i>cnorB</i>	cnorB2F	19	GACAAGNNNTACTGGTGGT	390	Braker & Tiedje, 2003
		cnorB6R	18	GAANCCCCANACNCCNGC		
	<i>nosZ</i>	nosZ1F	21	WCSYTGTTCMTCGACAGCCAG	259	Henry et al., 2006
		nosZ1R	23	ATGTCGATCARCTGVKCRTTYTC		

^a Amplicon length based on pure cultures used for standards

Primers used to create long amplicon standards were designed in this study to

target gene sequences from available pure cultures using the PrimerQuest tool from IDT (Table 2.2) available at the IDT website (<https://www.idtdna.com/PrimerQuest/>) (Rozen and Skaletsky, 2000). The gene fragments span the target qPCR amplicon region with an additional 50 bp or longer region on either end of the target sequence. Standards were diluted 10-fold from 10^6 copies μl^{-1} to 10^2 copies μl^{-1} for each target gene.

Table 2.2. Pure cultures and associated primers used to create qPCR standards. All primers were designed using the PrimerQuest tool from IDT (Rozen and Skaletsky, 2000).

Gene	Organism Name	Primer	Primer		Amplicon Length (bp)	Reference
			Length (bp)	Sequence (5'-3')		
<i>mcrA</i>	<i>Methanosarcina</i>	Forward	20	TCCAGACAAGCCGTGTATCC	729	This study
	<i>acetovirans</i> str C2A	Reverse	20	TCCTTGGCTCTGCGAAGTTG		
<i>pmoA</i>	<i>Methylobacterium</i>	Forward	22	CGCACGTTTGACTGGTTAATTT	729	This study
	<i>album</i> BG8	Reverse	20	TAGGTGGCTTGGGTAAATGC		
<i>norB</i>	<i>Paracoccus</i>	Forward	17	TGCTGATGGGCCTTTGG	542	This study
	<i>denitrificans</i> PD122	Reverse	18	GCCATAGAAGGCCAGGTG		
<i>nosZ</i>	<i>Paracoccus</i>	Forward	20	CCTGTTACCCGCTATATCC	706	This study
	<i>denitrificans</i> PD122	Reverse	18	AACAAGGTGCGGGTCTAC		

2.2.6.2 qPCR assay conditions

All qPCR reactions were run in triplicate using a total reaction volume of 25 μl . Each reaction was comprised of 12.5 μl of 2X iQ SYBR Green Supermix (Bio-Rad, US), 17.5 pmol of primer, and 3 μl of template DNA (with concentrations diluted

to between 3 and 10 ng μl^{-1}). Thermal cycling was conducted on an iCycler IQ (Bio-Rad) using protocols previously reported for the chosen primer sets (Braker and Tiedje, 2003; Costello and Lidstrom, 1999; Henry et al., 2006; Steinberg and Regan, 2009). Quantification analyses were carried out using both Data Analysis for Real-Time PCR (DART PCR) which inherently accounts for inhibition of qPCR in samples as well as C_t values reported via the Bio-Rad iCycler IQ software (Peirson et al., 2003). The two methods showed agreement thus C_t -based results are reported here. Melt curve analyses were conducted on all products to check for nonspecific amplification. Confirmation of a subset of qPCR products was done by Sanger sequencing at the Cornell University Biotechnology Resource Center.

2.2.7 Atypical nosZ denitrifiers and anaerobic methanotroph 16S rRNA analyses

To provide a more complete picture of the N_2O and CH_4 cycling community, samples were analyzed via PCR amplification and gel electrophoresis for presence/absence of ‘atypical’ *nosZ* containing denitrifiers and nitrite-dependent anaerobic methane oxidizing (n-damo) bacteria. ‘Atypical’ denitrifier and n-damo functional gene variants have previously been found in soil environments and are likely present across many soil types including leach field soils (Luesken et al., 2011; Sanford et al., 2012).

Many denitrifiers have an ‘atypical’ *nosZ* gene variant that is not captured by ‘typical’ *nosZ* gene primers (Sanford et al., 2012). To target these denitrifiers, atypical *nosZ* primers were designed using sequence alignments in ClustalW for 9 representative denitrifier groups identified by Sanford et al. (2012) (Sanford et al., 2012; Thompson et al., 1994). We chose to assay for 8 of the 9 groups, eliminating primer set 8 from analysis which targeted hyperthermophiles not likely to be found in our soil systems. Primer sequences for target denitrifier groups and annealing

temperatures for primer sets can be found in SI Table 2.1.

The p2f/p2r primer set was used to assay soil samples from all 9 sites for presence/absence of *Methylomirabilis oxyfera*-like bacteria (Ettwig et al., 2009). Primer sequences and annealing temperatures used for PCR reactions can be found in SI Table 2.1. A plasmid containing the 16S rRNA gene insert of n-damo like bacteria was used as a positive control (Vaksmas et al., 2016). All PCR reactions had a total reaction volume of 25 μ l and had the same reaction mixture used for qPCR with the exception that GoTaq Hot Start Polymerase (Promega) was used in place of 2X iQ SYBR Green Supermix. All PCR products were run on a 1% agarose gel and imaged for analysis.

2.2.8 Amplicon library sequencing

16S rRNA gene amplicon libraries targeting the V3-V4 region were created from extracted DNA pools using the universal primers S-D-Bact-0341-b-S-17/ S-D-Bact-0785-a-A-21 from Klindworth et al. (2013). The 25 μ l PCR reaction mixture was composed of 12.5 μ l of KAPA HiFi Master Mix (KAPA Biosystems, US), 5 μ l of 25 pmol of primer, and 2.5 μ l of template DNA. *mcrA* and *pmoA* amplicon libraries were amplified using the qPCR primers (**Error! Reference source not found.**). Amplicon concentrations were measured using a Qubit High sensitivity assay (Life Technologies, Carlsbad, CA, USA) prior to sequencing. Samples were sent for barcoding, pooling, and paired-end sequencing (2×250 bp) using the MiSeq platform (Illumina, San Diego, CA, USA) at the Cornell University Biotechnology Resource Center.

2.2.9 Microbial community analysis

Analysis of 16S rRNA sequencing reads was performed using the QIIME

(v1.9.1) platform (Caporaso et al., 2010). Paired-end reads were merged and quality filtered using default settings. Closed-reference operational taxonomic unit (OTU) picking was conducted against the Greengenes reference database v13.8 (August 2013) (McDonald et al., 2012). Clustering was used to group sequences into OTUs at 97% identity using the default uclust method (Edgar, 2010). RDP classifier was used to assign taxonomy for representative sequences of each OTU (Wang et al., 2007). Alpha diversity analysis was measured using Chao1 and Shannon diversity indices (Shannon, 1948; Wilkins et al., 2015). Beta diversity was calculated using the weighted UniFrac method in QIIME (Lozupone and Knight, 2005).

Downstream analyses of 16S rRNA data including ordinations were performed with R version 3.3.3 in the phyloseq (version 1.19.1) and vegan (version 2.4-4) packages (McMurdie et al., 2013; Oksanen et al., 2017; R Core Team, 2013). Principal Coordinate Analysis (PCoA) and constrained Distance-Based Redundancy Analysis (dbRDA) plots were generated in the vegan package of R using the *capscale* function based on the weighted UniFrac distance matrix. The *bioenv* function in vegan was used to determine which measured parameters (VWC, temperature, conductivity, CH₄ flux, N₂O flux) best explained the observed beta diversity. Variance Inflation Factors (VIF) were evaluated for the constraining parameters to determine if constraints were redundant (VIF score >10). Parameters with high VIF scores were eliminated from the analysis in an iterative process until all parameters were non-redundant (VIF < 5). All selected parameters were tested for significance ($p < 0.01$ based on ANOVA).

Additional analyses were conducted in R to assess the statistical significance of categorical variables in determining variation in microbial communities. Permutational multivariate analysis of variance using distance matrices (ADONIS) was used to analyze three variables based on 2000 permutations: depth (surface, subsurface), treatment (leach field, sand filter, control), and site (1 through 9).

mcrA and *pmoA* amplicon libraries were analyzed separately using the Burrows-Wheeler Aligner (BWA). BWA-MEM was used to pair and align reads to reference libraries of *mcrA* and *pmoA* sequences downloaded from the FunGene database (Fish et al., 2013; Li, 2013). The *mcrA* and *pmoA* databases were created using sequences from FunGene that had full taxonomic lineages. Reference sequence databases consisted of 943 and 931 sequences, for *mcrA* and *pmoA* respectively. After alignment, Samtools was used to count and merge files of individual samples into a summary file used for further analyses (Li et al., 2009). Taxonomy files were created using the UniProt Retrieve/ID mapping tool and manually assigned to each reference sequence (Pundir et al., 2016). Reads were normalized to relative abundance by dividing the reads assigned per family by the total number of assigned reads per sample.

2.2.10 Statistical analyses

All statistical analyses were performed with R (R Core Team, 2013). Linear mixed effects models (LME) were performed following the method of Truhlar et al. (2016), however each model was fit with the additional biomarker data sets. Statistical models were used to examine what drives GHG cycling gene abundances in leach field soils. Maximal models for GHG cycling gene abundances were created for each biomarker gene using site as the random variable and abundance of ‘partner’ genes (e.g. *mcrA* with *pmoA* or *nosZ* with *cnorB*) or ratio of production:consumption gene abundance (e.g. *mcrA:pmoA* and *cnorB:nosZ*), treatment (i.e. control, leach field, sand filter) and measured soil parameters (i.e. conductivity, VWC, temperature) as fixed effects. The ratio of production:consumption gene abundances was considered in models under the assumption that higher ratios (e.g. greater gene abundance of GHG producers as compared to GHG consumers) would correlate to higher GHG fluxes

compared to locations with lower production:consumption gene abundance ratios.

Additional LME models were created for methane or nitrous oxide gas fluxes to answer the question of what drives GHG fluxes from leach field soil systems. Maximal models were created using site as the random variable, with biomarker gene abundances or ratios of production:consumption biomarker gene abundances, treatment, and measured soil parameters as fixed effects.

All two-way interactions were examined, and minimal models were reached by sequentially removing non-significant fixed effects. Variance inflation factors were calculated for model parameters to determine if there was redundancy. Parameters with VIF scores greater than 10 were eliminated successively until all parameters in the model had VIF scores below 5. High correlation was observed between VWC and conductivity measurements in our data set (VIF >10). To avoid issues with collinearity in the LME models, conductivity was excluded from analysis. Normality and residual analyses were carried out for each analysis and both assumptions were satisfied for each model created.

2.3. Results

2.3.1 Abundance of GHG cycling genes in leach field soils

All four functional genes *mcrA*, *pmoA*, *cnorB*, and *nosZ* were present in all samples regardless of treatment type or depth (Figure 2.1). No treatment effect is apparent for any of the biomarker genes. Surface soil *mcrA* gene abundances were more variable across sites and treatment types ($1.48 \times 10^5 - 1.05 \times 10^9$ copies g^{-1} wet soil) than surface soil *pmoA* ($8.03 \times 10^5 - 5.6 \times 10^7$ copies g^{-1} wet soil), *cnorB* ($8.96 \times 10^6 - 1.69 \times 10^8$ copies g^{-1} wet soil), and *nosZ* ($3.10 \times 10^5 - 2.33 \times 10^7$ copies g^{-1} wet soil) gene abundances. The majority of sites and treatment types had higher surface gene abundances of *pmoA* than *mcrA*. Notably, site 9 leach field soil had an almost 20-fold

difference between *mcrA* and *pmoA* surface soil gene abundances with 1.05×10^9 and 5.6×10^7 copies g^{-1} wet soil, respectively. Surface *mcrA* gene abundance at this site was also the highest observed for any of the biomarker genes at any site, treatment type, or depth sampled in this study. *cnorB* gene copies were higher than *nosZ*, *pmoA*, and *mcrA* at each site and treatment with the exception of site 9 *mcrA*. Gene abundances of *cnorB* did not fall below 9×10^6 copies g^{-1} wet soil in surface soils or below 2.2×10^6 copies g^{-1} wet soil in subsurface soils. *nosZ* was lower in abundance than *cnorB* at any given site and treatment type.

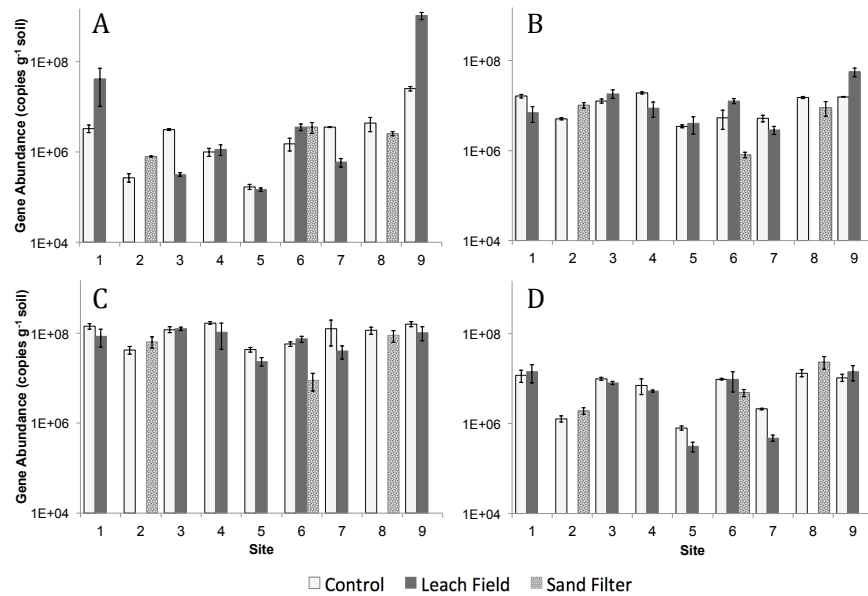


Figure 2.1. Surface soil gene abundances in copies per gram soil for *mcrA* (A), *pmoA* (B), *cnorB* (C), and *nosZ* (D) by treatment type (Control, Leach Field, and Sand Filter) for sites 1 through 9.

Generally, all four biomarker gene abundances were higher in surface soil than in subsurface soil regardless of treatment type (Figure 2.2). T-tests between surface and subsurface gene abundances confirmed this finding for *pmoA* ($p = 0.032$), *cnorB* ($p = 0.00064$), and *nosZ* ($p = 0.0015$) but not *mcrA* ($p = 0.42$). Several locations had greater *mcrA* gene abundances in subsurface samples as compared to surface samples, however the majority of locations had greater surface gene abundances of *mcrA*.

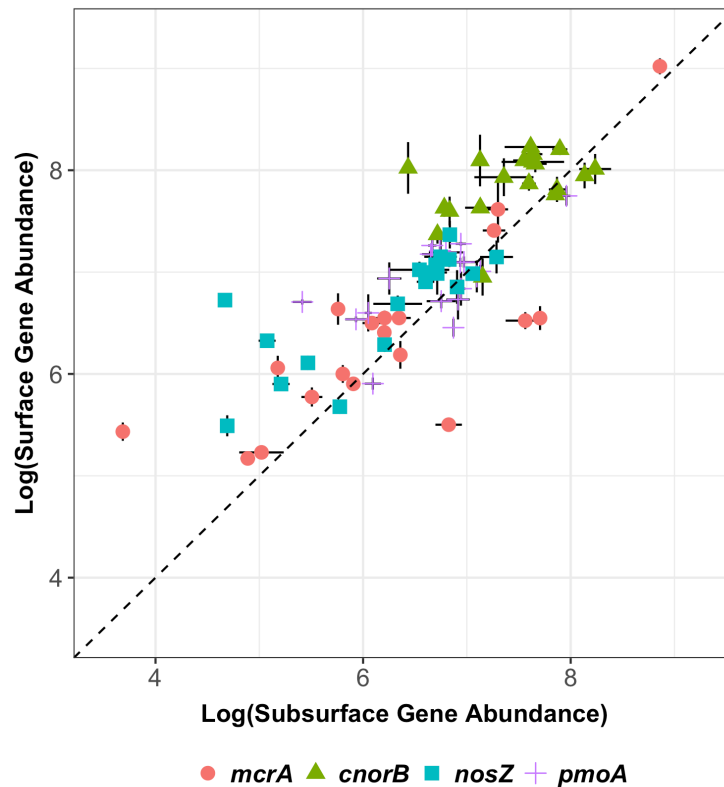


Figure 2.2. Comparison of log₁₀ gene abundances for surface samples and subsurface samples by site of *mcrA* (circle), *pmoA* (cross), *cnorB* (triangle), and *nosZ* (square). Dotted line indicates a 1-to-1 relationship. The majority of sites had greater biomarker gene abundances in the surface sample.

2.3.2 Modeling of GHG cycling gene abundances

LME models were fit for each biomarker gene to determine the effect of ‘partner’ (e.g. *mcrA* for *pmoA* and vice versa) gene abundance and measured soil parameters (VWC, conductivity, and temperature) on the modeled biomarker’s gene abundance (Figure 2.3). VWC had a significant effect on the abundance of *mcrA* ($p = 0.0398$) but not *pmoA*. *mcrA* and *pmoA* gene abundances were positively correlated with each other ($p < 0.0001$). No minimal model was created for *cnorB* or *nosZ* gene abundances as they were not significantly affected by treatment, measured soil

parameters, or the presence of a ‘partner’ gene.

The production:consumption gene ratio for CH₄ showed a significant relationship to VWC ($p = 0.0005$). Interestingly, there was a significant effect on the ratio of *mcrA:pmoA* by the leach field treatment ($p = 0.0935$) at a 90% confidence interval. No significant effect of any variable for the *cnorB:nosZ* ratios was found (Table 2.3).

Table 2.3. Results for LME models of biomarker gene abundances using site as the random effect. Individual biomarker genes were modeled using the ‘partner’ gene (e.g. *mcrA* modeled by *pmoA*), treatment, and soil parameters as effectors. Models for ratios of production to consumption gene abundances (e.g. *mcrA:pmoA*) with environmental parameters as effectors are also shown. Only models with at least one significant effect are presented. No significant effects were found for N₂O cycling genes. N.A. indicates the effector was not part of the model.

Biomarker LME			
Biomarker	'Partner' Biomarker		VWC
Gene			
<i>mcrA</i>	t = 5.32, $p < 0.0001$		t = 2.24, $p = 0.0398$
<i>pmoA</i>	t = 7.90, $p < 0.0001$		N.A.

LME with Biomarker Ratio			
Biomarker	Treatment		VWC
Ratio	Leach Field	Sand Filter	
<i>mcrA:pmoA</i>	t = 1.79, $p = 0.0935^*$	t = 0.793, $p = 0.44^*$	t = 4.39, $p = 0.0005$

Indicates not significant at a 95% confidence interval.

2.3.3 Biomarker abundances as drivers of GHG fluxes from leach field soils

Quantified biomarker gene abundances and measured GHG fluxes were used to examine whether there is a correlation between biomarker abundance and GHG emissions from leach field soils. First we compared GHG fluxes versus the ratio of production:consumption genes for each CH₄ and N₂O. Then we created statistical models for GHG fluxes using biomarker gene abundance and soil VWC. Additional statistical models were used to examine the effect of the ratio of production:consumption gene abundance on measured GHG fluxes.

Leach field CH₄ and N₂O flux measurements were previously reported by Truhlar et al. (2016) for 8 of the 9 sites in this study. Site 9 measurements are an additional dataset presented here. Average CH₄ gas fluxes (mg m⁻² day⁻¹) at each site showed no clear relationship with the ratio of *mcrA* to *pmoA* surface gene abundances below a ratio of 10 (Figure 2.3). Methane fluxes at sites 1 through 8 varied from -4.60 mg CH₄ m⁻² day⁻¹ to 38.2 mg CH₄ m⁻² day⁻¹, representing a range of net CH₄ producing, and consuming soils. Ratios of *mcrA:pmoA* gene abundance in surface soils ranged from 0.0174 to 6.01 for sites 1 through 8 with the majority of samples (79%) having a ratio below 1. The *mcrA:pmoA* ratio of site 9's leach field soil was 18.7 - 3 times greater than the next highest ratio. Site 9 also had the highest CH₄ emissions of any site and treatment type, 260 mg CH₄ m⁻² day⁻¹.

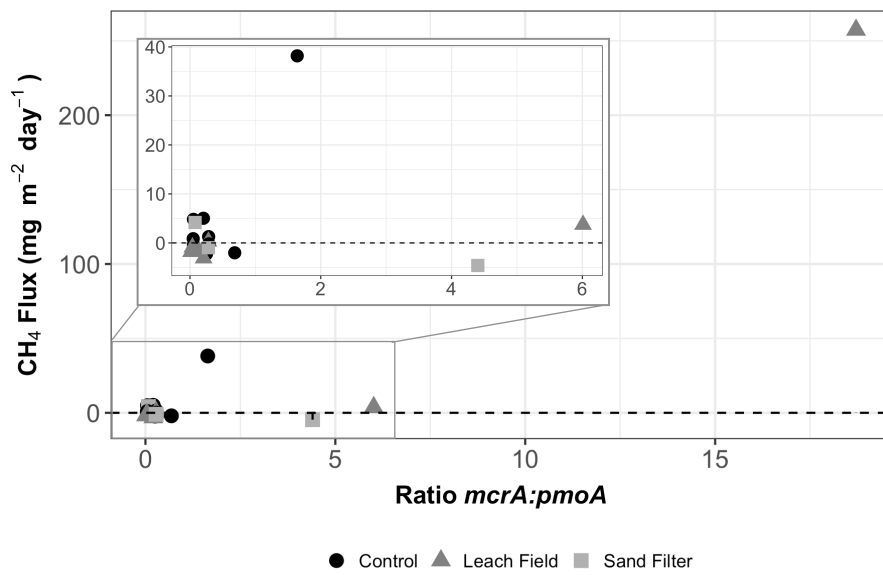


Figure 2.3. CH₄ fluxes (mg m⁻² day⁻¹) versus ratio of *mcrA:pmoA* gene abundances by treatment. Treatments are indicated by shape and color: Control (black circle), Leach Field (grey triangle), Sand Filter (light grey square). Inset shows data excluding site 9. The dotted line indicates zero net CH₄ emissions.

Average N₂O gas fluxes measured over the sampling period showed no relationship to the ratio of *cnorB:nosZ* surface gene abundances (Figure 2.4). All soils were net producers of N₂O, with fluxes from 0.146 mg N₂O m⁻² day⁻¹ to 14.9 mg N₂O m⁻² day⁻¹. Surface *cnorB:nosZ* gene ratios ranged from 1.84 up to 93.3 and had a wider range of values than those of *mcrA:pmoA*. However, *cnorB:nosZ* ratios never went below 1 due to consistently greater *cnorB* gene abundances as compared to the ‘typical’ *nosZ* abundances quantified in this study. Unlike Site 9’s leach field where the highest *mcrA:pmoA* gene abundance occurred at the location with the highest CH₄ emissions, the highest *cnorB:nosZ* ratio did not correspond to elevated N₂O emissions.

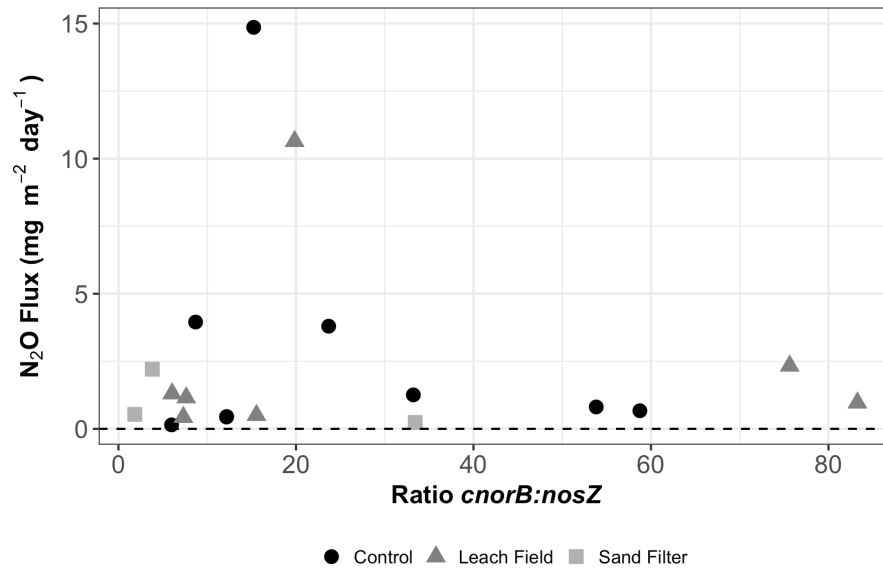


Figure 2.4. N_2O flux ($mg\ m^{-2}\ day^{-1}$) versus ratio of *cnorB:nosZ* gene abundances. Treatments are indicated by shape and color: Control (black circle), Leach Field (grey triangle), Sand Filter (light grey square). The dotted line indicates no net N_2O emissions.

To characterize the impact of the GHG cycling microbial community on GHG emissions, CH_4 and N_2O fluxes were modeled using functional gene abundances and VWC. The LME model results in Table 2.4 suggest that CH_4 fluxes were significantly positively affected by the abundance of *mcrA* ($p < 0.0001$) and *pmoA* ($p = 0.026$) as well as soil VWC ($p = 0.0106$). LME results additionally confirmed the ratio of *mcrA:pmoA* showed a significant positive relationship to CH_4 emissions ($p < 0.0001$) and a significant positive relationship to soil VWC ($p = 0.05$). However, there was no significant relationship between gene abundance of the N cycling biomarker genes to N_2O emissions at a 95% confidence interval.

Table 2.4. Results of LME models for CH₄ emissions using site as the random effect. Fluxes were modeled using fixed effects of either biomarker gene abundances or the ratio of production:consumption gene abundances and soil environmental parameters. Only significant effectors are shown. No significant effects were found for N₂O fluxes.

Gas LME with Biomarkers			
Gas	<i>mcrA</i>	<i>pmoA</i>	VWC
CH₄	t = 23.1, p < 0.0001	t = 2.71, p = 0.0257	t = 3.00, p = 0.0106

Gas LME with Biomarker Ratio		
Gas	Ratio <i>mcrA</i>:<i>pmoA</i>	VWC
CH₄	t = 6.079, p < 0.0001	t = 2.184, p = 0.050

2.3.4 Characterizing functional microbial communities in leach field soils

To gain a more complete understanding of the microbial communities in leach field soils we screened samples for presence/absence of atypical *nosZ* denitrifiers and anaerobic methanotrophs and performed high throughput sequencing on 16S rRNA, *mcrA*, and *pmoA* amplicon libraries. Determining presence or absence of atypical denitrifiers and anaerobic methanotrophs informs whether these populations should be further studied in soil systems in the future; while 16S rRNA and functional gene sequencing allows for a more in-depth look at microorganisms specifically involved in CH₄ cycling. 16S rRNA sequencing data was analyzed using principal coordinate and distance-based redundancy analyses to determine what drives microbial community diversity in leach field soils. Sequencing of the functional genes *mcrA* and *pmoA* was further used to examine the specific CH₄ populations of interest in this study and was compared to results from the 16S rRNA dataset.

2.3.4.1 Presence of atypical *nosZ* denitrifiers and anaerobic methanotrophs

Gel electrophoresis of PCR products suggests that denitrifiers with atypical *nosZ* sequences as well as anaerobic methane oxidizers are present in soils regardless of treatment. PCR products using the *nosZa9* primers targeting denitrifiers in the *Deltaproteobacteria* class were found in all but 3 samples (SI Figure 2.1). Sanger sequencing done on a subset of the products confirmed amplicons were from atypical *nosZ* genes belonging to *Anaeromyxobacter*-like organisms. BLAST results of trimmed sample sequences showed between 85 and 90% sequence identity to *Anaeromyxobacter* species. The remaining 7 primer sets for atypical *nosZ* genes were tested with samples pooled by treatment (e.g. leach field, sand filter, and control soils). However only the *nosZa7* primer set, designed to target bacteria from the *Chloroflexi* phylum, resulted in a PCR product of the correct size. The 6 atypical *nosZ* primer sets with no or nonspecific products belonged to several different groups of denitrifiers including those in the phyla *Bacteroidetes*, *Firmicutes*, and *Alpha-* and *Beta-proteobacteria* (SI Figure 2.2).

Results for primers specific to the 16S rRNA gene of *M. oxyfera*-like bacteria were mixed. Multiple bands were observed for most samples (SI Figure 2.3), however eight of the sites (a mix of leach field, sand filter, and control soils) had a PCR product of the correct size and Sanger sequencing confirmed the presence of NC10-like bacteria in these soils (GenBank Accession Number: MG970710).

2.3.4.2 16S rRNA and functional gene amplicon sequencing

After filtering out low quality sequences from the 16S rRNA dataset a total of 1,047,582 sequences were obtained. Assigned reads per sample ranged from 2,502 to 78,141 with a mean of 18,243 reads and a median read length of 444 bp. Singleton OTUs were removed resulting in the 22,656 unique OTUs used to calculate beta

diversity.

A 2D principal coordinate analysis (PCoA) on the weighted UniFrac distance matrix (Figure 2.5A) was used to describe the variation in microbial communities of sites 1 through 9. Constrained Distance-Based Redundancy Analysis (dbRDA) (Figure 2.5B) identified CH₄ flux, N₂O flux, and VWC as the parameters that best explained the variation in microbial community composition. The first two axes of the unconstrained plot (PC1 15.0% and PC2 12.1%) explain 27.1% of the phylogenetic variation in microbial communities (Figure 2.5A). The constrained ordination using CH₄ flux, VWC, and N₂O flux as explanatory variables explains approximately 64% (first axis 10.4% and second axis 6.96%) of the variation observed in the first two axes of the unconstrained PCoA plot (Figure 2.5B). Both soil VWC and CH₄ flux appear to strongly drive variations in microbial communities, while N₂O has a lesser effect.

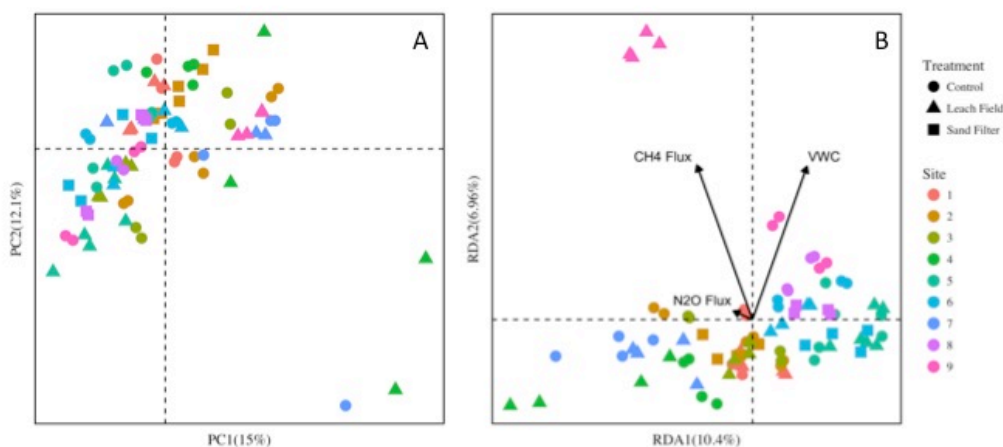


Figure 2.5. Microbial community structure in 9 septic system soils showing all treatment types (control (circle), leach field (triangle), and sand filter (square)) and depths (surface and subsurface). PCoA plot based on the pairwise weighted UniFrac distance matrix (A). Constrained dbRDA of soil microbial communities with environmental parameters CH₄ flux, VWC, and N₂O flux best explaining variation in microbial community structure (B).

ADONIS results based on 16S rRNA sequencing indicate that depth, treatment, and site all significantly affected microbial community composition, however depth and treatment did not explain a substantial portion of the variation (depth ($R^2 = 0.040$, $p < 0.001$), treatment ($R^2 = 0.044$, $p < 0.001$)). Site was a stronger explanatory variable ($R^2 = 0.37$, $p < 0.01$) than either depth or treatment.

Alpha diversity indices Chao1 and Shannon showed that within treatment microbial diversity was similar across the three treatments (SI Table 2.2). Chao1 values for control (9491) and sand filter (9922) soils were most similar with leach field having a lower value (7965). Shannon values showed a similar trend as the Chao1 indices with alpha diversity being the lowest in the leach field (7.18) and higher in control and sand filter soils (7.32 and 7.30, respectively).

Phylogenetic trees were constructed based on a subset of 16S rRNA gene sequences for microbial groups involved in CH_4 cycling (Figure 2.6 and Figure 2.7). The *Euryarchaeota* tree was constructed from all 126 sequences assigned to that phylum and shows that 16S rRNA reads belonging to methanogens from the *Methanosaetaceae* and *Methanomassiliicoccaceae* (predicted) families were found across all treatments while *Methanobacteriaceae* was found in leach field and sand filter but not control soils. Site 9 had a greater fraction of overall 16S rRNA reads assigned to methanogen species than any other site. Interestingly, site 9 leach field was also the only location with reads mapping to ANME-2D type microorganisms. ANME-2D are known to couple anaerobic methane oxidation to a variety of electron acceptors including nitrate and recently have been discovered in flooded soil systems (Vaksmas et al., 2016; Weber et al., 2017). The relatively low abundance values observed for archaea in the 16S rRNA tree are likely due to the low recovery of archaeal sequences (64.6% recovery) as compared to bacterial sequences (94.5% recovery) by the selected primers (Klindworth et al., 2013). Future work attempting to

characterize total bacterial and archaeal populations should select universal primers with greater recovery of archaeal sequences.

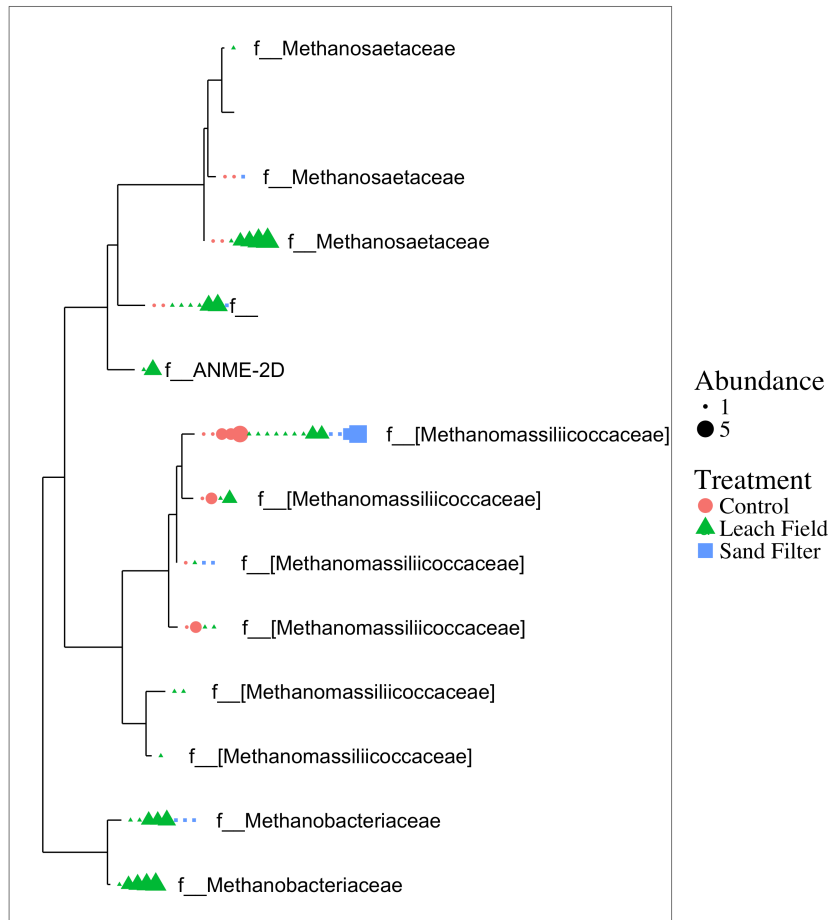


Figure 2.6. Phylogenetic tree based on 16S rRNA reads for families within the Euryarchaeota phylum. Read abundance is indicated by the size of the marker, and treatment is shown by shape: control (black circle), leach field (dark grey triangle), and sand filter (light grey square). Tree tips are labeled at the family level. Brackets ([]) indicate a predicted family. Blank tips indicate taxonomic information was not available at the family level from the Greengenes database.

16S rRNA sequencing data showed that aerobic methanotrophs including both Type I (*Methylococcaceae*) and Type II (*Methylocystaceae* and *Methylobacteriaceae*) as well as NC10 affiliated anaerobic methanotrophs (*Methylomirabiliaceae*) were present across all treatment types (Figure 2.7). A total of 1,072 sequences (approximately 0.1% of all sequences) mapped to one of these methanotrophs groups.

Methylococcaceae appear to dominate in leach field soils and the majority of OTUs were *Methylomonas*-type organisms (>85%) with a few *Methylosarcina* reads (<10%) and the rest being unassigned at the genus level.

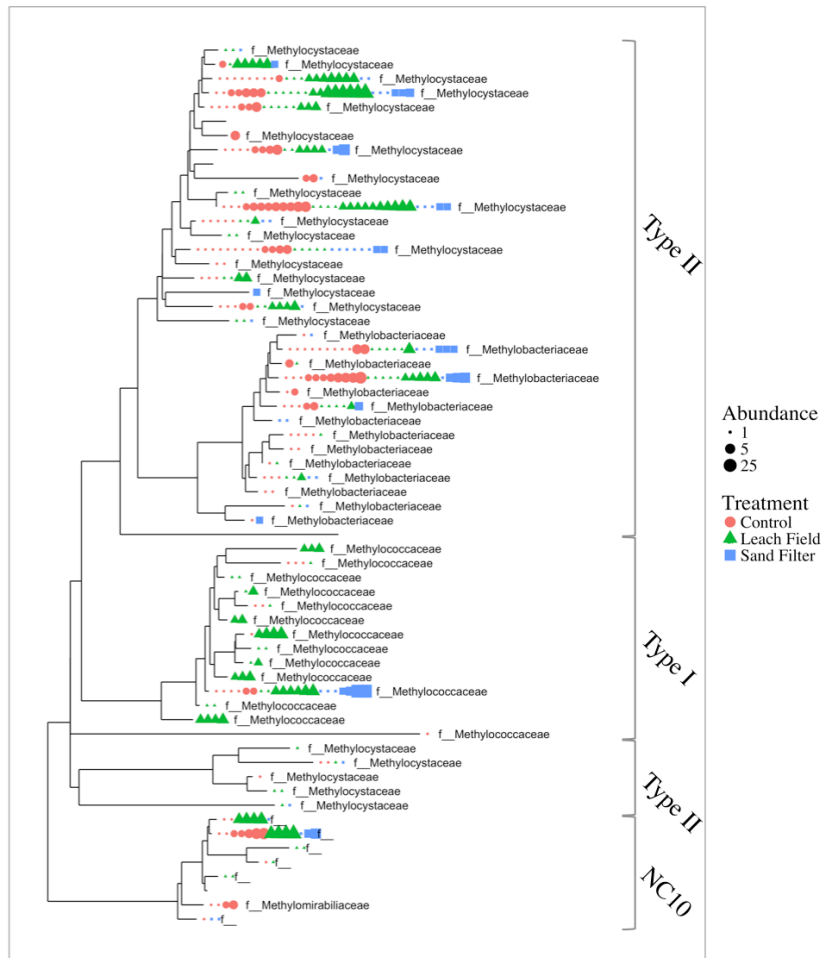


Figure 2.7. Phylogenetic tree based on 16S rRNA sequence reads of aerobic methanotrophs of the Gamma- and Alpha-proteobacteria as well as anaerobic methanotrophs of the NC10 phylum. Read abundance is indicated by the size of the marker, and treatment is shown by shape: control (black circle), leach field (dark grey triangle), and sand filter (light grey square). Tree tips are labeled at the family level. Blank tips indicate taxonomic information was not available at the family level from the Greengenes database.

Illumina sequencing of *mcrA* and *pmoA* libraries showed that treatment had little to no effect on the community composition of CH₄ cycling microorganisms (Figure 2.8 and SI Figure 2.4 and 2.5). Notably, the read depth of *mcrA* was

significantly greater than that of *pmoA* with mean mapped reads per sample of 13,745 for *mcrA* but only 16 for *pmoA* (total mapped reads across all samples were 1,268,909 and 1,523, respectively), making *mcrA* results overall more informative than *pmoA* results. It is unclear why fewer sequences were obtained for *pmoA*, however it may be attributed to unequal sample pooling (with a greater proportion of the sample going to *mcrA* and 16S rRNA libraries) as well as reference sequence database limitations, which excluded reference sequences with missing genus level taxonomic information potentially leading to high numbers of poor and/or failed alignments.

Relative abundances of *mcrA* reads did not differ between treatments at the family level. Methanogen families found in the 16S rRNA gene libraries were also found in the *mcrA* libraries including *Methanosaetaceae*, *Methanobacteriaceae*, and *Methanomassiliicoccaceae* (Figure 2.8). *mcrA* reads of the ANME-2D anaerobic methanotroph *Candidatus* Methanoperedeceae were found across all treatments; this result differed from the 16S rRNA sequencing results which detected ANME-2D sequences only in site 9 leach field soils.

pmoA sequencing results were limited with very few reads obtained overall resulting in detection of only three methanotroph groups: *Methylococcaceae*, *Methylocystaceae*, and candidate division NC10 (SI Figure 2.4). No reads were assigned to *Methanobacteriaceae* type methanotrophs, which were observed in the 16S rRNA libraries. At the genus level, *pmoA* reads confirmed the dominance of *Methylomonas*-type methanotrophs in leach field soils as compared to control or sand filter soils (SI Figure 2.5). Anaerobic methanotrophs of the NC10 phylum were found in both leach field and control soils but not sand filter soils in the *pmoA* libraries, this differed from 16S rRNA results that showed NC10 reads were present across all treatments (SI Figure 2.4).

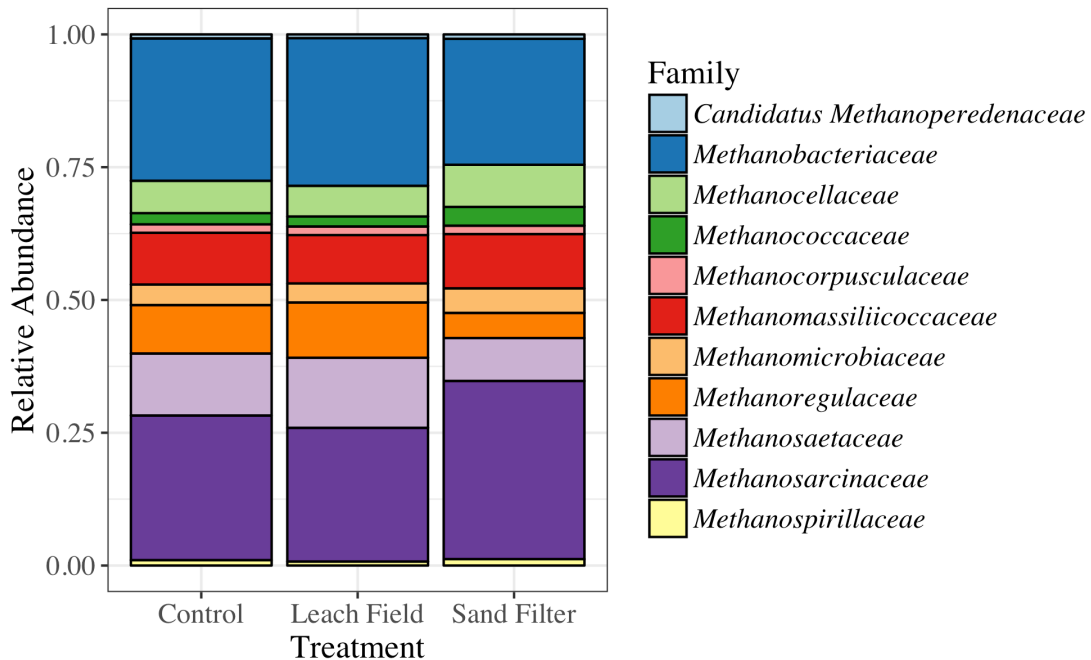


Figure 2.8. Relative abundance of *mcrA* reads assigned at the family level grouped by treatment. All 1,268,909 *mcrA* reads obtained from all 84 samples (control: n = 40, leach field: n = 30, sand filter: n=14).

2.4 Discussion

Understanding the ecology of microorganisms involved in GHG cycling is key to a better understanding of factors controlling GHG emissions from soil systems. Previous studies have used biomarker genes to explore the relationship between presence of key organisms involved in GHG cycling and net methane and nitrous oxide fluxes in soils across diverse environments (Billings and Tiemann, 2014; Dandie et al., 2008; Freitag et al., 2010; Lee et al., 2014). However, no previous study has coupled quantification of GHG cycling biomarkers to net CH₄ and N₂O fluxes in leach field soils using statistical models. Likewise, population and depth distributions of methanogens, methanotrophs and denitrifiers as well as high throughput sequencing characterization of microbial communities has not been previously studied in leach field soil systems.

2.4.1 Quantification of functional biomarkers in leach field soils

Presence of the functional genes *mcrA*, *pmoA*, *cnorB*, and *nosZ* was found in all sites, regardless of treatment type (leach field, sand filter, or control) or depth (surface or subsurface). Biomarker gene quantities were in typical ranges to those found in other soil systems, ranging from agricultural soils to peat bogs (Braker and Tiedje, 2003; Dandie et al., 2007; Freitag et al., 2010; Henry et al., 2006; Seo et al., 2013). In general, surface soils had greater biomarker gene abundances when compared to subsurface soils. A study by Seo et al. (2013) similarly showed greater abundance of *pmoA*, *mcrA*, and *nosZ* in rice paddy surface soils (< 10 cm) as compared to deeper soils (> 10 cm) suggesting the majority of GHG cycling is occurring in surface soil (Seo et al., 2013). Higher *pmoA* gene abundances are expected in aerobic surface soil environments favorable for methanotrophs, however the same trend was observed for *mcrA* gene abundances at the majority of sites suggesting methanogens are likewise more abundant in surface soils. Angel et al. (2012) showed that methanogens such as the *Methanosarcina* and *Methanocella* genera are robust to oxygen exposure; thus, the negative impact of oxygen on methanogen abundance may be outweighed by the benefit of access to elevated organic carbon in surface soils (Angel et al., 2012).

2.4.2 Modeling functional biomarker quantity in leach field soils

Soil properties, such as volumetric water content (VWC), are known to influence the structure of native microbial communities. Previous studies have shown a positive relationship between increased soil VWC and *mcrA* gene abundances (Christiansen et al., 2016; Ma et al., 2012). The same trend was observed in this study at site 9 where the highest abundance of *mcrA* gene copies occurred concomitantly

with the highest observed soil VWC (77.3 v/v). *mcrA* gene abundances at this site were more similar to those of traditionally flooded anaerobic environments such as rice paddies and peat bogs, likely due to anaerobic conditions created by a failing leach field system (Freitag et al., 2010; Ma et al., 2012). LME models confirmed the positive correlation between *mcrA* gene copies and soil VWC ($p = 0.0398$). However, gene abundances of *pmoA* were not significantly correlated with VWC and neither of the denitrifier genes showed a significant relationship with soil VWC. Average soil temperature over the sampling period (which ranged from 19.3 to 23.5 °C) did not significantly affect the abundance of any biomarker genes. Temperature has previously been shown to affect *nosZ* abundance, however this relationship was not significant in our study likely due to the limited temperature range (Jung et al., 2011).

Methanotrophs have been found to reside in close proximity to methanogens and a positive correlation between *pmoA* and *mcrA* gene abundances has been shown in other studies (Freitag et al., 2010; Lee et al., 2014). LME model results indicate a similar relationship is seen in our study, where the abundance of *pmoA* was significantly positively correlated with the abundance of *mcrA* and vice versa ($p < 0.0001$). Methanotrophs are thought to consume the majority of microbially produced methane, up to 80% globally, thus the co-occurrence of these populations suggests a potential for significant CH₄ mitigation from leach field and other soils (Cai et al., 2016; Conrad, 2009; Le Mer and Roger, 2001; Thauer et al., 2008).

2.4.3 Drivers of GHG fluxes from leach field soils

Eight of the 9 sites in this study were either net consumers or low rate emitters of methane. These 8 sites all had *mcrA:pmoA* ratios below 10, and all but two treatments from these sites had ratios below 1. Thus, at the majority of sites, methanotroph populations were greater than methanogen populations and were able to

keep pace with any methanogen activity. With the exception of site 9, this holds true even in cases where *mcrA* abundances are greater than *pmoA* abundances. Substantial methane production was measured at site 9, the only location where the *mcrA:pmoA* ratio exceeded 10. This suggests there may be a ‘threshold’ ratio above which methanotrophs are no longer capable of matching the activity of methanogens, resulting in net CH₄ emissions. LME models show that CH₄ fluxes are significantly positively correlated with the ratio of *mcrA:pmoA* gene abundances ($p < 0.0001$) and with soil VWC ($p = 0.05$). The relationship between CH₄ fluxes and soil VWC has been observed in a number of studies including one by McPhillips et al. (2016) which found high soil VWC was correlated with higher CH₄ fluxes from roadside ditches as compared to drier nearby lawns (Christiansen et al., 2016; McPhillips et al., 2016). Further studies on gene to transcript ratios for these key functional genes could clarify whether biomarker abundances in combination with soil VWC can be used to accurately predict GHG flux potential.

Although we found a significant relationship between CH₄ cycling genes and CH₄ emissions, we were unable to find a similar relationship for N₂O. Several studies have attempted to describe the relationship between abundance of N₂O cycling genes and N₂O emissions with mixed results (Angnes et al., 2013; Billings and Tiemann, 2014; Dandie et al., 2008). We found that ratios of *cnorB:nosZ* did not significantly correlate with N₂O emissions, however all soils were net producing and had *cnorB:nosZ* ratios greater than one. A study by Angnes et al. (2013) found a ratio of (*cnorB* + *qnorB*)/ *nosZ* greater than or equal to 100 was indicative of N₂O emission potential (Angnes et al., 2013). However, the *cnorB:nosZ* ratios in this study were all below 100 and the single observed ratio greater than 80 did not correspond to elevated N₂O flux. The lack of strong correlation in this and previous studies may be due, at least in part, to limitations of selecting primers that amplify only a subset of the

diversity found in N cycling genes. Indeed, we quantified *cnorB* but not *qnorB* as the latter has been observed in nondenitrifier bacteria strains, while the former is specific to denitrifiers (Dandie et al., 2007; Jung et al., 2011). Other studies have omitted *nor* completely, choosing to quantify the presence or activity of preceding denitrification steps (e.g. nitrate- and nitrite-reductase genes, *nar* and *nir*) (Cuhel et al., 2010; Hallin et al., 2009; Seo et al., 2013). Additionally, quantifying the ‘typical’ version of the *nosZ* gene to the exclusion of the diverse ‘atypical’ versions likely led to underestimation of denitrifier populations capable of consuming N₂O.

2.4.4 Presence of anaerobic methanotrophs and atypical denitrifiers

While our study focused specifically on aerobic methanotrophs, the relatively recent discovery of anaerobic methane oxidizing bacteria and archaea drove us to explore whether these populations were present in leach field soils. Both n-damo and ANME-2D can couple methane cycling to nitrogen cycling making them important potential players in soil GHG cycling. PCR products confirmed the presence of 16S rRNA gene sequences of *M. oxyfera*-like bacteria in 8 of 9 sites. 16S rRNA Illumina sequencing supported this finding with 16% of all methanotroph reads (e.g. Type I, Type II, and NC10) mapping to the *Candidatus* Methylomirabilis genus. This indicates potential for methane oxidation coupled to nitrite reduction in grassland soils regardless of the presence of a leach field.

ANME-2D have been discovered in soil environments from fresh water sediments to paddy soils (Raghoebarsing et al., 2006; Vaksmaa et al., 2016). Although we did not assay samples to determine presence of ANME groups, high-throughput sequencing of 16S rRNA libraries revealed that ANME-2D archaea were present in soils from leach field site 9, albeit at relatively low abundance with only 4 reads out of more than 14,000 mapping to ANME archaea. This was the only site with completely

saturated soils similar to conditions where ANME-2D methanotrophs have previously been found (Vaksmaa et al., 2016). *mcrA* amplicon library analysis supported the finding of ANME-2D archaea with reads mapping to *Candidatus* Methanoperedenaceae in 68 of the 84 samples across all treatment types. *Candidatus* Methanoperedens is thought to couple nitrate reduction to methane oxidation and despite the low read counts in this study, this ANME group has the potential to contribute significantly to methane oxidation in soils (Haroon et al., 2013). Based on these results, we suggest quantification of anaerobic methane oxidizers (including ANME-2D and n-damo) in septic leach field soils as they may contribute significantly to methane oxidation particularly in poorly-drained and/or fertilized soils. Quantification of these populations would allow for improved statistical modeling of CH₄ fluxes based on functional gene abundances ultimately leading to a better understanding of the carbon cycle.

Atypical denitrifying populations were also found in our soil samples. Both *Anaeromyxobacter* and *Chloroflexi* type organisms containing atypical *nosZ* genes were found across all treatments. 16S rRNA data confirmed the presence of these microorganisms with all samples having reads map to the *Chloroflexi* phylum and 75% of samples having reads map to *Anaeromyxobacter* type organisms. Based on these preliminary data, we suggest that qPCR of atypical *nosZ* genes in soil is needed to accurately capture a relationship between N₂O emissions and functional gene abundance.

2.4.5 16S rRNA and functional gene characterization of GHG cycling microbial communities

Constrained dbRDA ordination of the 16S rRNA gene amplicon libraries indicated that while treatment was not a significant driver of community composition,

soil VWC, CH₄ flux, and N₂O flux collectively explained 64% of the variation in the observed beta diversity (i.e. dissimilarity between samples). Site 9's leach field was unique in terms of CH₄ production and VWC and this influenced the dbRDA results, which highlighted site 9 leach field samples as the most dissimilar. This site also drove many of the relationships found in LME analyses for the CH₄ cycling biomarkers *mcrA* and *pmoA*. However, the N₂O cycling biomarkers, *cnorB* and *nosZ* gene copies were not significantly different at Site 9 as compared to the other 8 sites and N₂O emissions at this site were highest in control not leach field soils (0.232 vs. 0.007 mg m⁻² d⁻¹). The dbRDA and LME model results indicate that VWC is a strong driver for CH₄ cycling microorganisms but not necessarily N₂O cycling populations.

dbRDA results suggest that both CH₄ and N₂O fluxes significantly affect diversity of microbial communities present in the 9 sites ($p < 0.001$). Although we did not observe a significant relationship between selected N₂O biomarker gene abundances and net N₂O emissions in LME models, it is not surprising that N₂O fluxes explain some of the variation in soil microbial communities. Additionally, 16S rRNA gene amplicon analysis showed that location (i.e. site) was a significant explanatory variable for microbial diversity ($p < 0.001$). Although we did not analyze soil samples for pH, organic C, fixed N, or other nutrients, it is likely that sites have different soil characteristics that would significantly affect the composition of microbial populations.

High-throughput sequencing of *mcrA* and *pmoA* libraries was further used to characterize microbial populations controlling CH₄ cycling in septic leach field soils. Results for *pmoA* amplicon libraries were limited, with a mean of 16 reads per sample mapping to reference sequences (ranging from 0 to 362 assigned reads per sample). Although *pmoA* read depth was shallow, results indicate both Type I and Type II methanotrophs are present across all treatment types with Type II methanotrophs

being a greater proportion of reads in leach field soils as compared to control soils. Type II methanotrophs are regarded as low-affinity and more tolerant to low oxygen levels (Chowdhury and Dick, 2013; Knief, 2015). 16S rRNA sequencing results support this finding with Type II methanotrophs more abundant in the leach field treatment. Both 16S rRNA and *pmoA* sequencing indicated Type II *Methylomonas* were more abundant in leach field soils as compared to either control or sand filter soils. *mcrA* reads revealed no difference in methanogen community composition by treatment. Two families, *Methanosarinaceae* and *Methanobacteriaceae*, represented a majority of the *mcrA* reads.

The functional gene toolkit used in this study can be applied to other systems where GHG cycling is important to examine the abundance of microbial populations directly involved in GHG production and destruction. Quantifying transcripts of these biomarker genes *in situ* to look at activity of these communities over time and compared to net fluxes can help shed light on how the balance between the activity of organisms producing and consuming GHGs is ultimately reflected in GHG fluxes. Although we found that the presence of a leach field system had little impact on the overall structure of soil microbial communities, the site with a flooded leach field did show a markedly different community structure from other sites. Thus, we suggest proper installation and maintenance of leach fields in well-drained soils is essential to reducing greenhouse gas emissions from these systems.

2.5 Conclusions

Nine near-surface soils above septic leach field systems were studied to understand microbial presence, abundance, and diversity. Leach field soils resembled control lawn soils, suggesting that the leach field pipes are far enough below surface to have little impact on the near surface GHG cycling community. Populations harboring

mcrA, *pmoA* *cnorB*, and typical *nosZ* genes are more abundant in surface soils (0 - 4 inches) than subsurface soils (4 - 8 inches). VWC was a major driver of microbial community structure as well as GHG fluxes in this study, however due to the limited temperature range of this study it is unclear whether temperature could likewise be a significant driver of community structure. Atypical methanotrophs (n-damo and ANME-2D) and nitrous oxide (*Anaeromyxobacter* and *Chloroflexi*) consuming populations are present in near surface soils and need to be further studied to understand their relative contribution to GHG consumption.

Acknowledgements:

This work was supported by the New York State Water Resources Institute and the New York State Department of Environmental Conservation as well as the Cornell Cross-Scale Biogeochemistry & Climate IGERT Program under National Science Foundation (Grant No. 1069193). The authors would like to thank Mike Jetten and Annika Vaksmaa from Radboud Universiteit for the plasmid containing the 16S rRNA gene insert of n-damo like bacteria as well as Bridget Hegarty for primer design of the atypical *nosZ* primer sets.

References

- Angel, R., Claus, P., Conrad, R., 2012. Methanogenic archaea are globally ubiquitous in aerated soils and become active under wet anoxic conditions. *ISME J.* 6, 847–62. <https://doi.org/10.1038/ismej.2011.141>
- Angnes, G., Nicoloso, R.S., da Silva, M.L.B., de Oliveira, P.A. V, Higarashi, M.M., Mezzari, M.P., Miller, P.R.M., 2013. Correlating denitrifying catabolic genes with N₂O and N₂ emissions from swine slurry composting. *Bioresour. Technol.* 140, 368–75. <https://doi.org/10.1016/j.biortech.2013.04.112>
- Beal, E.J., House, C.H., Orphan, V.J., 2009. Manganese- and iron-dependent marine methane oxidation. *Science* 325, 184–7. <https://doi.org/10.1126/science.1169984>
- Billings, S.A., Tiemann, L.K., 2014. Warming-induced enhancement of soil N₂O efflux linked to distinct response times of genes driving N₂O production and consumption. *Biogeochemistry* 119, 371–386. <https://doi.org/10.1007/s10533-014-9973-2>
- Bourne, D.G., McDonald, I.R., Murrell, J.C., 2001. Comparison of pmoA PCR primer sets as tools for investigating methanotroph diversity in three Danish soils. *Appl. Environ. Microbiol.* 67, 3802–9.
- Braker, G., Tiedje, J.M., 2003. Nitric oxide reductase (norB) genes from pure cultures and environmental samples. *Appl. Environ. Microbiol.* 69, 3476–83.
- Cai, Y., Zheng, Y., Bodelier, P.L.E., Conrad, R., Jia, Z., 2016. Conventional methanotrophs are responsible for atmospheric methane oxidation in paddy soils. *Nat. Commun.* 7, 11728. <https://doi.org/10.1038/ncomms11728>
- Caporaso, J.G., Kuczynski, J., Stombaugh, J., Bittinger, K., Bushman, F.D., Costello, E.K., Fierer, N., Peña, A.G., Goodrich, J.K., Gordon, J.I., Huttley, G.A., Kelley,

- S.T., Knights, D., Koenig, J.E., Ley, R.E., Lozupone, C.A., McDonald, D., Muegge, B.D., Pirrung, M., Reeder, J., Sevinsky, J.R., Turnbaugh, P.J., Walters, W.A., Widmann, J., Yatsunenko, T., Zaneveld, J., Knight, R., 2010. QIIME allows analysis of high-throughput community sequencing data. *Nat. Methods* 7, 335–336. <https://doi.org/10.1038/nmeth.f.303>
- Chowdhury, T.R., Dick, R.P., 2013. Ecology of aerobic methanotrophs in controlling methane fluxes from wetlands. *Appl. Soil Ecol.* 65, 8–22. <https://doi.org/10.1016/j.apsoil.2012.12.014>
- Christiansen, J.R., Levy-Booth, D., Prescott, C.E., Grayston, S.J., 2016. Microbial and Environmental Controls of Methane Fluxes Along a Soil Moisture Gradient in a Pacific Coastal Temperate Rainforest. *Ecosystems* 19, 1255–1270. <https://doi.org/10.1007/s10021-016-0003-1>
- Conrad, R., 2009. The global methane cycle: recent advances in understanding the microbial processes involved. *Environ. Microbiol. Rep.* 1, 285–92. <https://doi.org/10.1111/j.1758-2229.2009.00038.x>
- Costello, A.M., Lidstrom, M.E., 1999. Molecular characterization of functional and phylogenetic genes from natural populations of methanotrophs in lake sediments. *Appl. Environ. Microbiol.* 65, 5066–74.
- Cuhel, J., Simek, M., Laughlin, R.J., Bru, D., Chèneby, D., Watson, C.J., Philippot, L., 2010. Insights into the effect of soil pH on N₂O and N₂ emissions and denitrifier community size and activity. *Appl. Environ. Microbiol.* 76, 1870–8. <https://doi.org/10.1128/AEM.02484-09>
- Dandie, C.E., Burton, D.L., Zebarth, B.J., Henderson, S.L., Trevors, J.T., Goyer, C., 2008. Changes in bacterial denitrifier community abundance over time in an agricultural field and their relationship with denitrification activity. *Appl. Environ. Microbiol.* 74, 5997–6005. <https://doi.org/10.1128/AEM.00441-08>

- Dandie, C.E., Miller, M.N., Burton, D.L., Zebarth, B.J., Trevors, J.T., Goyer, C.,
2007. Nitric oxide reductase-targeted real-time PCR quantification of denitrifier
populations in soil. *Appl. Environ. Microbiol.* 73, 4250–8.
<https://doi.org/10.1128/AEM.00081-07>
- Dedysh, S.N., Dunfield, P.F., Derakshani, M., Stubner, S., Heyer, J., Liesack, W.,
2003. Differential detection of type II methanotrophic bacteria in acidic peatlands
using newly developed 16S rRNA-targeted fluorescent oligonucleotide probes.
FEMS Microbiol. Ecol. 43, 299–308. [https://doi.org/10.1111/j.1574-
6941.2003.tb01070.x](https://doi.org/10.1111/j.1574-6941.2003.tb01070.x)
- Diaz-Valbuena, L.R., Leverenz, H.L., Cappa, C.D., Tchobanoglous, G., Horwath,
W.R., Darby, J.L., 2011. Methane, carbon dioxide, and nitrous oxide emissions
from septic tank systems. *Environ. Sci. Technol.* 45, 2741–7.
<https://doi.org/10.1021/es1036095>
- Edgar, R.C., 2010. Search and clustering orders of magnitude faster than BLAST.
Bioinformatics 26, 2460–2461. <https://doi.org/10.1093/bioinformatics/btq461>
- Ettwig, K.F., Butler, M.K., Le Paslier, D., Pelletier, E., Mangenot, S., Kuypers,
M.M.M., Schreiber, F., Dutilh, B.E., Zedelius, J., de Beer, D., Gloerich, J.,
Wessels, H.J.C.T., van Alen, T., Luesken, F., Wu, M.L., van de Pas-Schoonen,
K.T., Op den Camp, H.J.M., Janssen-Megens, E.M., Francoijs, K.-J.,
Stunnenberg, H., Weissenbach, J., Jetten, M.S.M., Strous, M., 2010. Nitrite-
driven anaerobic methane oxidation by oxygenic bacteria. *Nature* 464, 543–8.
<https://doi.org/10.1038/nature08883>
- Ettwig, K.F., van Alen, T., van de Pas-Schoonen, K.T., Jetten, M.S.M., Strous, M.,
2009. Enrichment and molecular detection of denitrifying methanotrophic
bacteria of the NC10 phylum. *Appl. Environ. Microbiol.* 75, 3656–62.
<https://doi.org/10.1128/AEM.00067-09>

- Fish, J.A., Chai, B., Wang, Q., Sun, Y., Brown, C.T., Tiedje, J.M., Cole, J.R., 2013. FunGene: the functional gene pipeline and repository. *Front. Microbiol.* 4, 291. <https://doi.org/10.3389/fmicb.2013.00291>
- Freitag, T.E., Prosser, J.I., 2009. Correlation of methane production and functional gene transcriptional activity in a peat soil. *Appl. Environ. Microbiol.* 75, 6679–87. <https://doi.org/10.1128/AEM.01021-09>
- Freitag, T.E., Toet, S., Ineson, P., Prosser, J.I., 2010. Links between methane flux and transcriptional activities of methanogens and methane oxidizers in a blanket peat bog. *FEMS Microbiol. Ecol.* 73, 157–65. <https://doi.org/10.1111/j.1574-6941.2010.00871.x>
- Friedrich, M.W., 2005. Methyl-Coenzyme M Reductase Genes: Unique Functional Markers for Methanogenic and Anaerobic Methane-Oxidizing Archaea. *Methods Enzymol.* 397, 428–442.
- Hallam, S.J., Putnam, N., Preston, C.M., Detter, J.C., Rokhsar, D., Richardson, P.M., DeLong, E.F., 2004. Reverse methanogenesis: testing the hypothesis with environmental genomics. *Science* 305, 1457–62. <https://doi.org/10.1126/science.11100025>
- Hallin, S., Jones, C.M., Schloter, M., Philippot, L., 2009. Relationship between N-cycling communities and ecosystem functioning in a 50-year-old fertilization experiment. *ISME J.* 3, 597–605. <https://doi.org/10.1038/ismej.2008.128>
- Haroon, M.F., Hu, S., Shi, Y., Imelfort, M., Keller, J., Hugenholtz, P., Yuan, Z., Tyson, G.W., 2013. Anaerobic oxidation of methane coupled to nitrate reduction in a novel archaeal lineage. *Nature* 500, 567–70. <https://doi.org/10.1038/nature12375>
- Hendriks, J., Oubrie, A., Castresana, J., Urbani, A., Gemeinhardt, S., Saraste, M., 2000. Nitric oxide reductases in bacteria. *Biochim. Biophys. Acta - Bioenerg.*

- 1459, 266–273. [https://doi.org/10.1016/S0005-2728\(00\)00161-4](https://doi.org/10.1016/S0005-2728(00)00161-4)
- Henry, S., Bru, D., Stres, B., Hallet, S., Philippot, L., 2006. Quantitative detection of the *nosZ* gene, encoding nitrous oxide reductase, and comparison of the abundances of 16S rRNA, *narG*, *nirK*, and *nosZ* genes in soils. *Appl. Environ. Microbiol.* 72, 5181–9. <https://doi.org/10.1128/AEM.00231-06>
- Hui, C., Guo, X., Sun, P., Lin, H., Zhang, Q., Liang, Y., Zhao, Y.-H., 2017. Depth-specific distribution and diversity of nitrite-dependent anaerobic ammonium and methane-oxidizing bacteria in upland-cropping soil under different fertilizer treatments. *Appl. Soil Ecol.* 113, 117–126. <https://doi.org/10.1016/j.apsoil.2017.02.005>
- IPCC, 2006. National Greenhouse Gas Inventories. Prepared by the National Greenhouse Gas Inventories Programme. Japan.
- Jung, J., Yeom, J., Kim, J., Han, J., Lim, H.S., Park, H., Hyun, S., Park, W., 2011. Change in gene abundance in the nitrogen biogeochemical cycle with temperature and nitrogen addition in Antarctic soils. *Res. Microbiol.* 162, 1018–1026. <https://doi.org/10.1016/j.resmic.2011.07.007>
- Kinnicutt, L.P., Winslow, C.-E.A., Pratt, R.W., 1919. *Sewage Disposal*, Second. ed. John Wiley & Sons, Inc., New York.
- Klindworth, A., Pruesse, E., Schweer, T., Peplies, J., Quast, C., Horn, M., Glöckner, F.O., 2013. Evaluation of general 16S ribosomal RNA gene PCR primers for classical and next-generation sequencing-based diversity studies. *Nucleic Acids Res.* 41, e1. <https://doi.org/10.1093/nar/gks808>
- Knief, C., 2015. Diversity and Habitat Preferences of Cultivated and Uncultivated Aerobic Methanotrophic Bacteria Evaluated Based on *pmoA* as Molecular Marker. *Front. Microbiol.* 6, 1346. <https://doi.org/10.3389/fmicb.2015.01346>
- Le Mer, J., Roger, P., 2001. Production, oxidation, emission and consumption of

- methane by soils: A review. *Eur. J. Soil Biol.* 37, 25–50.
[https://doi.org/10.1016/S1164-5563\(01\)01067-6](https://doi.org/10.1016/S1164-5563(01)01067-6)
- Lee, H.J., Kim, S.Y., Kim, P.J., Madsen, E.L., Jeon, C.O., 2014. Methane emission and dynamics of methanotrophic and methanogenic communities in a flooded rice field ecosystem. *FEMS Microbiol. Ecol.* 88, 195–212.
<https://doi.org/10.1111/1574-6941.12282>
- Leverenz, H.L., Tchobanoglous, G., Darby, J.L., 2010. Evaluation of GHG Emissions from Septic Systems.
- Levy-Booth, D.J., Prescott, C.E., Grayston, S.J., 2014. Microbial functional genes involved in nitrogen fixation, nitrification and denitrification in forest ecosystems. *Soil Biol. Biochem.* <https://doi.org/10.1016/j.soilbio.2014.03.021>
- Li, H., 2013. Aligning sequence reads, clone sequences and assembly contigs with BWA-MEM.
- Li, H., Handsaker, B., Wysoker, A., Fennell, T., Ruan, J., Homer, N., Marth, G., Abecasis, G., Durbin, R., 1000 Genome Project Data Processing Subgroup, 2009. The Sequence Alignment/Map format and SAMtools. *Bioinformatics* 25, 2078–2079. <https://doi.org/10.1093/bioinformatics/btp352>
- Lozupone, C., Knight, R., 2005. UniFrac: a new phylogenetic method for comparing microbial communities. *Appl. Environ. Microbiol.* 71, 8228–35.
<https://doi.org/10.1128/AEM.71.12.8228-8235.2005>
- Luesken, F.A., Zhu, B., van Alen, T.A., Butler, M.K., Diaz, M.R., Song, B., Op den Camp, H.J.M., Jetten, M.S.M., Ettwig, K.F., 2011. pmoA Primers for detection of anaerobic methanotrophs. *Appl. Environ. Microbiol.* 77, 3877–80.
<https://doi.org/10.1128/AEM.02960-10>
- Luton, P.E., Wayne, J.M., Sharp, R.J., Riley, P.W., 2002. The mcrA gene as an alternative to 16S rRNA in the phylogenetic analysis of methanogen populations

- in landfill. *Microbiology* 148, 3521–3530.
- Ma, K., Conrad, R., Lu, Y., 2012. Responses of methanogen *mcrA* genes and their transcripts to an alternate dry/wet cycle of paddy field soil. *Appl. Environ. Microbiol.* 78, 445–54. <https://doi.org/10.1128/AEM.06934-11>
- McDonald, D., Price, M.N., Goodrich, J., Nawrocki, E.P., DeSantis, T.Z., Probst, A., Andersen, G.L., Knight, R., Hugenholtz, P., 2012. An improved Greengenes taxonomy with explicit ranks for ecological and evolutionary analyses of bacteria and archaea. *ISME J.* 6, 610–8. <https://doi.org/10.1038/ismej.2011.139>
- McMurdie, P.J., Holmes, S., Kindt, R., Legendre, P., O’Hara, R., 2013. phyloseq: An R Package for Reproducible Interactive Analysis and Graphics of Microbiome Census Data. *PLoS One* 8, e61217. <https://doi.org/10.1371/journal.pone.0061217>
- McPhillips, L.E., Groffman, P.M., Schneider, R.L., Walter, M.T., 2016. Nutrient Cycling in Grassed Roadside Ditches and Lawns in a Suburban Watershed. *J. Environ. Qual.* 45, 1901. <https://doi.org/10.2134/jeq2016.05.0178>
- Meng, H., Wang, Y.-F., Chan, H.-W., Wu, R.-N., Gu, J.-D., 2016. Co-occurrence of nitrite-dependent anaerobic ammonium and methane oxidation processes in subtropical acidic forest soils. *Appl. Microbiol. Biotechnol.* 100, 7727–7739. <https://doi.org/10.1007/s00253-016-7585-6>
- Molodovskaya, M., Warland, J., Richards, B.K., Öberg, G., Steenhuis, T.S., 2011. Nitrous Oxide from Heterogeneous Agricultural Landscapes: Source Contribution Analysis by Eddy Covariance and Chambers. *Soil Sci. Soc. Am. J.* 75, 1829. <https://doi.org/10.2136/sssaj2010.0415>
- Oksanen, A.J., Blanchet, F.G., Kindt, R., Legendre, P., Minchin, P.R., Hara, R.B.O., Simpson, G.L., Soly, P., Stevens, M.H.H., Wagner, H., 2017. *Vegan: Community Ecology Package* 46–56. <https://doi.org/ISBN-0-387-95457-0>
- Orphan, V.J., House, C.H., Hinrichs, K.U., McKeegan, K.D., DeLong, E.F., 2001.

- Methane-consuming archaea revealed by directly coupled isotopic and phylogenetic analysis. *Science* 293, 484–7.
<https://doi.org/10.1126/science.1061338>
- Peirson, S.N., Butler, J.N., Foster, R.G., 2003. Experimental validation of novel and conventional approaches to quantitative real-time PCR data analysis. *Nucleic Acids Res.* 31, e73.
- Pundir, S., Martin, M.J., O'Donovan, C., UniProt Consortium, 2016. UniProt Tools, in: *Current Protocols in Bioinformatics*. John Wiley & Sons, Inc., Hoboken, NJ, USA, p. 1.29.1-1.29.15. <https://doi.org/10.1002/0471250953.bi0129s53>
- R Core Team, 2013. R: A language and environment for statistical computing.
- Raghoebarsing, A. a, Pol, A., van de Pas-Schoonen, K.T., Smolders, A.J.P., Ettwig, K.F., Rijpstra, W.I.C., Schouten, S., Damsté, J.S.S., Op den Camp, H.J.M., Jetten, M.S.M., Strous, M., 2006. A microbial consortium couples anaerobic methane oxidation to denitrification. *Nature* 440, 918–21.
<https://doi.org/10.1038/nature04617>
- Rozen, S., Skaletsky, H., 2000. Primer3 on the WWW for General Users and for Biologist Programmers. *Bioinforma. Methods Protoc.* 132, 365–386.
<https://doi.org/10.1385/1-59259-192-2:365>
- Sanford, R.A., Wagner, D.D., Wu, Q., Chee-Sanford, J.C., Thomas, S.H., Cruz-García, C., Rodríguez, G., Massol-Deyá, A., Krishnani, K.K., Ritalahti, K.M., Nissen, S., Konstantinidis, K.T., Löffler, F.E., 2012. Unexpected nondenitrifier nitrous oxide reductase gene diversity and abundance in soils. *Proc. Natl. Acad. Sci. U. S. A.* 109, 19709–14. <https://doi.org/10.1073/pnas.1211238109>
- Semrau, J., Chistoserdov, A., Lebron, J., Costello, A., Davagnino, J., Kenna, E., Holmes, A., Finch, R., Murrell, J., Lidstrom, M., 1995. Particulate methane monooxygenase genes in methanotrophs. *J. Bacteriol.* 177, 3071–3079.

- Semrau, J.D., DiSpirito, A.A., Yoon, S., 2010. Methanotrophs and copper. *FEMS Microbiol. Rev.* 34, 496–531. <https://doi.org/10.1111/j.1574-6976.2010.00212.x>
- Seo, J., Jang, I., Gebauer, G., Kang, H., 2013. Abundance of Methanogens, Methanotrophic Bacteria, and Denitrifiers in Rice Paddy Soils. *Wetlands* 34, 213–223. <https://doi.org/10.1007/s13157-013-0477-y>
- Shannon, C.E., 1948. A mathematical theory of communication. *Bell Syst. Tech. J.* 27, 379–423. <https://doi.org/10.1145/584091.584093>
- Shen, L. -d., Wu, H. -s., Gao, Z. -q., Li, J., Liu, X., 2016. Presence of diverse Candidatus Methyloirabilis oxyfera-like bacteria of NC10 phylum in agricultural soils. *J. Appl. Microbiol.* 120, 1552–1560. <https://doi.org/10.1111/jam.13119>
- Shen, L., Liu, S., He, Z., Lian, X., Huang, Q., He, Y., Lou, L., Xu, X., Zheng, P., Hu, B., 2015. Depth-specific distribution and importance of nitrite-dependent anaerobic ammonium and methane-oxidising bacteria in an urban wetland. *Soil Biol. Biochem.* 83, 43–51. <https://doi.org/10.1016/j.soilbio.2015.01.010>
- Steinberg, L.M., Regan, J.M., 2009. mcrA-targeted real-time quantitative PCR method to examine methanogen communities. *Appl. Environ. Microbiol.* 75, 4435–42. <https://doi.org/10.1128/AEM.02858-08>
- Steinberg, L.M., Regan, J.M., 2008. Phylogenetic comparison of the methanogenic communities from an acidic, oligotrophic fen and an anaerobic digester treating municipal wastewater sludge. *Appl. Environ. Microbiol.* 74, 6663–71. <https://doi.org/10.1128/AEM.00553-08>
- Tate, K.R., 2015. Soil methane oxidation and land-use change – from process to mitigation. *Soil Biol. Biochem.* 80, 260–272. <https://doi.org/10.1016/j.soilbio.2014.10.010>
- Thauer, R.K., Kaster, A.-K., Seedorf, H., Buckel, W., Hedderich, R., 2008.

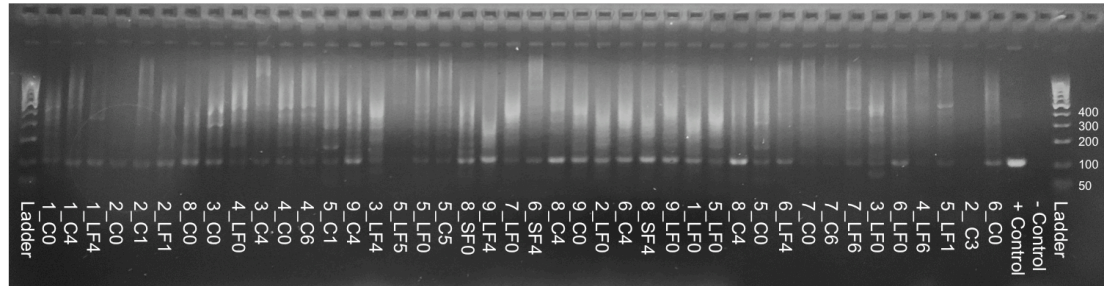
- Methanogenic archaea: ecologically relevant differences in energy conservation. *Nat. Rev. Microbiol.* 6, 579–91. <https://doi.org/10.1038/nrmicro1931>
- Thompson, J.D., Higgins, D.G., Gibson, T.J., 1994. CLUSTAL W: improving the sensitivity of progressive multiple sequence alignment through sequence weighting, position-specific gap penalties and weight matrix choice. *Nucleic Acids Res.* 22, 4673–4680. <https://doi.org/10.1093/nar/22.22.4673>
- Truhlar, A.M., Rahm, B.G., Brooks, R.A., Nadeau, S.A., Makarsky, E.T., Walter, M.T., 2016. Greenhouse Gas Emissions from Septic Systems in New York State. *J. Environ. Qual.* 45, 1153. <https://doi.org/10.2134/jeq2015.09.0478>
- US EPA, 2012. Global Anthropogenic Non-CO₂ Greenhouse Gas Emissions: 1990-2030 [WWW Document]. URL http://www.epa.gov/climatechange/Downloads/EPAactivities/EPA_Global_Non_CO2_Projections_Dec2012.pdf (accessed 4.13.15).
- USEPA, 2002. Decentralized Wastewater Systems Technology Fact Sheets [WWW Document]. URL <https://www.epa.gov/septic/onsite-wastewater-treatment-and-disposal-systems> (accessed 12.16.16).
- Vaksmaa, A., Lüke, C., van Alen, T., Valè, G., Lupotto, E., Jetten, M.S.M., Ettwig, K.F., 2016. Distribution and activity of the anaerobic methanotrophic community in a nitrogen-fertilized Italian paddy soil. *FEMS Microbiol. Ecol.* 92, fiw181. <https://doi.org/10.1093/femsec/fiw181>
- Wang, Q., Garrity, G.M., Tiedje, J.M., Cole, J.R., 2007. Naive Bayesian classifier for rapid assignment of rRNA sequences into the new bacterial taxonomy. *Appl. Environ. Microbiol.* 73, 5261–7. <https://doi.org/10.1128/AEM.00062-07>
- Wang, Y., Zhu, G., Harhangi, H.R., Zhu, B., Jetten, M.S.M., Yin, C., Op den Camp, H.J.M., 2012. Co-occurrence and distribution of nitrite-dependent anaerobic ammonium and methane-oxidizing bacteria in a paddy soil. *FEMS Microbiol.*

- Lett. 336, 79–88. <https://doi.org/10.1111/j.1574-6968.2012.02654.x>
- Weber, H.S., Habicht, K.S., Thamdrup, B., 2017. Anaerobic Methanotrophic Archaea of the ANME-2d Cluster Are Active in a Low-sulfate, Iron-rich Freshwater Sediment. *Front. Microbiol.* 8, 619. <https://doi.org/10.3389/fmicb.2017.00619>
- Wilkins, D., Lu, X.-Y., Shen, Z., Chen, J., Lee, P.K.H., 2015. Pyrosequencing of *mcrA* and archaeal 16S rRNA genes reveals diversity and substrate preferences of methanogen communities in anaerobic digesters. *Appl. Environ. Microbiol.* 81, 604–13. <https://doi.org/10.1128/AEM.02566-14>
- Winneberger, J.H.T., 1983. Amazon.com: Septic-Tank Systems: A Consultant's Toolkit - The Septic Tank, Vol. II. ed. Ann Arbor Science, Ann Arbor.
- Wu, M.L., Ettwig, K.F., Jetten, M.S.M., Strous, M., Keltjens, J.T., van Niftrik, L., 2011. A new intra-aerobic metabolism in the nitrite-dependent anaerobic methane-oxidizing bacterium *Candidatus "Methyloirabilis oxyfera"*. *Biochem. Soc. Trans.* 39, 243–8. <https://doi.org/10.1042/BST0390243>

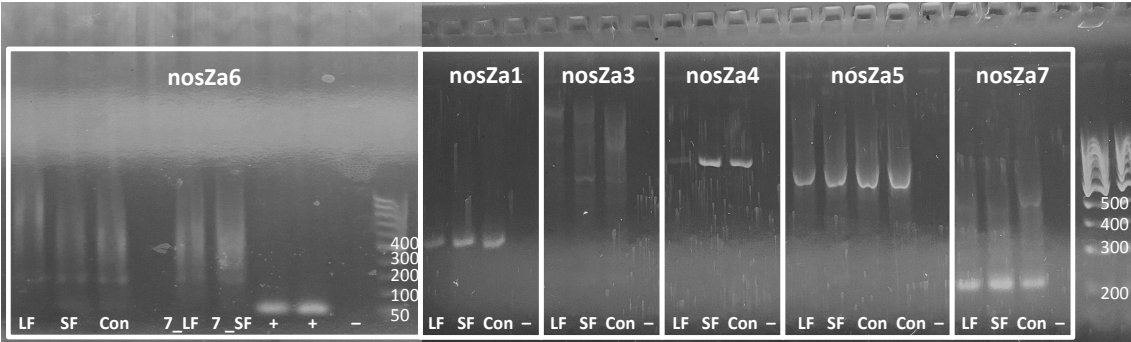
Chapter 2: Supplemental Information

SI Table 2.1. Primer sequences and length, amplicon size, and annealing temperatures for genes of 'atypical' methanotrophs and denitrifiers. Denitrifier groups based on Sanford et al., 2012.

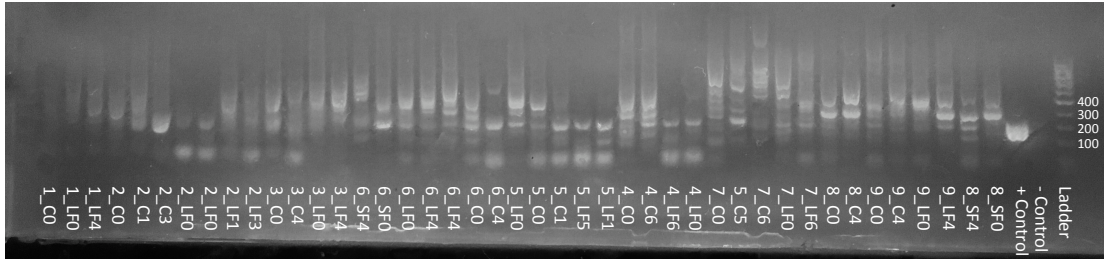
Target Microbial Community	Gene	Represented Phylum or Class	Primer	Primer Length (bp)	Sequence (5'-3')	Amplicon Length (bp)	Annealing Temperature (T _a , °C)	Reference
n-damo Bacteria	16S	NC10	p2f	14	GGGGAAGCTGCCAGCGTCAAG	291	63	Eitwig et al., 2009
			p2r	14	CTCAGCGACTTCGAGTACAG			
'Atypical' Denitrifiers	nosZ	<i>Bacteroidetes</i>	nosZa1F	23	ACATGACCKMATHCGCTCGCAC	118	57	This study
			nosZa1R	20	AAKCGTGGGGYACRTCCCA			
		<i>Aquificae, Chlorobi</i>	nosZa2F	29	TTCTWYACWTCKTAYAYACRGARCAGGC	95	61	This study
			nosZa2R	17	TTCCAGTTDACYGCMGC			
		<i>Firmicutes</i>	nosZa3F	23	GAYGARGAYATYACCCAYGGHIT	140	53	This study
			nosZa3R	17	GCYGARCAAGAGTISGT			
			nosZa4F	20	AAACKATCAITGAARGAGCGAAA			
			nosZa4R	26	CTTGGCTGRTAAGTYTTAGC			
		<i>Epsilonproteobacteria</i>	nosZa5F	26	TYGARHTVCKCCHTATATGCARGAT	136	54	This study
			nosZa5R	27	CCDGGTTCRAAHGGAGG			
			nosZa6F	23	CAGTACCAGGTCAAGGCYGCCGA			
			nosZa6R	34	TCTTTGGCGCGTTTCTGCTCSAGGWAGGTTTGGC			
		<i>Chloroflexi</i>	nosZa7F	20	GGCCGCTBCTGCCRCARA	120	60	This study
			nosZa7R	20	ATCTGGGCRTAGTCCGGYTC			
nosZa9F	17		CGGCGTGGACKTCYCGC					
<i>Deltaproteobacteria</i>	nosZa9R	20	CTCCCGGGHGAAGKCCCTTG	162	62	This study		



SI Figure 2.1. PCR reaction results for the nosZa9 primer set shows products for all but 3 samples and the negative control (LF = Leach Field, SF = Sand Filter, C = Control, - = negative control, + = positive control). A subset of samples were sequenced to confirm the product as related to *Anaeromyxobacter*-like nosZ genes.



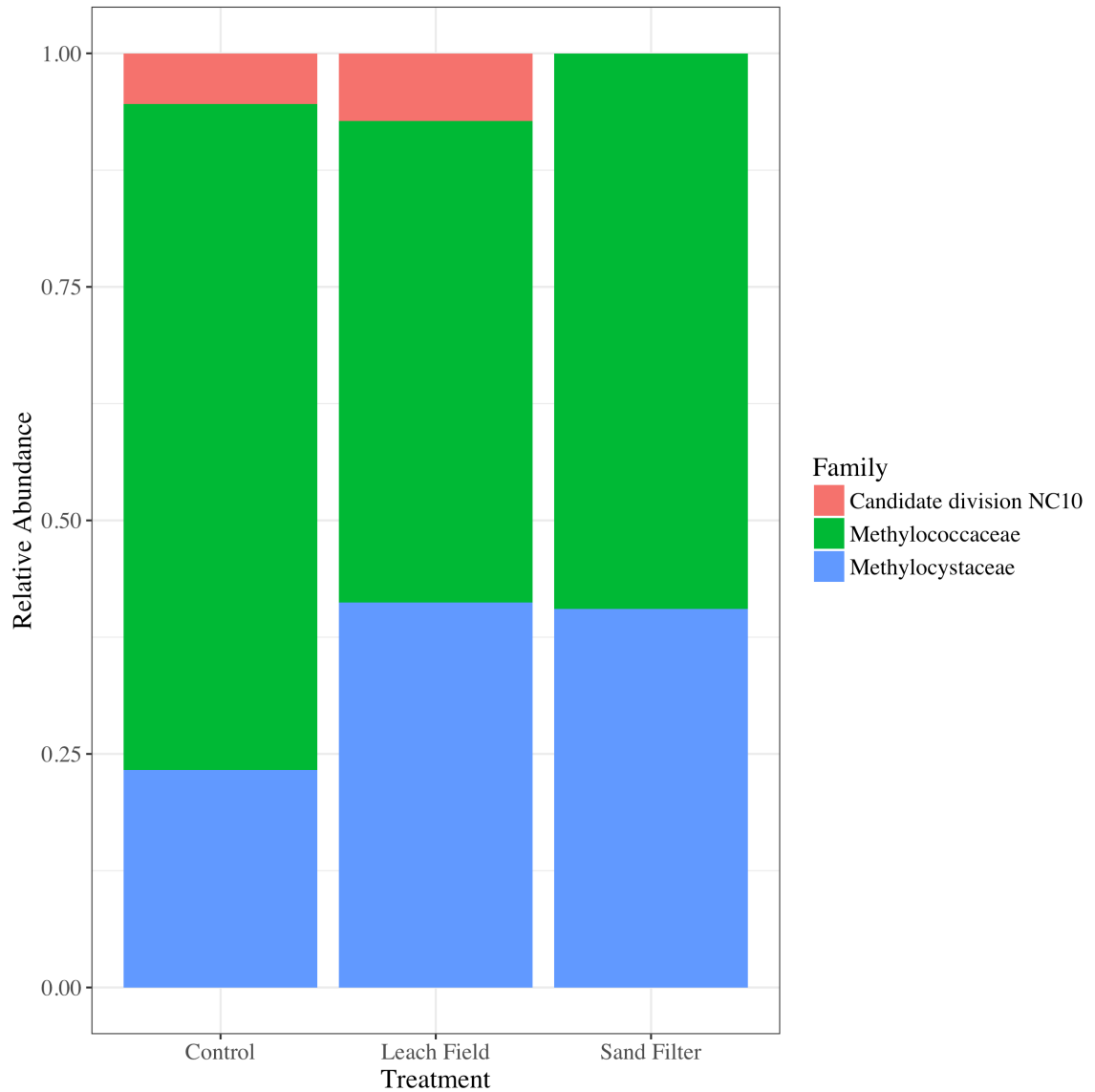
SI Figure 2.2. PCR reaction results for 'atypical' nosZ primer sets nosZa1, nosZa2, nosZa3, nosZa4, nosZa5, nosZa6, and nosZa7 for pooled samples (LF = Leach Field, SF = Sand Filter, Con = Control, - = negative control, + = positive control). Only primer set nosZa7 had a product of the correct size indicating the presence of denitrifiers from the *Chloroflexi* phylum.



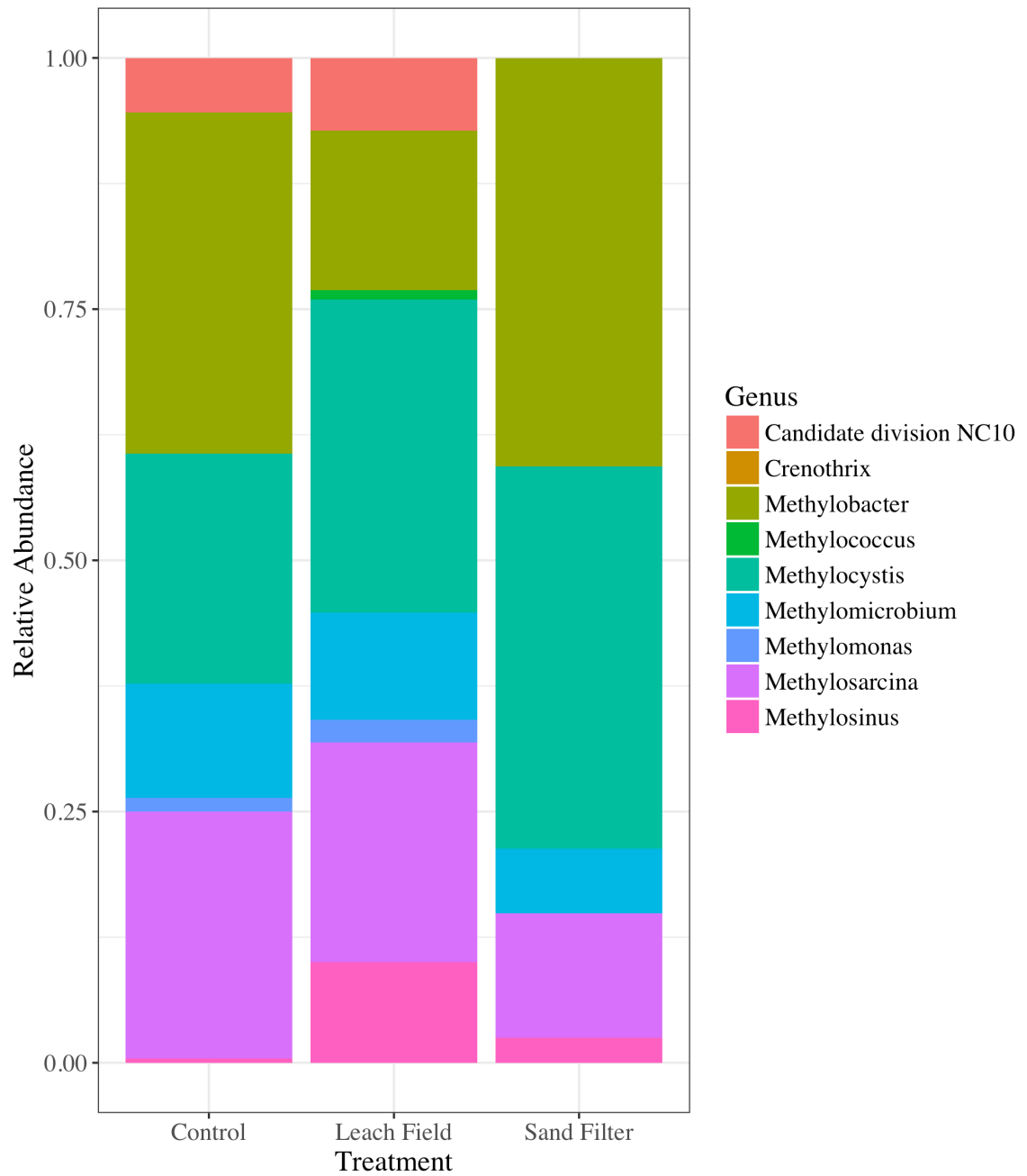
SI Figure 2.3. PCR reaction results for primer set p2f/p2r targeting the 16S rRNA gene of anaerobic methanotrophs from the NC10 phylum. Multiple banding and nonspecific products were seen for most samples. Products of the correct size were submitted for sequencing and confirmed the presence of *Methylomirabilis*-like bacteria in leach field soils.

SI Table 2.2. Alpha diversity as measured by Chao1 and Shannon indices, based on total reads and number of OTUs shown.

Samples	Total reads	OTUs	Chao	Shannon
Leach Field	326,499	6,941	7965	7.19
Sand Filter	191,212	4,475	9922	7.30
Control	529,871	11,240	9491	7.32



SI Figure 2.4. Relative abundance of *pmoA* reads assigned at the family level by treatment.



SI Figure 2.5. Relative abundance of *pmoA* reads at the genus level, grouped by treatment.

CHAPTER 3

MICROBIAL COMMUNITIES CONTROLLING METHANE AND NUTRIENT CYCLING IN LEACH FIELD SOILS

Abstract

Septic systems inherently rely on microbial communities in the septic tank and leach field to attenuate pollution from household sewage. Operating conditions of septic leach field systems, especially the degree of water saturation, are likely to impact microbial biogeochemical cycling, including carbon (C), nitrogen (N), and phosphorus (P), as well as greenhouse gas (GHG) emissions to the atmosphere. To study the impact of flooding on microbial methane (CH₄) and nutrient cycling, two leach field soil columns were constructed. One system was operated as designed and the other was operated in both flooded and well-maintained conditions. CH₄ emissions were significantly higher in flooded soils (with means between 0.047 and 0.33 g CH₄ m⁻² d⁻¹) as compared to well-drained soils (means between -0.0025 and 0.004 g CH₄ m⁻² d⁻¹). Subsurface CH₄ profiles were also elevated under flooded conditions and peaked near the wastewater inlet. Gene abundances of *mcrA*, a biomarker for methanogens, were also greatest near the wastewater inlet. In contrast, gene abundances of *pmoA*, a biomarker for methanotrophs, were greatest in surface soils at the interface of CH₄ produced subsurface and atmospheric oxygen. 16S rRNA, *mcrA*, and *pmoA* amplicon library sequencing revealed microbial community structure in the soil columns differed from that of the original soils and was driven largely by CH₄ fluxes and soil VWC. Additionally, active microbial populations differed from those present at the gene level. Flooding did not appear to affect N or P removals in the soil

columns (between 75 and 99% removal). COD removal was variable throughout the experiment, and was negatively impacted by flooding. Our study shows septic system leach field soils are dynamic environments where CH₄ and nutrients are actively cycled by microbial populations. Our results suggest proper siting, installation, and routine maintenance of leach field systems is key to reducing the overall impact of these systems on water and air quality.

3.1 Introduction

The World Health Organization (WHO) estimates 1 in 6 people globally rely on septic systems to treat domestic wastewater on-site (WHO, 2017). Inexpensive solutions for on-site wastewater treatment (OWTS), such as septic systems, are popular in low-resource areas where they account for 56% of on-site improved sanitation in urban settings and 38% in rural settings (WHO, 2017). Decentralized systems are also prevalent in the U.S. and Europe where approximately 25% of U.S. and 26% of European households rely on septic systems (US EPA, 2012; Williams et al., 2012). Septic systems can achieve treatment levels comparable to larger, energy-intensive wastewater treatment plants while maintaining many of the same public health and environmental benefits (USEPA, 2002). Despite the popularity of these low-cost OWTSs, little is known about their impact on the environment. Specifically, how failing septic leach field systems impact both air and water quality is poorly understood.

Because septic systems require infrequent service and are inconspicuous by nature, failures can remain unnoticed and un-repaired. Failing systems causing ground and/or surface water contamination can be difficult to identify and diagnose. Few permitting agencies in the U.S. and Europe conduct inspections of systems after installation (Withers et al., 2014). Consequently, the number of failing septic systems in the U.S. and Europe is unknown and even less data on system failures is available for low-resource countries. Currently, there are no requirements for states in the U.S. to collect data on septic system failures and those that do create their own definition of “failure,” ranging from “sewage back-up” to “surface and/or ground water

contamination” (USEPA, 2002). Many leach field systems fail by flooding due to improper installation in locations with poorly-draining soils, steep slopes, or high ground water tables (USEPA, 2002). Several studies have examined septic systems’ impact on groundwater; however, to our knowledge no previous work has compared the air and water quality impacts of a failing system to those of a well-maintained system (Cogger and Carlile, 1984; Katz et al., 2011; Richards et al., 2016; Withers et al., 2014).

In terms of greenhouse gas (GHG) emissions, well-maintained septic systems have been estimated to release between 0.22 and 0.27 tonne CO₂-equivalents (CO₂e) capita⁻¹ year⁻¹ to the environment, with leach field emissions representing roughly 20% of those emissions (Diaz-Valbuena et al., 2011; Truhlar et al., 2016). The percentage of failing systems in the U.S. could range anywhere from 0.5% to 70% by state, based on a USEPA (2002) report, while in Europe estimates based on watershed surveys suggest failures are as high as 70% (Withers et al., 2014). If systems fail at the high end of these estimates, their contributions to GHG emissions as well as their impacts on groundwater could be significantly greater than previously thought.

Leach field systems rely on soil microbial communities to remove nutrients from septic effluent and as a consequence serve to prevent eutrophication of down gradient waterways. Additionally, these communities may be responsible for significant mitigation of GHG emissions (mainly in the form of methane (CH₄) and nitrous oxide (N₂O)) from septic systems. Microorganisms involved in CH₄ production (methanogens) and consumption (methanotrophs) can be studied using the functional genes *mcrA* and *pmoA*, respectively, and have previously been shown to

correlate with CH₄ emission patterns from soil systems (Freitag et al., 2010; Lee et al., 2014). Flooded leach field soils likely support microbial communities distinct from those of a well-maintained system, which may lead to significant differences in observed CH₄ emissions.

As we attempt to better evaluate OWTSSs, it is important to determine how ‘failing’ systems impact air and water quality. The objective of this study was to compare two lab-scale septic leach field soil columns, under either well-maintained or flooded operation, in four categories: (1) measured surface CH₄ fluxes; (2) measured subsurface CH₄ concentration profiles, (3) distribution and activity of key microbial populations with a particular focus on those involved in CH₄ cycling; (4) measured effectiveness at removing nutrients from wastewater (organic C, N, P).

3.2 Methods

3.2.1 Soil column construction

Two soil columns were designed to meet the minimum spacing requirements specified in the New York State Department of Health and Bureau of Water Supply Protection's *Onsite Wastewater Treatment Systems Design Manual* (2012) (Figure 3.1). Soil columns were constructed in August 2015 from a 1.2 m section of PVC pipe (Schedule 80, 8 cm ID) filled with soil excavated from an operational leach field system (Site 7 in Fernández-Baca et al. (2018) and Truhlar et al. (2016)). The leach field system had well-draining soils and had been operational for 10 years with no history of flooding and no observed biomat at the time of excavation. Representative samples were taken for soils above and below the leach field lateral and submitted to Cornell Nutrient Analysis Laboratory (CNAL) for analysis. Soils were relatively dry

loam/silt loam with circumneutral pH and bulk densities of 1.19 and 1.39 g ml⁻¹ for above and below the lateral, respectively (SI Table 3.1). The top 24 cm of soil were collected intact from above the existing leach field system. Approximately 5 cm of gravel was then back-filled into the column before inserting the dosing system. The wastewater dosing structure, hereafter referred to as the inlet, was constructed from a 2.5-cm ID PVC pipe with 0.64 cm holes drilled 5 cm apart. The structure was inserted through a pre-dilled hole in the soil column and caulked to prevent leaks. An additional 15 cm of gravel was added to mimic the construction of an in-field leach field system. To ensure the soil column microbial communities were acclimated to receiving septic tank effluent, they were back-filled with soil excavated from below the laterals of the operational system.

Rhizon pore water samplers (Rhizosphere, Cat. No. 19.21.23F) were inserted at approximately 7.6, 23, 46, 71, and 100 cm below the soil surface (Figure 3.1). Soil volumetric water content (VWC) was continuously monitored with EC-5 Soil Moisture Sensors (Decagon Devices, Cat. No. 40593) inserted at 15 cm and 64 cm below the soil surface (above and below the inlet, respectively) using the Em-50 5-channel data logger for data collection (Decagon Devices, Cat. No. 40800).

3.2.2 Soil column operation

Soil columns were dosed with a synthetic wastewater mix (SI Table 3.2) adapted from Aiyuk and Verstraete (2004) to achieve a waste stream chemically comparable to septic tank effluent based on reported effluent characteristics in Cooper et al. (2015). The synthetic wastewater did not have large particulate matter but had total suspended solids (TSS) of approximately 200 mg l⁻¹. Low TSS is expected in

settled water leaving the septic tank and Cooper et al. (2015) reported TSS values between 18 and 89 mg l⁻¹ for septic effluent. Although the synthetic wastewater has higher TSS the particle size distribution is likely more homogenous than authentic effluent with lower mean particle sizes leading to greater infiltration in the soil columns. Wastewater was sparged with N₂ for 1 hour and stored in a sealed, collapsible 10 L carboy under an N₂ headspace at 4°C in the dark, immediately adjacent to the soil columns which were held at temperature (25°C) throughout the experiment.

Both soil columns received wastewater through the inlet using computer controlled peristaltic pumps and were operated as either flooded or well-maintained systems (Figure 3.1). Experimental columns were operated from August 2015 until August 2016 (13 months) and were dosed 6 times daily for a total of 103.5 ml d⁻¹ (approximately 24.4 l m⁻² d⁻¹) representing a daily COD load of 62.1 mg COD d⁻¹. The systems were operated within the dosing range of typical leach field systems specified by New York State, which range from 18.3 to 48.9 l m⁻² d⁻¹ (NYS Depart. of Health, 2012). Peristaltic pumps were used to pump out effluent via a 1.3 cm hole drilled at the bottom of the column fitted with a push-to-connect and collected in 1 l Nalgene bottles.

In the first phase of monitoring referred to hereafter as Phase I (February 2016 to August 2016), Column A was operated under continuously flooded conditions while Column B was well-maintained. This was achieved by dosing wastewater until there was visible pooling at the soil surface in both columns at which point the effluent pump was turned on for Column B only to drain the system until VWC in the shallow

sensor registered ‘dry’ soils ($0.1 \text{ m}^3 \text{ m}^{-3}$). In Phase II, starting August 2016, the water table in Column B was increased to mimic the flooded conditions in Column A by continuously pumping wastewater into Column B until flooding was observed at the soil surface. Both columns were remained flooded for 6 months. In Phase III, starting February 2017, Column B was drained over a period of several months returning to a well-maintained state.

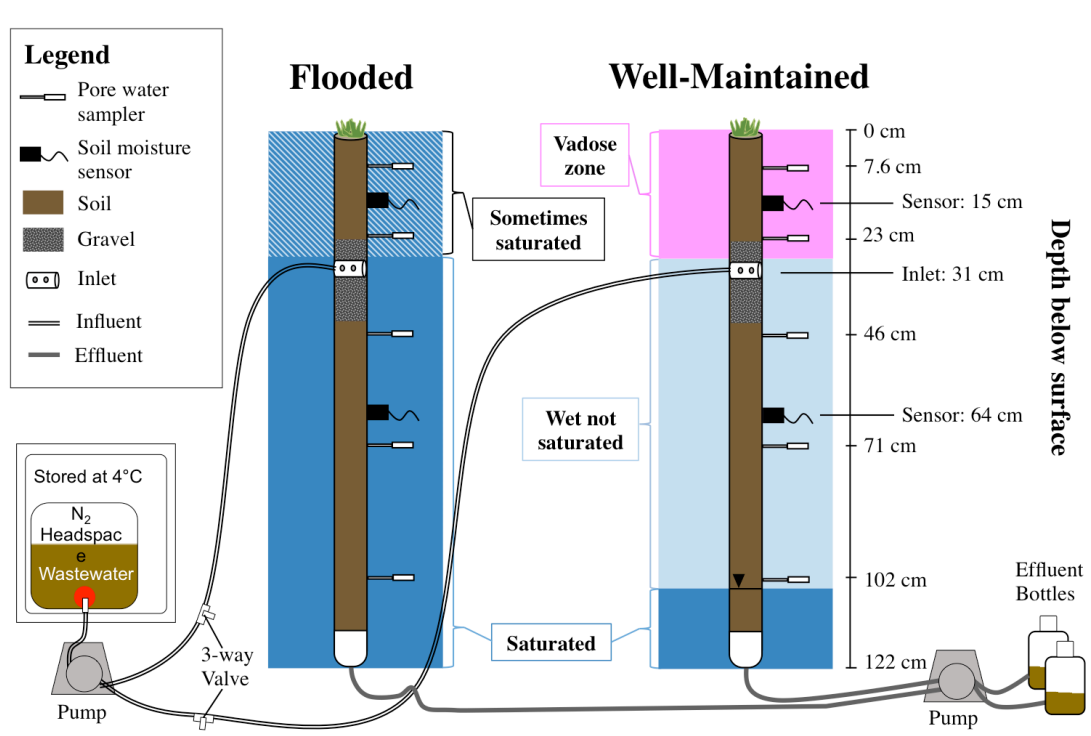


Figure 3.1. Experimental lab column set-up constructed using soil from an active leach field system. Figure shows flooded vs. well-maintained operation and depths of pore water samplers, soil moisture sensors, and distribution (inlet) pipe. Soil columns were dosed with synthetic wastewater by peristaltic pumps. Effluent wastewater was pumped out from the base of the soil columns and into 1 l Nalgene bottles.

3.2.3. Surface methane flux measurements

Soil flux measurements were taken following a modified field flux chamber method established by Molodovskaya et al. (2011). Briefly, PVC caps fitted to the soil columns' were adapted to hold a septum for gas sampling as well as a 23-gauge needle

to provide headspace venting. After caps were placed over each column, 5 ml headspace gas samples were taken through the septa every 10 minutes for 30 minutes and injected into pre-sealed 9 ml vials. Gas samples were analyzed within 12 hours via gas chromatography, using a flame ionization detector (Hewlett-Packard 5890 Series) and a 2.4 m long 3/10 cm-ID 60/80 Carbopack B column (Supelco). Gas fluxes were determined by fitting a linear regression to CH₄ concentrations over time, the regression slope was taken as the rate of gas flux and was then divided by the soil column surface area for a per m² flux rate. Boxplots used to visualize flux data define the inter quartile range (IQR) as between 25% and 75% of data. Outliers were defined as measurements less than or greater than 1.5 times the IQR and were not included in testing significance as they likely represent ebullition events. T-tests were used to test significance of observed differences in CH₄ emissions between operation phases for each column using a 95% confidence interval.

3.2.4 Influent, effluent, and pore water sampling

Influent, effluent, and pore water samples were taken biweekly. Influent was sampled by switching the position of a 3-way valve leading to each inlet to allow sample collection in 15 ml centrifuge tubes. Fresh effluent samples were collected directly from the 1 l Nalgene bottles. 10 ml pore water samples were collected via the installed samplers at each depth (Figure 3.1). All water samples were filtered and stored at 4°C for later nutrient analysis.

Pore water dissolved CH₄ concentrations were measured immediately after sampling by injecting 5 ml of sample into a pre-sealed 9 ml vial, shaking for 5 minutes, and sampling the headspace for GC-FID analysis. Dissolved CH₄

concentrations were back-calculated using Henry's Constant for CH₄ partitioning in water at room temperature (25°C). All water samples were analyzed for ammonium (NH₄⁺), nitrate/nitrite (NO₃⁻ and NO₂⁻), soluble reactive phosphorus (PO₄³⁻), and chemical oxygen demand (COD). Nutrient concentrations were determined using published colorimetric assays modified for a Tecan Infinite M200 Pro microplate reader: ammonium (Bower and Holm-Hansen, 1980); nitrate/nitrite (Miranda et al., 2001); SRP (APHA, 2012). Influent and effluent samples were analyzed for COD removal using the CHEMetrics kit (Cat. No. K-7365). All samples were analyzed in duplicate and monthly averages were calculated for each column influent and effluent.

3.2.5 Soil sampling, nucleic acid extractions, and qPCR

Soils were sampled three times throughout the experiment within a 3 cm vertical distance of each pore water sampler. A flame-sterilized drill bit was used to drill through the PVC to take soil samples with a sterile 0.3 cm diameter corer approximately 6 cm long. After sampling, the hole was flushed with N₂ gas to displace ambient oxygen and sealed with a rubber stopper then caulked to ensure a water and air-tight seal. Soil samples were manually homogenized and subsampled for duplicate nucleic acid extractions and gravimetric dry weight determination. Dry weight determination was used to estimate the dry weight per wet weight of each soil sample used in extractions and was done by drying approximately 1g soil samples at 105°C (±1°C) for 24 h.

Nucleic acids were extracted using the RNeasy PowerSoil Total RNA kit and RNeasy PowerSoil DNA Elution kit (Qiagen). Approximately 2 g of soil were extracted following the manufacturer's protocol. All samples were spiked with 4 µl of

1×10^9 copies μl^{-1} of luciferase RNA (Promega) as an internal control prior to cell lysis. DNA was quantified using the Quant-iT PicoGreen dsDNA assay (Molecular Probes, Eugene, OR) and quality checked with a NanoDrop spectrophotometer (Nanodrop ND-1000, ThermoScientific, Waltham, MA).

Following RNA isolation, the RQ1 RNase-free DNase kit (Promega) was used to remove contaminating DNA following manufacturer's instructions. RNA concentrations were measured using the Quant-it RNA assay kit (Invitrogen). cDNA was synthesized from the DNase-treated RNA using the Advanced iScript cDNA synthesis kit (Bio-Rad) according to manufacturer's instructions.

QPCR reactions were run in triplicate using a total reaction volume of 25 μl . Each reaction was comprised of 2X iQ SYBR Green Supermix (Bio-Rad), 17.5 pmol of primer, and 3 μl of template DNA (with diluted concentrations of approximately 10 ng μl^{-1}). Thermal cycling was conducted on an iCycler IQ (Bio-Rad) following published protocols for the selected primers for *mcrA*, *pmoA*, and 16S rRNA genes (SI Table 3.3) (Costello and Lidstrom, 1999; Ferris et al., 1996; Luton et al., 2002; Steinberg and Regan, 2009). Quantification analysis was done using Ct values from the iCycler IQ software. Melt curve analyses were conducted on all products and a subset of samples was sent for Sanger sequencing to confirm amplification of target genes (data not shown).

3.2.6 Illumina sequencing of 16S rRNA, *mcrA* and *pmoA* libraries

Duplicate DNA samples from each column at the 7.6-cm depth from two sampling dates were selected for high throughput sequencing community analysis. Gene amplicon libraries for *mcrA* and *pmoA* were created using the qPCR primers

with added adapters for Illumina sequencing compatibility. 16S rRNA amplicon libraries were created by amplifying the hypervariable V3-V4 region using the universal primers S-D-Bact-0341-b-S-17/ S-D-Bact-0785-a-A-21 (Klindworth et al., 2013). DNA samples from the original leach field and control soils at the same depth were also sequenced for comparison to the soil column communities. Additionally, duplicate cDNA samples from each column at the 7.6-cm depth were sequenced to examine the active microbial populations in the soil columns. The Qubit dsDNA High Sensitivity assay (Life Technologies, Carlsbad, CA, USA) was used to measure amplicon concentrations for a randomly sampled subset of reactions. Samples were submitted to Cornell University Biotechnology Resource Center for barcoding, pooling, and paired-end (2×250 bp) sequencing on the MiSeq platform (Illumina, San Diego, CA, USA).

3.2.7 Analyses of 16S rRNA, *mcrA*, and *pmoA* amplicon libraries

Resulting 16S rRNA, *mcrA*, and *pmoA* sequencing data was processed as described in Fernández-Baca et al. (2018). 16S rRNA sequencing data was analyzed using QIIME (v 1.9.1) and the Greengenes reference database v 13.8 (August 2013). Functional gene sequence analyses were done with BWA-MEM and a curated reference database from FunGene (Caporaso et al., 2010; Fernández-Baca et al., 2018; Fish et al., 2013; Li, 2013; McDonald et al., 2012). Alpha diversity was measured using both Chao1 and Shannon diversity indices (Shannon, 1948; Wilkins et al., 2015). Principal Coordinate Analysis (PCoA) and constrained Distance-Based Redundancy Analysis (dbRDA) plots were created with R version 3.3.3 using the phyloseq (version 1.19.1) and vegan (version 2.4-4) packages and the weighted

UniFrac distance matrix. Variance inflation factors were checked for dbRDA constraining parameters ($VIF < 5$) and for significance ($p < 0.01$ based on ANOVA)

3.3 Results

3.3.1 Soil volumetric water content

Soil VWC was monitored throughout the sampling period above and below the inlet (Figure 3.2). From August 2015 to February 2016, the start-up phase, VWC was monitored until measurements stabilized and during this time no other samples were taken. Phase I began after measurements stabilized, during this phase Column A was flooded and VWC was maintained at or above $0.26 \text{ m}^3 \text{ m}^{-3}$ (mean of 0.326 and $0.294 \text{ m}^3 \text{ m}^{-3}$ at 15 cm and 64 cm below the surface, respectively). Column A remained flooded for the duration of the experiment through all phases of operation. In contrast, Column B shallow (15 cm depth) soils were dry (mean of $0.114 \text{ m}^3 \text{ m}^{-3}$) during Phase I and deep soils (64 cm depth) were saturated (mean of $0.316 \text{ m}^3 \text{ m}^{-3}$). In Phase II, Column B mean VWC increased to $0.30 \text{ m}^3 \text{ m}^{-3}$ in both shallow and deep soils confirming flooded conditions. Column B was drained over several months in Phase III. After March 2017 there were occasional spikes in the shallow sensor for Column B indicating intermittent flooding. However after mid June, the VWC sensors showed Column B had consistently drier soils (means of 0.169 and $0.146 \text{ m}^3 \text{ m}^{-3}$ for shallow and deep soil, respectively).

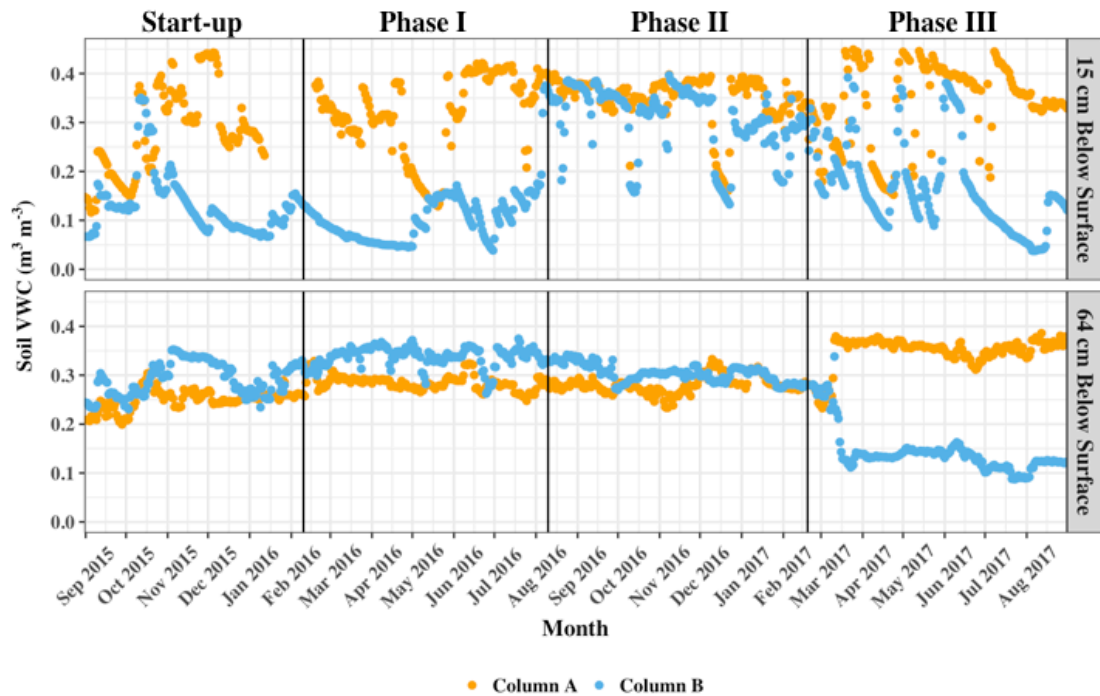


Figure 3.2. Soil volumetric water content ($\text{m}^3 \text{m}^{-3}$) measured continuously above the inlet (15 cm below the surface) and below the inlet (64 cm below the surface) in both soil columns. Vertical lines indicate phases of operation.

3.3.2 Atmospheric CH_4 flux measurements

CH_4 surface fluxes varied over the two-year operation period (Figure 3.3). During Phase 1, Column A had significantly higher methane fluxes than B ($p = 0.036$, Figure 3.3a). In Phase II, both columns had similar methane emissions ($p > 0.05$, Figure 3.3b). In the final phase of operation, CH_4 fluxes again diverged with Column A emitting significantly more CH_4 than Column B ($p = 0.012$, **Error! Reference source not found.**c) but at a lower mean rate than before. Over the course of operation, the total CH_4 emissions ranged in Column A from a mean of $0.11 \text{ g CH}_4 \text{ m}^{-2} \text{ d}^{-1}$ in Phase 1 to a mean of $0.20 \text{ g CH}_4 \text{ m}^{-2} \text{ d}^{-1}$ in Phase II, dropping to $0.047 \text{ g CH}_4 \text{ m}^{-2} \text{ d}^{-1}$ in the final phase. There were no significant differences between fluxes from Column A over

time. In Column B, Phase I and III had average methane emissions close to zero (means fluxes of 0.004 and -0.0025 g CH₄ m⁻² d⁻¹), while during Phase II there was a significant increase in mean methane emissions to 0.33 g CH₄ m⁻² d⁻¹ ($p = 0.046$, Figure 3.3a and Figure 3.3b).

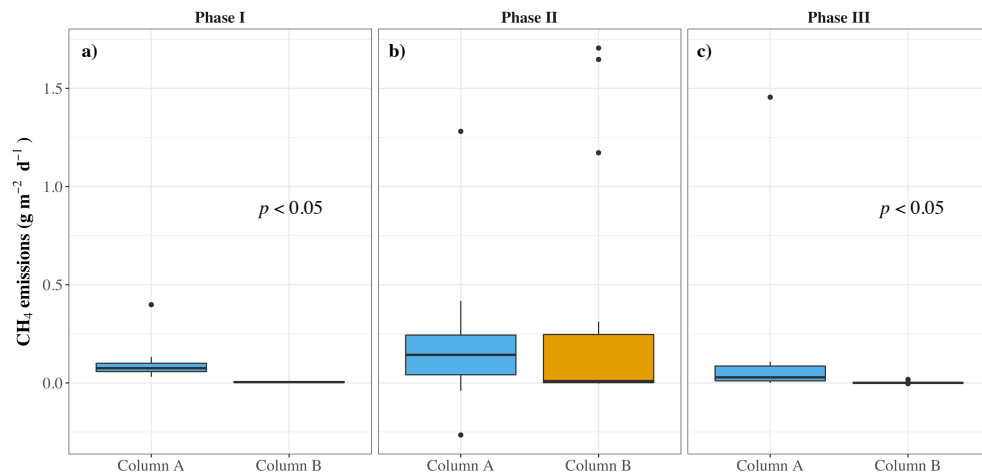


Figure 3.3. Boxplots of flux measurements for three different periods of operation, a) Phase I Column A flooded, Column B well-maintained ($n = 10$); b) Phase II both columns flooded ($n = 16$); c) Phase III Column A flooded, Column B drained ($n = 11$). Significant differences are shown at a 95% confidence interval. Inter-quartile range (IQR) defined between 25% and 75% of data, median shown by black bar. Upper and lower whiskers indicate the highest and lowest data point within 1.5 times the IQR.

3.3.3 Subsurface CH₄ concentration profiles

CH₄ depth profiles of the two soil columns evolved over the course of the experiment (Figure 3.4). During Phase I, subsurface CH₄ concentrations ranged from atmospheric to a peak of 15.8 mg l⁻¹ in Column A and 0.637 mg l⁻¹ in Column B (Figure 3.4a). During Phase II in Column B, average monthly methane concentrations 46 cm below the surface increased steadily from 1.87 to 9.28 mg l⁻¹, while in Column A peak subsurface CH₄ concentrations ranged from 5.18 to 17.5 mg l⁻¹ in the same time period (Figure 3.4b). In Phase III, Column B was drained and methane concentrations above the inlet dropped over time to atmospheric, while below the inlet

peak methane concentrations remained high with observed concentrations between 1.3 and 12.3 mg l⁻¹ from March to August 2017 (Figure 3.4c).

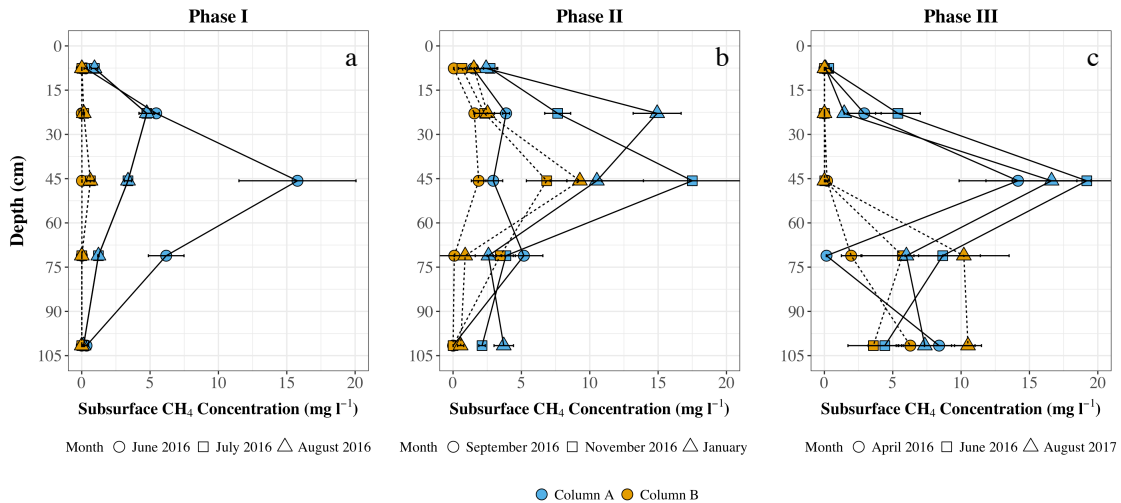


Figure 3.4. Mean monthly methane depth profiles for Column A and B, a) Phase I Column A flooded, Column B well-maintained; b) Phase II Column A flooded, Column B flooding; c) Phase III Column A flooded, Column B drained.

3.3.4 *mcrA*, *pmoA*, and 16S rRNA gene and transcript abundances

Gene abundances of 16S rRNA, *mcrA*, and *pmoA* varied across sampling dates and with depth (Figure 3.5). *mcrA* gene copies were highest near the wastewater inlet in both columns with abundances up to 7.11×10^7 and 2.07×10^7 *mcrA* copies g⁻¹ dry weight soil (soil_{dw}) for Column A and B, respectively. The lowest *mcrA* gene abundances were observed in surface soil samples (0 and 8 cm). In contrast, the highest observed *pmoA* gene abundances occurred in surface samples (up to 1.99×10^8 and 5.80×10^7 copies g⁻¹ soil_{dw} for Column A and B, respectively) and decreased with depth. 16S rRNA gene copies followed a similar pattern, with greater abundances near the surface and decreasing with depth.

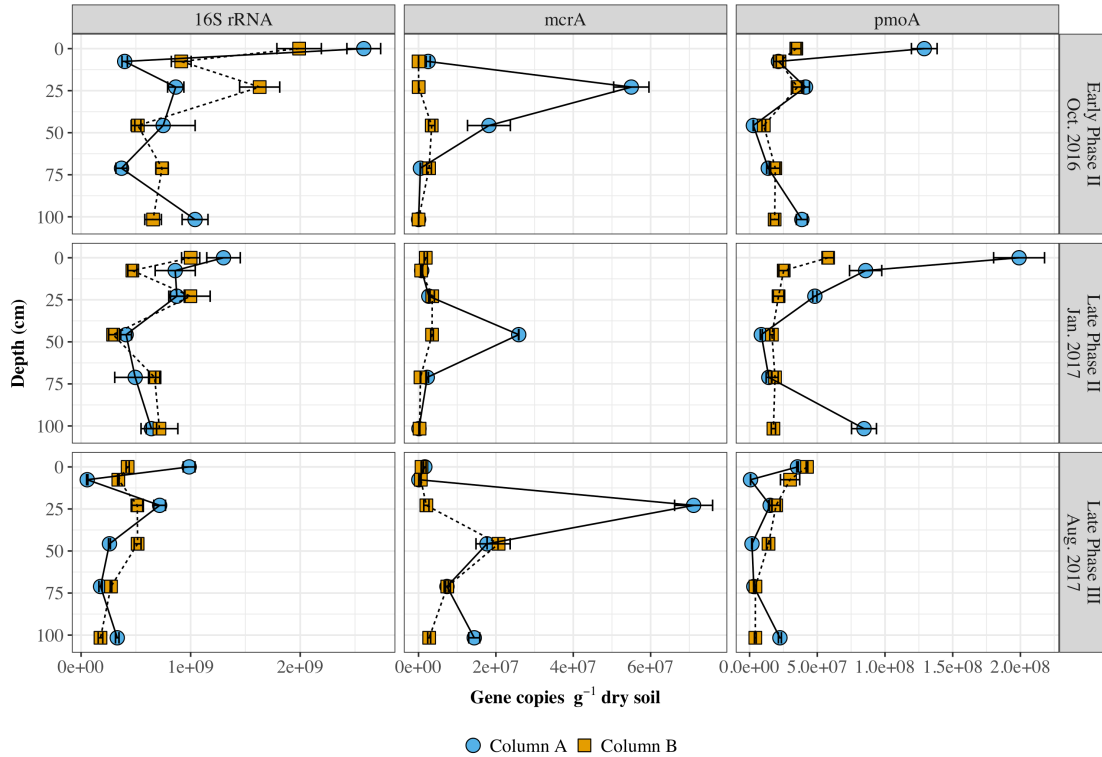


Figure 3.5. Gene copies of 16S rRNA, *mcrA*, and *pmoA* per gram of dry soil on three sampling dates for Column A (solid line) and Column B (dashed line). Error bars indicate the standard error between duplicate extractions and triplicate qPCR reactions.

Transcript abundances of *mcrA* and *pmoA* were used to estimate the activity of CH_4 cycling microorganisms, while 16S rRNA transcript quantification was used to estimate baseline microbial activity (Figure 3.6). Both 16S rRNA and *pmoA* transcript abundances showed similar trends to gene abundances, where the highest observed transcript levels were found in near-surface soils and decreased with depth. Results for *mcrA* showed methanogen activity was not necessarily restricted to soils surrounding the inlet, but occurred throughout the soil column depth.

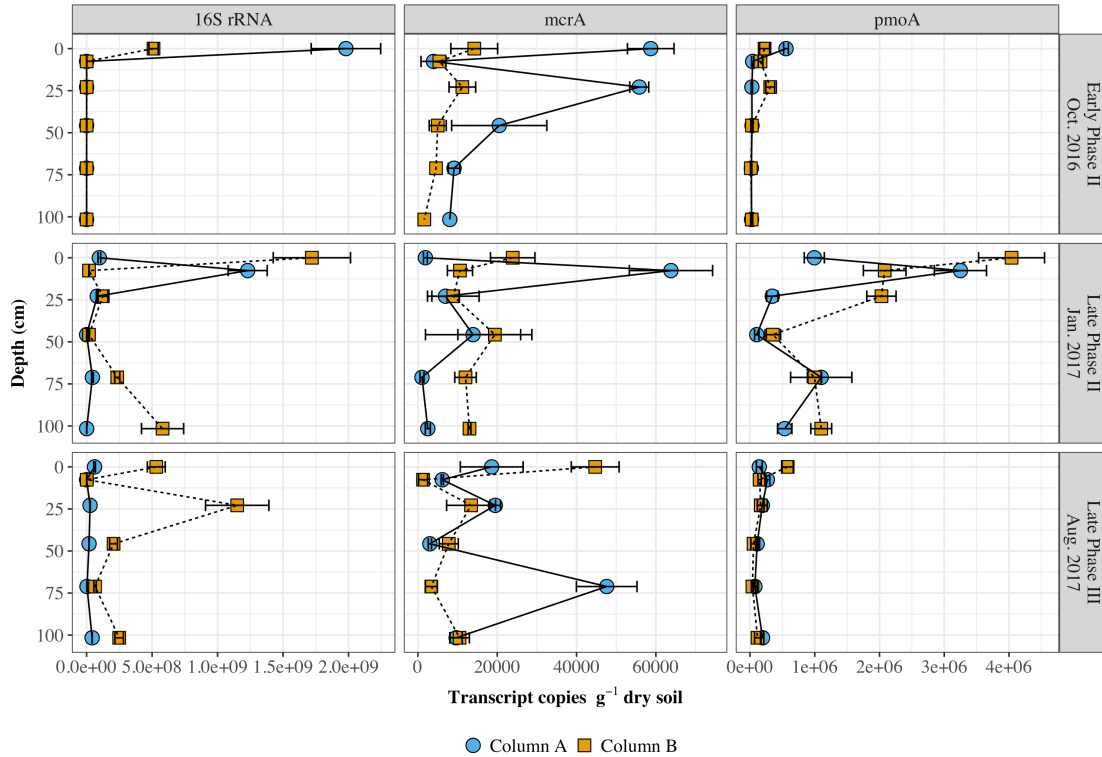


Figure 3.6. Transcript abundances over depth of 16S rRNA, *mcrA*, and *pmoA* per gram soil for Column A (solid line) and Column B (dashed line) on three sampling dates. Error bars indicate the standard error between duplicate extractions and triplicate qPCR reactions.

Ratios of *mcrA* to *pmoA* gene abundances were compared to mean monthly subsurface concentrations of CH₄ in both soil columns for each of the three sampling dates (SI Figure 3.1). A significant positive relationship between $\log_{10}(\text{mcrA}:\text{pmoA}$ gene abundances) and $\log_{10}(\text{mean monthly CH}_4 \text{ concentrations mg l}^{-1})$ was found for one sampling date in Column B ($r^2 = 0.829$, $p = 0.0318$). Weak positive correlations were observed for all other sampling dates (r^2 ranging from 0.23 to 0.65 and p -values between 0.110 and 0.414). Additionally, weak positive relationships were observed between CH₄ concentrations and ratios of *mcrA*:*pmoA* transcript abundances, however again these correlations were not significant at a 95% confidence interval (SI Figure 3.2).

3.3.5 16S rRNA, mcrA, and pmoA amplicon library sequencing

16S rRNA sequencing data was quality filtered and low quality sequences were removed resulting in a total of 105,113 reads. Mean assigned reads per sample for DNA was 12,502 (ranging from 6,706 to 17,672) and for cDNA was 6,838 (ranging from 21 to 14,422) with a median read length of 444 bp. Singleton OTUs were removed resulting in 17,492 unique OTUs.

PCoA and constrained dbRDA plots were created to visualize variations in microbial community structure at the DNA level (Figure 3.7). PCoA revealed samples clustered together based on treatment (i.e. Column A, B, and original soil). The dbRDA constraining parameters, surface CH₄ flux and soil VWC, explained approximately 79% of the variation observed in the unconstrained plot (PC1 = 22.7% and PC2 = 11.2%). An additional PCoA plot was used to examine differences in community diversity between gene and transcript libraries (SI Figure 3.3), which revealed the microbial communities in the columns, diverged even more at the transcript level.

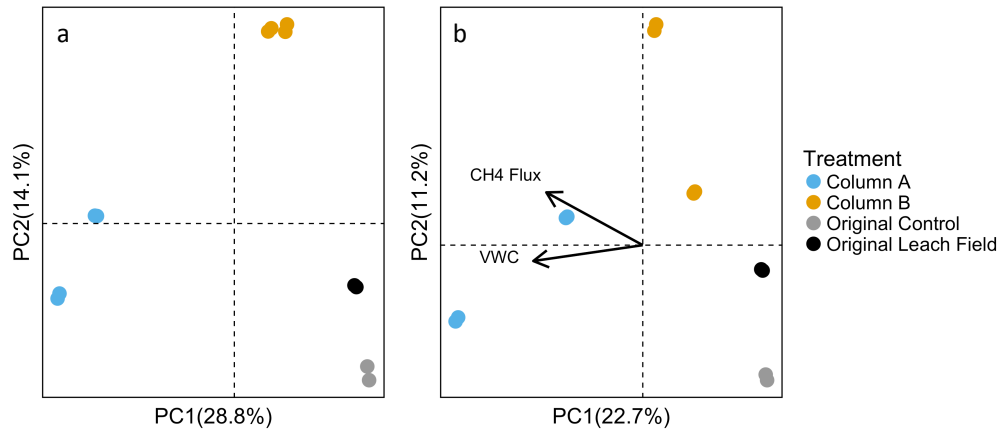


Figure 3.7. PCoA (a) and dbRDA (b) constrained by CH₄ fluxes and soil VWC. Both analyses were based on the weighted UniFrac distance matrix of 16S rRNA sequencing data for DNA samples.

Functional gene sequencing of *mcrA* and *pmoA* amplicon libraries was further used to study CH₄ cycling populations. Sequencing results for *mcrA* and *pmoA* amplicon libraries were varied, with more total reads assigned for *mcrA* (87,979) than for *pmoA* (853). Mean mapped reads per sample was 12,242 for *mcrA* and 420 for *pmoA* samples.

Methanogen diversity in the experimental columns and original soils was studied using the *mcrA* amplicon libraries at the family and genus level (Figure 3.8a and SI Figure 3.4a). Relative abundance of *Methanosaetaceae* increased in Column A (39% of reads) as compared to Column B (14% of reads) and the original soils (12.1% and 17.4% for leach and control soils, respectively).

Methanotroph populations were examined using the functional gene *pmoA* at both the family and genus level (Figure 3.8b and SI Figure 3.4b). *Methylococcaceae* and *Methylocystaceae*, Type I and Type II methanotroph families, respectively, dominated both soil columns and original soils with Column A having a relatively greater number of reads associated with *Methylocystaceae* (54% of reads mapped to

this family) as compared to Column B and original soils (less than 15% of mapped reads per sample). A large fraction of reads from Column B (30%) and the original leach field soils (16%) were assigned to candidate division NC10 phylum organisms, which are thought to couple methane oxidation to nitrite reduction (Luesken et al., 2011). In the 16S rRNA sequencing data, loss of methanotroph diversity in Column A is evident at the genus level, where Type II *Methylocystis* and *Methylobacter* make up more than 80% of the assigned reads and the Type I methanotroph *Methyломicrobium* has disappeared (SI Figure 3.5).

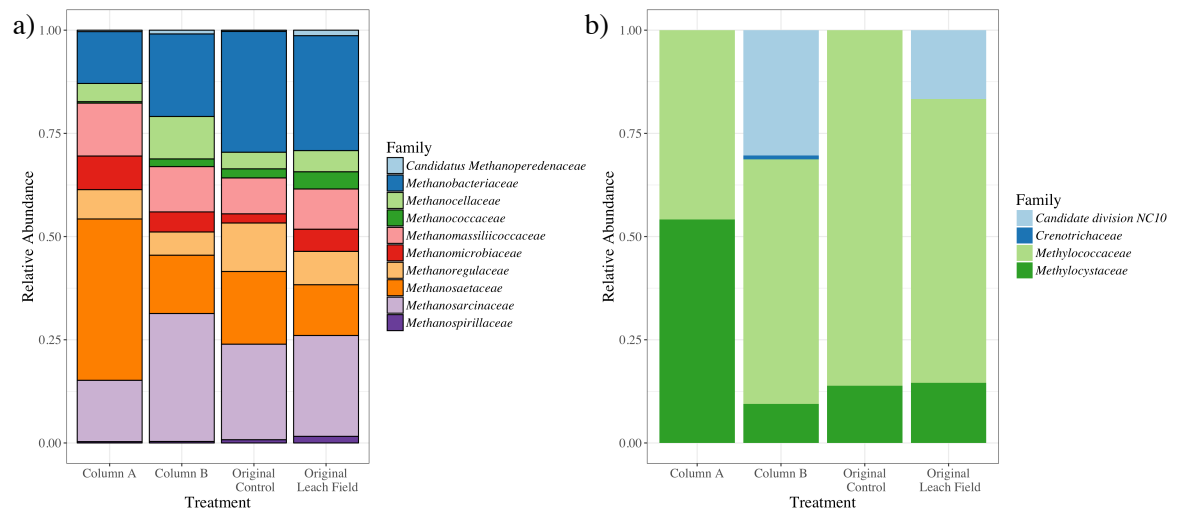


Figure 3.8. Functional gene sequencing results for a) *mcrA* and b) *pmoA* amplicon libraries. Relative abundances for Column A, Column B and original soils (leach field and control) are shown at the family level. Total number of assigned reads was higher for *mcrA* (78,258) compared to *pmoA* (853).

Chao1 and the Shannon diversity values calculated from the 16S rRNA sequencing data, indicate that the original soils had the greatest observed diversity with Chao1 values of 8787 and 9559 and Shannon values of 7.55 and 7.59 for original control and leach field soils, respectively. Column B had a Chao1 value of 8239 and Shannon index of 7.37, while Column A had the lowest calculated diversity (5371 and

6.74, for Chao1 and Shannon, respectively).

3.3.6 Nutrient and COD removal

Influent and effluent concentrations of NH_4^+ , PO_4^{3-} , and COD were compared for flooded and well-maintained soil columns (Figure 3.9). Removal for both NH_4^+ and PO_4^{3-} appears to be unaffected by flooding. However, NH_4^+ removal did decline during Column B's transition period from flooded to well-maintained conditions. Nitrate and nitrite were produced at low levels in both columns and ranged from 0 to 15 mg l^{-1} as N. COD removal was variable, but higher in Column B (75% removal) prior to flooding as compared to Column A (25% removal) and declined after flooding. Nutrient concentrations were also measured with depth (data not shown) and peak concentrations for NH_4^+ , PO_4^{3-} , and nitrate and nitrite were observed near the inlet decreasing with depth.

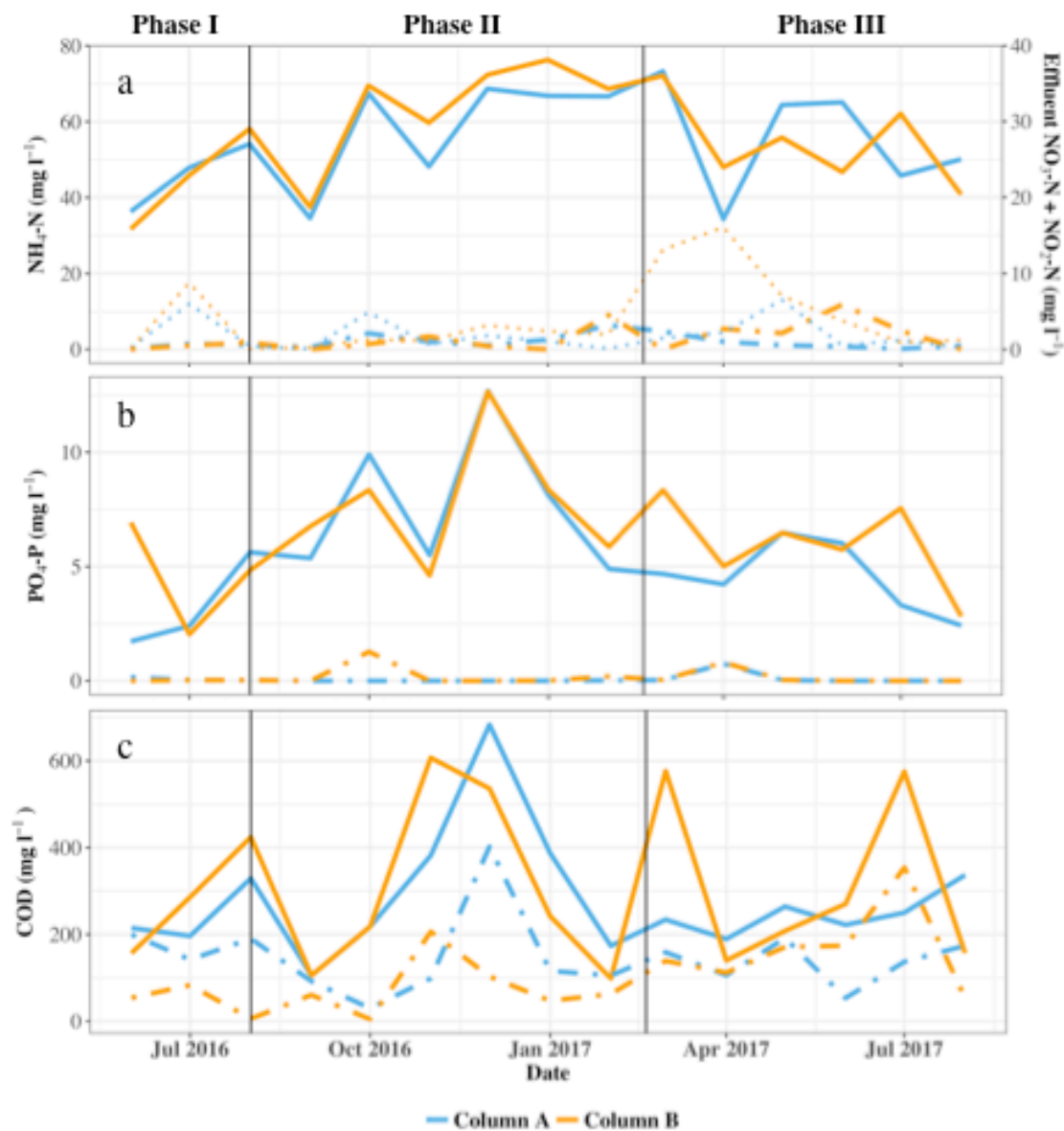


Figure 3.9. Influent (solid line) and effluent (dashed line) concentrations of (a) $\text{NH}_4\text{-N}$ and effluent concentrations of $\text{NO}_3\text{-N} + \text{NO}_2\text{-N}$ (dotted line), (b) $\text{PO}_4\text{-P}$, (c) COD for Column A and B, with vertical lines marking the three phases of operation.

3.4 Discussion

3.4.1 CH_4 cycling in leach field soil columns

CH_4 emissions from Column B during ‘well-maintained’ operation (Phases I and III) were comparable to well-maintained leach field systems measured in central New York which range from low rate net CH_4 consuming ($-0.004 \text{ g CH}_4 \text{ m}^{-2} \text{ d}^{-1}$) to net

emitting sites ($0.005 \text{ g CH}_4 \text{ m}^{-2} \text{ d}^{-1}$) (Truhlar et al., 2016). Under flooded conditions, the soil columns exhibited increased CH_4 emissions compared to non-flooded conditions and had emissions similar to those observed in flooded leach field soils measured in summer of 2014 (mean $0.26 \text{ g CH}_4 \text{ m}^{-2} \text{ d}^{-1}$) (Fernández-Baca et al., 2018). Ebullition events observed during the flooded phases of operation had peak rates of 1.45 and $1.71 \text{ g CH}_4 \text{ m}^{-2} \text{ d}^{-1}$ for Column A and B, respectively, and were comparable to emissions from traditionally flooded soils such as rice paddies (0.24 to $1.44 \text{ g CH}_4 \text{ m}^{-2} \text{ d}^{-1}$) and peat bogs (0.21 to $0.4 \text{ g CH}_4 \text{ m}^{-2} \text{ d}^{-1}$), indicating GHG emissions from leach fields could be significantly higher than previously thought (Deppe et al., 2010; Freitag et al., 2010; Lee et al., 2014).

Subsurface CH_4 profiles evolved over time with changes in soil VWC. In Phase I, Column B accumulated low amounts of CH_4 at depth. In contrast, Column A had CH_4 concentrations between 5 to $20 \text{ mg CH}_4 \text{ l}^{-1}$. During Phase II, the two columns exhibited similar CH_4 depth profiles with peak concentrations occurring near the inlet and decreasing both above and below. Subsurface CH_4 concentrations in rice paddy and pasture soils have previously been shown to peak below surface (between 8 and 40 cm deep) and decrease with depth. This pattern may be attributed to a combination of upward diffusion and low or no production of CH_4 in deeper mineral soils (Chamberlain et al., 2016; Lee et al., 2015; Vaksmaa et al., 2017). Similarly in the experimental columns a combination of diffusion and microbial CH_4 oxidation likely explain the low CH_4 concentration in shallow soils.

High soil VWC has been correlated to increased CH_4 emissions in soil environments as varied as pastures, roadside storm water ditches, and bogs

(Chamberlain et al., 2016; Deppe et al., 2010; McPhillips et al., 2016). Truhlar et al. (2016) estimated the leach field of well-maintained systems in central New York had a mean CH₄ flux of 0.0196 g m⁻² d⁻¹, this study suggests a flooded system could have peak emissions 100 times greater. Thus, proper installation and continued maintenance of septic system leach fields is essential to reducing net GHG emissions from these systems.

3.4.2 CH₄ cycling community composition

Methanogens and methanotrophs were present throughout both soil columns but had distinct depth profiles. Methanogens were more abundant near the wastewater inlet as indicated by greater *mcrA* gene copies and less abundant both above and below. Although Angel et al. (2012) showed that certain methanogen species are robust to oxygen exposure, we found that our lowest *mcrA* gene abundances were observed at the surface (0 - 2.5 cm depth). However, at the transcript level we found that methanogens were active in near-surface soils as suggested by the 1.5 to 2 fold higher *mcrA* transcript levels observed in surface soils as compared to deeper soils (below 23 cm).

In contrast, methanotroph populations were more abundant near-surface, and became less abundant with depth. Lee et al. (2015) and Reim et al. (2012) observed similar profiles in flooded rice paddy soils where methanotroph abundances were highest in near-surface soil at the interface of oxygen-methane gradients. As O₂ availability decreases, aerobic methanotroph populations also declined, even as CH₄ concentrations increased, suggesting that soil methanotroph populations are driven largely by O₂ availability. Oxygen concentrations were measured several times during

Phase II in this study (data not shown) and were found to be below detection (dissolved oxygen detection limit was $0.025 \text{ mg O}_2 \text{ l}^{-1}$) below the 8 cm depth. Thus, decreasing O_2 concentrations between the 8 and 23 cm depths may be responsible for the decline in methanotroph populations with depth.

mcrA and *pmoA* gene abundances have previously been correlated to CH_4 production potential in rice paddies and peat bogs (Freitag et al., 2010; Ma et al., 2013, 2012). We explored similar biomarker abundance to CH_4 emission relationships in the leach field soil columns using \log_{10} of *mcrA:pmoA* gene or transcript abundances and mean monthly CH_4 concentrations at each sampling depth (SI Figure 3.1 and 3.2). Moderately strong correlations were found (between r^2 of 0.230 and 0.829) indicating a positive relationship between the biomarker gene ratio and CH_4 concentrations, however the observed relationship was only significant for samples from January 2017 in Column B ($r^2 = 0.829$, $p = 0.0318$). This relationship appears to be driven in large part by *mcrA* gene abundances, which alone was significantly correlated to CH_4 concentrations for the January 2017 sampling date ($r^2 = 0.810$, $p = 0.0386$), whereas *pmoA* gene abundances showed no significant correlations for any date. The link between biomarker abundances and CH_4 potential may be obscured by differences in pore water and soil sample volumes. Soil samples were taken over a relatively small volume (approximately 0.23 cm^2) while pore water samplers pulled from a larger volume of soil, potentially integrating small volumes of high activity with larger volumes of low activity.

3.4.3 Microbial community composition in leach field soils

16S rRNA, *mcrA*, and *pmoA* libraries were analyzed to characterize the

microbial community structure in leach field soils with an emphasis on examining populations controlling CH₄ cycling. The 16S rRNA libraries revealed that communities from the experimental leach field soil columns had diverged from those of the original soils at the DNA level. This variation was explained, in part, by soil VWC and CH₄ emissions of the soil columns (Figure 3.7). Soil microbial communities from original control and leach field soils were more similar to each other than either Column A or B at the gene level. At the transcript level, greater divergence in community structure was observed, indicating that active microbial populations differ from those present at the gene level (SI Figure 3.3). Krause et al. (2010) observed a similar disparity between total and active microbial populations when examining methanotroph populations via *pmoA* gene and transcript abundances in flooded rice paddy soils.

pmoA amplicon libraries revealed two aerobic methanotroph families were present across all samples: *Methylocystaceae* and *Methylococcaceae*. *Methylococcaceae* represented the majority of reads in all soil samples with the exception of Column A where it accounted for 45.9% of reads. This was in contrast to results from 16S rRNA libraries (SI Figure 3.5), which suggested that *Methylocystaceae* was dominant across all samples (greater than 85% of reads in all samples). Loss of methanotroph diversity in Column A observed in the *pmoA* amplicon libraries was supported by 16S rRNA sequencing results; however family and genus level assignments differed considerably between the two datasets. A majority of the 16S rRNA reads aligned to Type II methanotrophs (greater than 75% of reads) while in the *pmoA* library the majority of reads were Type I methanotrophs and

had a low relative abundance of Type II methanotrophs (less than 18.0% in all samples except Column A which had 54.1% of reads assigned to Type II). Lee et al. (2014) similarly found that taxonomic affiliations based on *pmoA* libraries differed from those based on the 16S rRNA libraries that could be attributed to primer biases or incomplete gene sequence information in reference databases.

mcrA amplicon libraries revealed *Methanosaetaceae*, *Methanosarcinaceae*, *Methanobacteriaceae*, and *Methanomassilicoccaceae* families combined represented the majority of reads (approximately 43%) across all soil samples. These families as well as *Methanoregulaceae*, *Methanocellaceae* and *Methanospirillaceae*, have previously been found in soil environments such as rice paddies and wetlands suggesting leach field soils have similar methanogen profiles to other high VWC soils (Bridgham et al., 2013). Interestingly, *mcrA* libraries revealed the presence of the anaerobic methanotrophic archaea *Candidatus Methanoperedenceae* (ANME-2d clade), thought to couple methane oxidation to nitrate reduction, in low abundance across all samples (Haroon et al., 2013). Column A had the most distinct methanogen profile with a loss of many of the low abundance genera observed in Column B and the original soils and an increase in the relative abundance of *Methanosaeta* relative to other genera. The decrease in methanogen diversity observed in Column A parallels that found in the *pmoA* and 16S rRNA libraries and is supported by statistical diversity indices Chao1 and Shannon. Due to primer biases against archaeal sequences, reads were sparse for the *Euryarchaeaota* phylum (21 total mapped reads) in the 16S rRNA amplicon library and precluded comparisons between *mcrA* and 16S rRNA sequencing datasets.

The use of synthetic wastewater in this study likely impacted the soil microbial community structure. In addition to having readily available C sources such as acetate, there were no large particles that would be more resistant to microbial attack and could reduce effluent infiltration into soil. Additionally, authentic septic effluent could introduce high numbers of methanogens and, to a lesser degree, methanotrophs to leach field soils. The probable presence of anaerobic methanotrophs in septic tank effluent should also not be disregarded. Thus, *in situ* leach field systems would have a constant input of methane-cycling populations not mimicked in the study system. However, *in situ* systems likely reach a ‘steady-state’ in terms of microbial populations that do not fluctuate substantially over time unless there is a significant disturbance such as a change in soil VWC. The findings in this study reflect a system that has been substantially disturbed from ‘steady-state.’

3.4.4 Nitrogen, phosphorus, and COD removal

Septic systems can impact ground and surface water by leaching high loads of nutrients (N and P), COD, and pathogens (Richards et al., 2016; USEPA, 2002). In this study, the soil columns were able to remove N and P effectively despite flooding. Both NH_4^+ and PO_4^{3-} were removed at greater than 75% efficiency during all operational phases. High N and P removals have previously been reported in well-maintained leach field systems but had not previously been measured in flooded system (Gill et al., 2009; Pell, et al. 1990). In this study P is likely retained by complexation with aluminum (Al) or iron (Fe) oxides. Sequences of *Acidovorax* sp. and *Thiobacillus* sp., which can both oxidize iron anaerobically coupled to nitrate reduction, were found in the soil columns indicating potential for Fe-oxidation

creating minerals available for P sorption (Carlson et al., 2013).

16S rRNA amplicon sequencing also revealed the presence of nitrifier, denitrifier and ammonia oxidizing microorganisms, indicating full or partial denitrification may be responsible for the high NH_4^+ removals observed. Reads assigned to nitrifier genera including *Nitrospira* sp. were found in both columns with relative abundances of 0.4% and 0.8% for Column A and B, respectively. Well-known denitrifier genera including *Pseudomonas*, *Bradyrhizobium*, and *Rhodanobacter*, as well as ‘atypical’ denitrifiers’ including *Anaeromyxobacter* sp., sequences were also found albeit at a low relative abundances (less than 0.1% in both experimental columns) (Ma et al., 2008; Sanford et al., 2012).

COD removal was impacted by flooding, suggesting flooded leach fields could introduce high COD loads to nearby ground water. Furthermore, although both N and P had high removals in this study, further work should be done to better understand the biogeochemical cycling occurring in these systems, as previous studies suggested septic systems can contribute significantly to ground water contamination of N and P (Bunnell et al., 1999; Cooper et al., 2015; Withers et al., 2014). Thus, proper installation of leach field systems with sufficient spacing between laterals and the local ground water table is critical to maintaining high removal efficiencies without impacting nearby ground and/or surface water.

3.5 Conclusions

Two lab-scale leach field soil columns were constructed to study how flooding impacts CH_4 and nutrient cycling in these systems. CH_4 fluxes and subsurface concentrations increased under failing-by-flooding conditions indicating soil VWC is

a major driver of CH₄ production in leach field soils. *mcrA* gene copies were greatest near the wastewater inlet, in contrast, *pmoA* gene abundances were greatest in surface soils. Soil column microbial community structure shifted significantly from the original leach field soils at the DNA level and was explained by CH₄ emissions and soil VWC. Active microbial populations differed from populations at the gene level, suggesting analysis of both gene and transcripts is important to understanding microbial community and CH₄ cycling dynamics. Flooding did not appear to affect nutrient removals, however did negatively impact COD removal. Based on these results, we suggest proper maintenance of leach field systems to avoid flooding, is essential to mitigating their methane emissions and reducing their impact on water quality.

Acknowledgements

Thanks to M. Todd Walter in Biological and Environmental Engineering at Cornell University for allowing us to excavate soils from his active leach field for our soil column experiments. We would like to thank Jennifer Cooper from University of Rhode Island and Erica Gardner for their help with systems design and set-up. Thanks also go to Brian Rahm from the Water Resources Institute of New York State for input on the study.

References

- Aiyuk, S., Verstraete, W., 2004. Sedimentological evolution in an UASB treating SYNTHES, a new representative synthetic sewage, at low loading rates. *Bioresour. Technol.* 93, 269–78. <https://doi.org/10.1016/j.biortech.2003.11.006>
- Angel, R., Claus, P., Conrad, R., 2012. Methanogenic archaea are globally ubiquitous in aerated soils and become active under wet anoxic conditions. *ISME J.* 6, 847–62. <https://doi.org/10.1038/ismej.2011.141>
- APHA, 2012. Standard methods for the examination of water and wastewater Title, 22nd ed. Washington, D.C.
- Bower, C.E., Holm-Hansen, T., 1980. A Salicylate–Hypochlorite Method for Determining Ammonia in Seawater. *Can. J. Fish. Aquat. Sci.* 37, 794–798. <https://doi.org/10.1139/f80-106>
- Bridgham, S.D., Cadillo-Quiroz, H., Keller, J.K., Zhuang, Q., 2013. Methane emissions from wetlands: Biogeochemical, microbial, and modeling perspectives from local to global scales. *Glob. Chang. Biol.* 19, 1325–1346. <https://doi.org/10.1111/gcb.12131>
- Bunnell, J.F., Zampella, R.A., Morgan, M.D., Gray, D.M., 1999. A comparison of nitrogen removal by subsurface pressure dosing and standard septic systems in sandy soils. *J. Environ. Manage.* 56, 209–219. <https://doi.org/10.1006/JEMA.1999.0273>
- Caporaso, J.G., Kuczynski, J., Stombaugh, J., Bittinger, K., Bushman, F.D., Costello, E.K., Fierer, N., Peña, A.G., Goodrich, J.K., Gordon, J.I., Huttley, G.A., Kelley,

- S.T., Knights, D., Koenig, J.E., Ley, R.E., Lozupone, C.A., McDonald, D., Muegge, B.D., Pirrung, M., Reeder, J., Sevinsky, J.R., Turnbaugh, P.J., Walters, W.A., Widmann, J., Yatsunenko, T., Zaneveld, J., Knight, R., 2010. QIIME allows analysis of high-throughput community sequencing data. *Nat. Methods* 7, 335–336. <https://doi.org/10.1038/nmeth.f.303>
- Carlson, H.K., Clark, I.C., Blazewicz, S.J., Iavarone, A.T., Coates, J.D., 2013. Fe(II) oxidation is an innate capability of nitrate-reducing bacteria that involves abiotic and biotic reactions. *J. Bacteriol.* 195, 3260–8. <https://doi.org/10.1128/JB.00058-13>
- Chamberlain, S.D., Gomez-Casanovas, N., Walter, M.T., Boughton, E.H., Bernacchi, C.J., DeLucia, E.H., Groffman, P.M., Keel, E.W., Sparks, J.P., 2016. Influence of transient flooding on methane fluxes from subtropical pastures. *J. Geophys. Res. Biogeosciences* 121, 965–977. <https://doi.org/10.1002/2015JG003283>
- Cogger, C.G., Carlile, B.L., 1984. Field Performance of Conventional and Alternative Septic Systems in Wet Soils¹. *J. Environ. Qual.* 13, 137. <https://doi.org/10.2134/jeq1984.00472425001300010025x>
- Cooper, J.A., Loomis, G.W., Kalen, D. V., Amador, J.A., 2015. Evaluation of Water Quality Functions of Conventional and Advanced Soil-Based Onsite Wastewater Treatment Systems. *J. Environ. Qual.* 44, 953. <https://doi.org/10.2134/jeq2014.06.0277>
- Costello, A.M., Lidstrom, M.E., 1999. Molecular characterization of functional and phylogenetic genes from natural populations of methanotrophs in lake sediments. *Appl. Environ. Microbiol.* 65, 5066–74.

- Deppe, M., Knorr, K.-H., McKnight, D.M., Blodau, C., 2010. Effects of short-term drying and irrigation on CO₂ and CH₄ production and emission from mesocosms of a northern bog and an alpine fen. *Biogeochemistry* 100, 89–103.
<https://doi.org/10.1007/s10533-010-9406-9>
- Diaz-Valbuena, L.R., Leverenz, H.L., Cappa, C.D., Tchobanoglous, G., Horwath, W.R., Darby, J.L., 2011. Methane, carbon dioxide, and nitrous oxide emissions from septic tank systems. *Environ. Sci. Technol.* 45, 2741–7.
<https://doi.org/10.1021/es1036095>
- Fernández-Baca, C.P., Truhlar, A.M., Omar, A.-E.H., Rahm, B.G., Walter, M.T., Richardson, R.E., 2018. Methane and nitrous oxide cycling microbial communities in soils above septic leach fields: Abundances with depth and correlations with net surface emissions. *Sci. Total Environ.* 640–641, 429–441.
<https://doi.org/10.1016/J.SCITOTENV.2018.05.303>
- Ferris, M.J., Muyzer, G., Ward, D.M., 1996. Denaturing gradient gel electrophoresis profiles of 16S rRNA-defined populations inhabiting a hot spring microbial mat community. *Appl. Environ. Microbiol.* 62, 340–6.
- Fish, J.A., Chai, B., Wang, Q., Sun, Y., Brown, C.T., Tiedje, J.M., Cole, J.R., 2013. FunGene: the functional gene pipeline and repository. *Front. Microbiol.* 4, 291.
<https://doi.org/10.3389/fmicb.2013.00291>
- Freitag, T.E., Toet, S., Ineson, P., Prosser, J.I., 2010. Links between methane flux and transcriptional activities of methanogens and methane oxidizers in a blanket peat bog. *FEMS Microbiol. Ecol.* 73, 157–65. <https://doi.org/10.1111/j.1574-6941.2010.00871.x>

- Gill, L.W., O’Luanaigh, N., Johnston, P.M., Misstear, B.D.R., O’Suilleabhain, C.,
2009. Nutrient loading on subsoils from on-site wastewater effluent, comparing
septic tank and secondary treatment systems. *Water Res.* 43, 2739–2749.
<https://doi.org/10.1016/J.WATRES.2009.03.024>
- Haroon, M.F., Hu, S., Shi, Y., Imelfort, M., Keller, J., Hugenholtz, P., Yuan, Z.,
Tyson, G.W., 2013. Anaerobic oxidation of methane coupled to nitrate reduction
in a novel archaeal lineage. *Nature* 500, 567–70.
<https://doi.org/10.1038/nature12375>
- Katz, B.G., Eberts, S.M., Kauffman, L.J., 2011. Using Cl/Br ratios and other
indicators to assess potential impacts on groundwater quality from septic
systems: A review and examples from principal aquifers in the United States. *J.*
Hydrol. 397, 151–166. <https://doi.org/10.1016/j.jhydrol.2010.11.017>
- Klindworth, A., Pruesse, E., Schweer, T., Peplies, J., Quast, C., Horn, M., Glöckner,
F.O., 2013. Evaluation of general 16S ribosomal RNA gene PCR primers for
classical and next-generation sequencing-based diversity studies. *Nucleic Acids*
Res. 41, e1. <https://doi.org/10.1093/nar/gks808>
- Krause, S., Lüke, C., Frenzel, P., 2010. Succession of methanotrophs in oxygen-
methane counter-gradients of flooded rice paddies. *ISME J.* 4, 1603–7.
<https://doi.org/10.1038/ismej.2010.82>
- Lee, H.J., Jeong, S.E., Kim, P.J., Madsen, E.L., Jeon, C.O., 2015. High resolution
depth distribution of Bacteria, Archaea, methanotrophs, and methanogens in the
bulk and rhizosphere soils of a flooded rice paddy. *Front. Microbiol.* 6, 639.
<https://doi.org/10.3389/fmicb.2015.00639>

- Lee, H.J., Kim, S.Y., Kim, P.J., Madsen, E.L., Jeon, C.O., 2014. Methane emission and dynamics of methanotrophic and methanogenic communities in a flooded rice field ecosystem. *FEMS Microbiol. Ecol.* 88, 195–212.
<https://doi.org/10.1111/1574-6941.12282>
- Li, H., 2013. Aligning sequence reads, clone sequences and assembly contigs with BWA-MEM.
- Luesken, F. a, van Alen, T. a, van der Biezen, E., Frijters, C., Toonen, G., Kampman, C., Hendrickx, T.L.G., Zeeman, G., Temmink, H., Strous, M., Op den Camp, H.J.M., Jetten, M.S.M., 2011. Diversity and enrichment of nitrite-dependent anaerobic methane oxidizing bacteria from wastewater sludge. *Appl. Microbiol. Biotechnol.* 92, 845–54. <https://doi.org/10.1007/s00253-011-3361-9>
- Luton, P.E., Wayne, J.M., Sharp, R.J., Riley, P.W., 2002. The *mcrA* gene as an alternative to 16S rRNA in the phylogenetic analysis of methanogen populations in landfill. *Microbiology* 148, 3521–3530.
- Ma, K., Conrad, R., Lu, Y., 2013. Dry/Wet cycles change the activity and population dynamics of methanotrophs in rice field soil. *Appl. Environ. Microbiol.* 79, 4932–9. <https://doi.org/10.1128/AEM.00850-13>
- Ma, K., Conrad, R., Lu, Y., 2012. Responses of methanogen *mcrA* genes and their transcripts to an alternate dry/wet cycle of paddy field soil. *Appl. Environ. Microbiol.* 78, 445–54. <https://doi.org/10.1128/AEM.06934-11>
- Ma, W.K., Bedard-Haughn, A., Siciliano, S.D., Farrell, R.E., 2008. Relationship between nitrifier and denitrifier community composition and abundance in predicting nitrous oxide emissions from ephemeral wetland soils. *Soil Biol.*

- Biochem. 40, 1114–1123. <https://doi.org/10.1016/j.soilbio.2007.12.004>
- McDonald, D., Price, M.N., Goodrich, J., Nawrocki, E.P., DeSantis, T.Z., Probst, A., Andersen, G.L., Knight, R., Hugenholtz, P., 2012. An improved Greengenes taxonomy with explicit ranks for ecological and evolutionary analyses of bacteria and archaea. *ISME J.* 6, 610–8. <https://doi.org/10.1038/ismej.2011.139>
- McPhillips, L.E., Groffman, P.M., Schneider, R.L., Walter, M.T., 2016. Nutrient Cycling in Grassed Roadside Ditches and Lawns in a Suburban Watershed. *J. Environ. Qual.* 45, 1901. <https://doi.org/10.2134/jeq2016.05.0178>
- Miranda, K.M., Espey, M.G., Wink, D.A., 2001. A rapid, simple spectrophotometric method for simultaneous detection of nitrate and nitrite. *Nitric Oxide* 5, 62–71. <https://doi.org/10.1006/niox.2000.0319>
- Molodovskaya, M., Warland, J., Richards, B.K., Öberg, G., Steenhuis, T.S., 2011. Nitrous Oxide from Heterogeneous Agricultural Landscapes: Source Contribution Analysis by Eddy Covariance and Chambers. *Soil Sci. Soc. Am. J.* 75, 1829. <https://doi.org/10.2136/sssaj2010.0415>
- New York State Department of Health Bureau of Water Supply Protection, 2012. Residential Onsite Wastewater Treatment Systems Design Handbook, 2012th ed. New York State Department of Health Bureau of Water Supply Protection, Albany.
- Pell, M., Nhyberg, F., Ljunggren, H., 1990. MICROBIAL NUMBERS AND ACTIVITY DURING INFILTRATION OF SEPTIC-TANK EFFLUENT IN A SUBSURFACE SAND FILTER. *Wat. Res* 24, 1347–1354.
- Reim, A., Lüke, C., Krause, S., Pratscher, J., Frenzel, P., 2012. One millimetre makes

- the difference: high-resolution analysis of methane-oxidizing bacteria and their specific activity at the oxic-anoxic interface in a flooded paddy soil. *ISME J.* 6, 2128–39. <https://doi.org/10.1038/ismej.2012.57>
- Richards, S., Paterson, E., Withers, P.J.A., Stutter, M., 2016. Septic tank discharges as multi-pollutant hotspots in catchments. *Sci. Total Environ.* 542, 854–863. <https://doi.org/10.1016/J.SCITOTENV.2015.10.160>
- Sanford, R.A., Wagner, D.D., Wu, Q., Chee-Sanford, J.C., Thomas, S.H., Cruz-García, C., Rodríguez, G., Massol-Deyá, A., Krishnani, K.K., Ritalahti, K.M., Nissen, S., Konstantinidis, K.T., Löffler, F.E., 2012. Unexpected nondenitrifier nitrous oxide reductase gene diversity and abundance in soils. *Proc. Natl. Acad. Sci. U. S. A.* 109, 19709–14. <https://doi.org/10.1073/pnas.1211238109>
- Shannon, C.E., 1948. A mathematical theory of communication. *Bell Syst. Tech. J.* 27, 379–423. <https://doi.org/10.1145/584091.584093>
- Steinberg, L.M., Regan, J.M., 2009. *mcrA*-targeted real-time quantitative PCR method to examine methanogen communities. *Appl. Environ. Microbiol.* 75, 4435–42. <https://doi.org/10.1128/AEM.02858-08>
- Truhlar, A.M., Rahm, B.G., Brooks, R.A., Nadeau, S.A., Makarsky, E.T., Walter, M.T., 2016. Greenhouse Gas Emissions from Septic Systems in New York State. *J. Environ. Qual.* 45, 1153. <https://doi.org/10.2134/jeq2015.09.0478>
- US EPA, 2012. Global Anthropogenic Non-CO₂ Greenhouse Gas Emissions: 1990-2030 [WWW Document]. URL http://www.epa.gov/climatechange/Downloads/EPAactivities/EPA_Global_Non_CO2_Projections_Dec2012.pdf (accessed 4.13.15).

- US EPA, 2002. Onsite Wastewater Treatment and Disposal Systems. Washington, D.C.
- USEPA, 2002. Decentralized Wastewater Systems Technology Fact Sheets [WWW Document]. URL <https://www.epa.gov/septic/onsite-wastewater-treatment-and-disposal-systems> (accessed 12.16.16).
- Vaksmaa, A., van Alen, T.A., Ettwig, K.F., Lupotto, E., Valè, G., Jetten, M.S.M., Lüke, C., 2017. Stratification of Diversity and Activity of Methanogenic and Methanotrophic Microorganisms in a Nitrogen-Fertilized Italian Paddy Soil. *Front. Microbiol.* 8, 2127. <https://doi.org/10.3389/fmicb.2017.02127>
- WHO; UNICEF; JMP, 2017. Progress on Drinking Water, Sanitation, and Hygiene 2017 [WWW Document]. URL <https://washdata.org/> (accessed 10.15.18).
- Wilkins, D., Lu, X.-Y., Shen, Z., Chen, J., Lee, P.K.H., 2015. Pyrosequencing of *mcrA* and archaeal 16S rRNA genes reveals diversity and substrate preferences of methanogen communities in anaerobic digesters. *Appl. Environ. Microbiol.* 81, 604–13. <https://doi.org/10.1128/AEM.02566-14>
- Williams, R., Keller, V., Voß, A., Bärlund, I., Malve, O., Riihimäki, J., Tattari, S., Alcamo, J., 2012. Assessment of current water pollution loads in Europe: estimation of gridded loads for use in global water quality models. *Hydrol. Process.* 26, 2395–2410. <https://doi.org/10.1002/hyp.9427>
- Withers, P.J., Jordan, P., May, L., Jarvie, H.P., Deal, N.E., 2014. Do septic tank systems pose a hidden threat to water quality? *Front. Ecol. Environ.* 12, 123–130. <https://doi.org/10.1890/130131>

Chapter 3: Supplemental Information

SI Table 3.1. Soil characteristics for excavated soil used to fill experimental soil columns.

Soil Column Location	Soil Sample Depth	Texture (Calculated /Estimated)	Particle Size Distribution			Bulk Density (g ml ⁻¹)	Soil Moisture %	NH ₄ -N (mg kg ⁻¹)	NO ₃ (mg kg ⁻¹)	pH	Total N (%)	Total C (%)
			Sand	Silt	Clay							
Above lateral	0 - 10 in	Fine Silt Loam/ Silt Loam	55.5	36.2	8.4	1.39	0.98	3.01	2.65	7.6	0.10	1.2
Below lateral	Below 22 in*	Loam/ Silt Loam	41.3	45.9	12.7	1.19	1.08	4.12	2.73	6.8	0.13	1.4

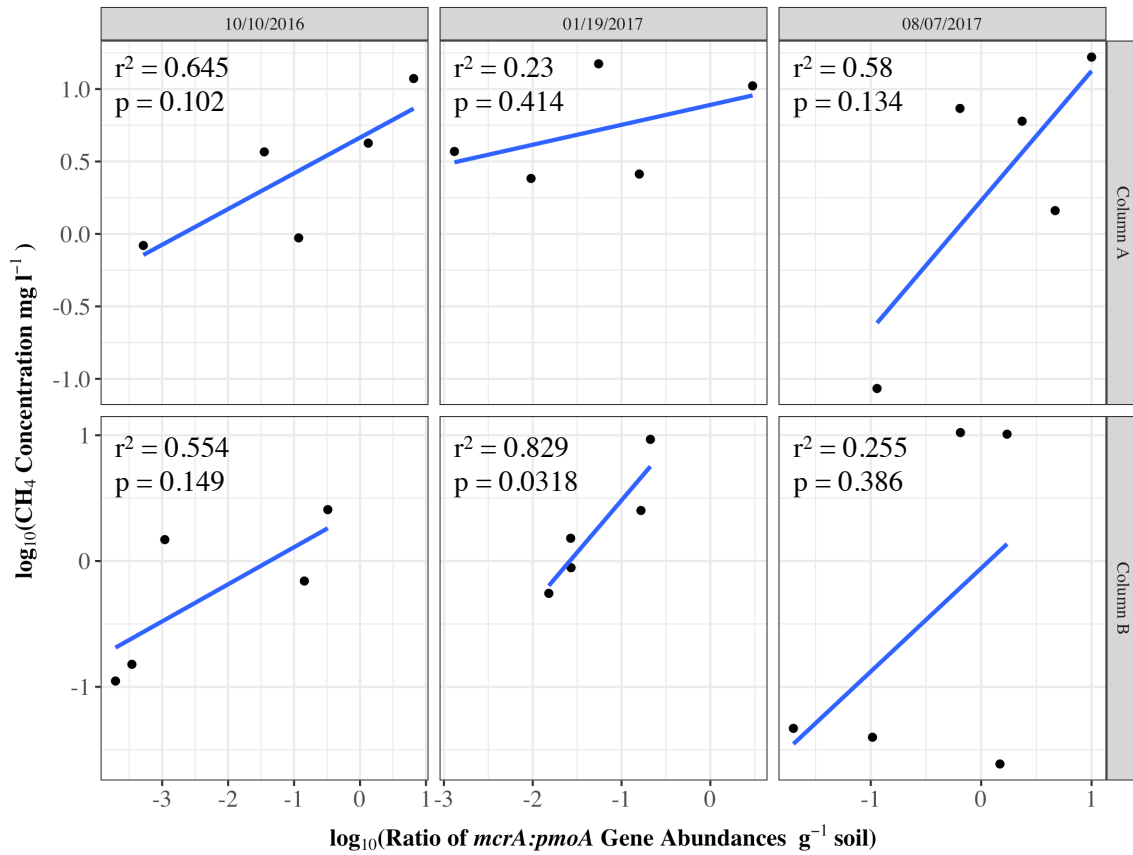
*Soil was collected below the lateral in the active leach field.

SI Table 3.2. Synthetic wastewater recipe adapted from Aiyuk & Verstraete (2004).

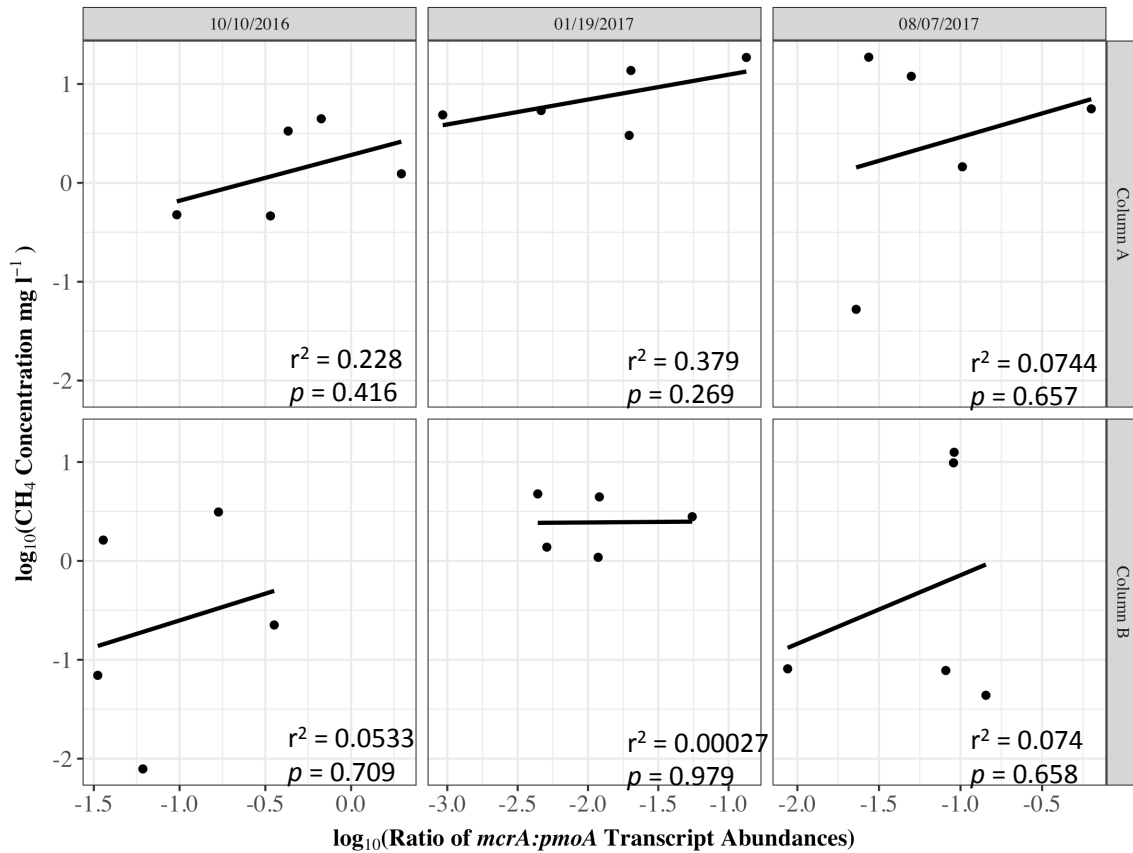
Component	Amount (mg L ⁻¹)
<i>Chemical compounds</i>	
Urea	1600
NH ₄ Cl	200
Na-acetate · 3H ₂ O	2250
Peptone	300
MgHPO ₄ · 3H ₂ O	500
K ₂ HPO ₄ · 3H ₂ O	400
FeSO ₄ · 7H ₂ O	100
CaCl ₂	100
<i>Food ingredients</i>	
Starch	2100
Milk powder	2000
Dried yeast	900
Vegatable oil	500
<i>Trace metals</i>	
Cr(NO ₃) ₃ · 9H ₂ O	15
CuCl ₂ · 2H ₂ O	10
MnSO ₄ · H ₂ O	2
NiSO ₄ · 6H ₂ O	5
PbCl ₂	2
ZnCl ₂	5

SI Table 3.3. Primers used to amplify *mcrA* and *pmoA* in qPCR assays (Costello and Lidstrom, 1999; Ferris et al., 1996; Luton et al., 2002; Steinberg and Regan, 2009). Amplicon length is based on the pure culture used to create qPCR standards.

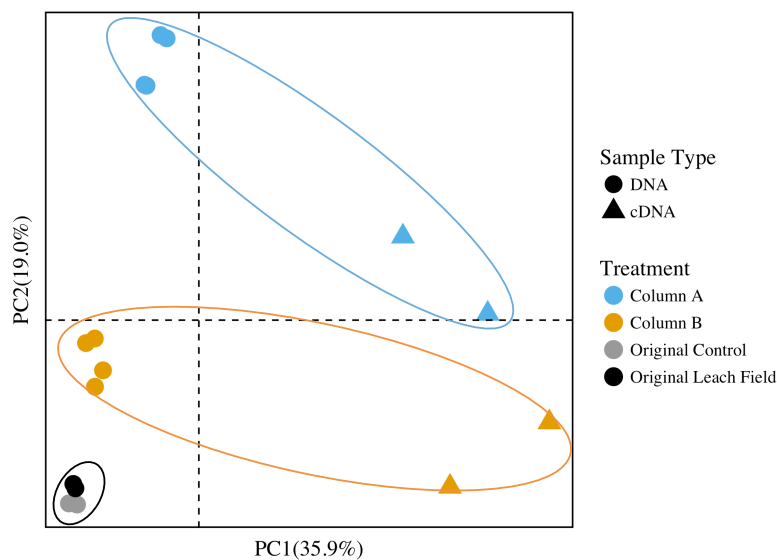
Target		Primer			Amplicon	
Microbial	Gene	Primer	Length	Sequence (5'-3')	Length	Reference(s)
Community			(bp)		(bp)	
Methanogens	<i>mcrA</i>	mlasF	23	GGTGGTGTMGDDTTCACMCARTA	490	Steinberg & Regan, 2009; Luton et al., 2002
		mcrA rev	24	CGTTCATBGCCTAGTTVGGRTAGT		
Methanotrophs	<i>pmoA</i>	A189F	18	GGNGACTGGGACTTCTGG	508	Costello & Lidstrom, 1999
		mb661R	19	CCGGMGCAACGTCYTTACC		
General	16S	1055F	16	ATGGYTGTCGTCAGCT	337	Ferris et al., 1996
Bacterial	rRNA	1392R	15	ACGGGCGGTGTGTAC		



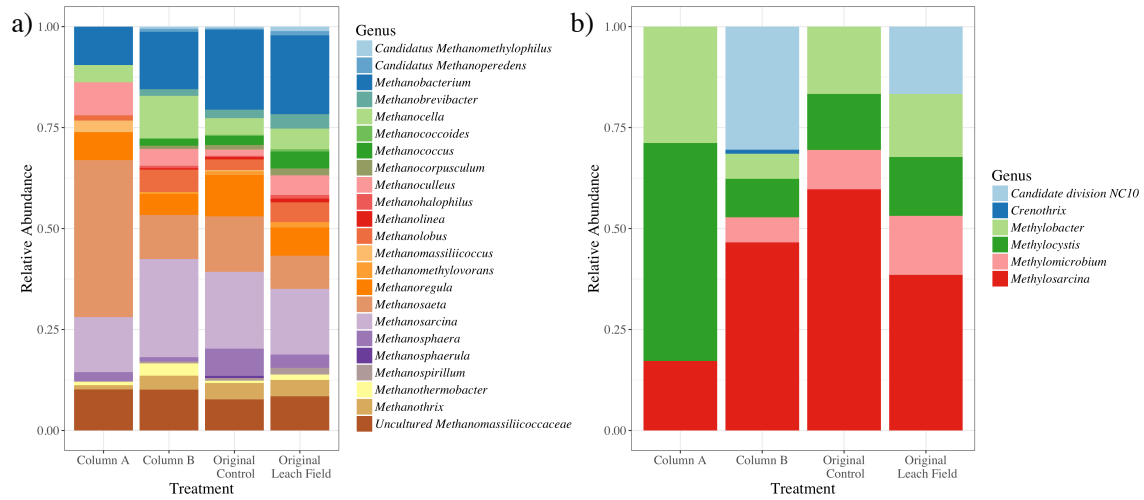
SI Figure 3.1. Measure CH₄ concentrations versus the ratio of *mcrA* to *pmoA* gene abundances by sampling date for Column A and B.



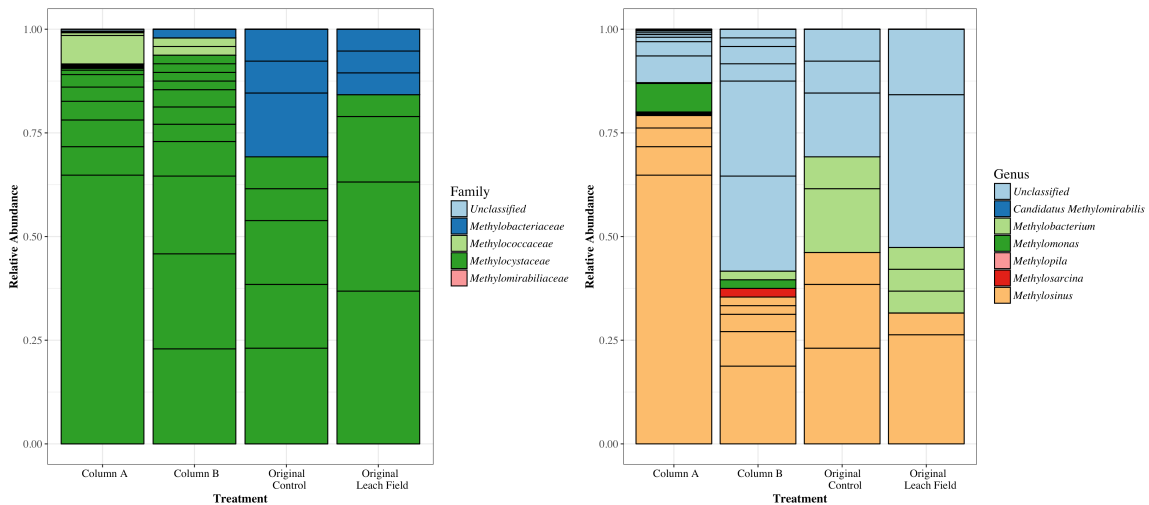
SI Figure 3.2. Ratio of *mcrA* to *pmoA* transcript abundances vs measured CH₄ depth concentrations.



SI Figure 3.3. PCoA based on weighted UniFrac distance matrix of 16S rRNA sequencing data; DNA samples (circles), cDNA samples (triangles) and treatment (original control and leach field soils and experimental Columns A and B).



SI Figure 3.4. Functional gene sequencing results for a) *mcrA* and b) *pmoA* amplicon libraries. Relative abundances for Column A, Column B and original soils (leach field and control) are shown at the genus level. Genus level reads are shown if their abundance is greater than 1% of reads by sample.



SI Figure 3.5. 16S rRNA Amplicon library sequencing results for methanotroph groups including the bacterial families *Methylococcaceae*, *Methylocystaceae*, and *Methylobacteriaceae* and the NC10 phylum (546 total reads across all samples). a) 16S rRNA methanotroph relative abundance with reads assigned at the family level and, b) reads assigned at the genus level.

CHAPTER 4

VARIED TRENDS IN CH₄, N₂O, AND CO₂ FLUXES STIMULATED BY RAIN EVENTS IN WELL-DRAINED SOILS ABOVE LEACH FIELDS

Abstract

Septic systems are a common form of onsite wastewater treatment for rural households in the U.S. Notwithstanding their prevalence, treatment performance is seldom monitored onsite, and little is known about leach field system greenhouse gas (GHG) emissions and microbial cycling. This study aimed to measure a leach field soil system's response to a rapid increase in soil volumetric water content (VWC) from a rain event. Methane (CH₄), carbon dioxide (CO₂), and nitrous oxide (N₂O) emissions and subsurface concentrations in leach field soils were monitored for 4 weeks prior to a wetting event. Following baseline measurements, a rain event was simulated and GHG fluxes and subsurface concentrations were measured in leach field and control lawns for 3 hours after wetting. GHG cycling microbial communities were likewise monitored before and after rain using the functional genes *mcrA* and *pmoA* for CH₄ cycling and *cnorB* and *nosZ* for N₂O cycling. Baseline GHG fluxes and subsurface measurements showed no significant differences between control and leach field soils. However, following the rain event, GHGs were significantly greater from leach field soils for CO₂ ($p = 0.017$) and N₂O ($p = 0.035$), but not for CH₄ ($p > 0.05$). Microbial populations did not change significantly over the rain event experiment at the DNA level, but shifts were seen at the transcript level for CH₄ cycling biomarkers with relatively greater increases in transcript abundances for production genes (*mcrA*) as compared to consumption genes (*pmoA*). These results indicate that GHG emissions caused by a rain event can be significantly higher than previously reported emissions

from leach field systems. Furthermore, GHG emission trends differ across the three measured gases in terms of timing and intensity of fluxes to the atmosphere.

4.1 Introduction

More than 1 in 5 homes in the U.S. rely on septic systems for onsite wastewater treatment (US EPA, 2012). Despite their prevalence, these systems have been understudied in terms of their treatment effectiveness and impacts on water and air quality, particularly with respect to greenhouse gas (GHG) emissions. Additionally, the associated microbial communities controlling GHG cycling in these systems are poorly understood, specifically their response to rapid changes in soil volumetric water content (VWC). Only a few studies have attempted to measure GHG emissions from the soil dispersal component (i.e. leach field) of septic systems (Diaz-Valbuena et al., 2011; Truhlar et al., 2016). Leach fields introduce high concentrations of organic carbon and nutrients, such as nitrogen (N) and phosphorus (P), to the subsurface which can stimulate native soil microbial populations to cycle nutrients and in the process create and cycle greenhouse gases such as methane (CH₄), nitrous oxide (N₂O), and carbon dioxide (CO₂).

A study by Truhlar et al. (2016) found that greenhouse gas emissions from leach field systems accounted for approximately 19% of the total GHG emissions from well-functioning septic tank systems (total emissions were estimated to be 0.27 tonne CO₂-equivalents (CO₂e) capita⁻¹ year⁻¹). However, differences in soil GHG emissions between leach field and control treatments were significant only for N₂O fluxes and not for CH₄ or CO₂ fluxes. Truhlar et al. also measured roof vent emissions from septic systems and found that roof vent and leach field soil emissions were similar for CO₂ but were significantly greater in the roof vent compared to leach field soils for both CH₄ and N₂O. The discrepancy between roof vent and leach field

emissions for these two potent greenhouse gases suggests there may be significant microbial cycling of CH₄ and N₂O in soils above leach field systems.

Previous work has found that soil volumetric water content (VWC) is a significant driver of GHG emissions from leach field and other terrestrial systems (e.g. peat bogs and rice paddies) particularly for CH₄ (Fernández-Baca et al., 2018b; Kotiaho et al., 2010; Lee et al., 2014; S. C. Whalen, 2010). Likewise, a study by Fernández-Baca et al. (2018b) found soil VWC was correlated to gene abundances of biomarkers for CH₄ cycling in leach field soils including *mcrA*, a gene encoding the α -subunit of methyl coenzyme M reductase found in all known methanogens and involved in the final step of methane production, and *pmoA*, a gene encoding a subunit of the particulate version of methane monooxygenase (pMMO) found in the vast majority of known aerobic methanotrophs which is responsible for the first step of methane oxidation (Colin Murrell and Radajewski, 2000; Steinberg and Regan, 2009). Although sustained increases in soil VWC have been shown to increase CH₄ emissions in a variety of environments from leach field to pasture and forest soils, the response of soils to an instantaneous increase in VWC from a wetting event has not been explored in leach field soils (Chamberlain et al., 2016; Christiansen et al., 2016; Fernández-Baca et al., 2018b). Well-drained and upland soils are thought to be net CH₄ sinks, responsible for consuming up to 80% CH₄ produced in subsurface soils, however their response to a wetting event could change the CH₄ flux dynamics of these soils transforming them from net sinks to net sources (Wilson et al., 2016).

Similarly, increases in N₂O emissions can be driven by increases in soil VWC particularly in soils that are characteristically dry such as grasslands (Davidson, 1992;

Smith et al., 2003; Wilson et al., 2016). While temperature is known to be a strong driver of N₂O emissions, due to stimulation of microbial respiration leading to a reduction of available O₂, an increase in soil VWC has been shown to have a similar effect, particularly in wetted soils (Kim et al., 2012; Smith et al., 2003). Because leach field soils already have higher N₂O fluxes to the atmosphere than control soils, their N₂O response to a rain event could be significant (Truhlar et al., 2016). The N₂O cycle is particularly complicated at the microbial scale as there are several denitrification steps preceding the production and consumption of N₂O. Full denitrification of nitrate (NO₃⁻) to nitrogen gas (N₂) is dependent on the sequential reduction of nitrate to nitrite, nitric oxide, nitrous oxide and finally N₂ by the enzymes nitrate reductase (Nar), nitrite reductase (Nir), nitric oxide reductase (Nor), and nitrous oxide reductase (Nos), respectively. The functional genes *cnorB* and *nosZ* (encoding for the enzymes Nor and Nos, respectively) have been used to quantify the microbial populations directly involved in the cycling of N₂O in environmental soil samples and have previously been used for target denitrifying populations found in leach field soils (Braker and Tiedje, 2003; Dandie et al., 2008; Fernández-Baca et al., 2018b; Henry et al., 2006).

Diaz-Valbuena et al. (2011) measured dissolved gas concentrations from septic tank effluent and found that concentrations ranged from 0.0 to 3.6 mg l⁻¹ for CH₄ and 0.6 to 12 mg l⁻¹ for CO₂. They were unable to detect any dissolved N₂O but did not report detection limits for dissolved N₂O measurements, thus any N₂O in the septic effluent may have been just below their quantification limit. Despite these potential subsurface inputs of dissolved CH₄ and CO₂ in the leach field Diaz-Valbuena et al.

(2011) found negligible atmospheric emissions of CH₄ and CO₂ from leach field soils under ideal operating conditions (i.e. not flooded). This suggests soil microbial populations may be mitigating emissions of leachate CH₄ by cycling the subsurface inputs of dissolved CH₄ and CO₂ from leach field systems. Moreover, native soil microbial communities may be stimulated to produce CH₄ and N₂O in anaerobic soil niches from subsurface nutrient inputs of septic effluent, which have high concentrations of both carbon and nitrogen (Cooper et al., 2015). *In situ*, subsurface measurements of key greenhouse gases have not previously been measured in leach field soils, thus the potential for microbial communities to be cycling gases subsurface is unknown. Coupling surface fluxes and subsurface measurements of GHG concentrations is valuable to understanding the dynamic soil microbial cycling of these gases in soils.

The aim of this study was to examine the dynamic GHG flux and microbial response in leach field soils and control soils to an instantaneous increase in soil water content due to a simulated precipitation event. To this aim, we measured surface greenhouse gas emissions in leach field and control soils before and after a significant rain event. Furthermore, we aimed to characterize the subsurface profile *in situ* of leach field soils and control lawn soils. In addition to GHG measurements, we quantified CH₄ and N₂O cycling functional gene and transcript abundances to examine the temporal relationship between measured GHG emissions and key populations controlling GHG cycling in these systems after a rain event.

4.2 Materials and Methods

4.2.1 Study site description

The study site is located in central New York and has previously been characterized (Site 7 in Truhlar et al. (2016) and Fernández-Baca et al. (2018b)). The study site has unfertilized, well-draining, grass-covered soils that are characteristically dry. Control lawn soils are defined as soils roughly 6 m upslope from the leach field system. All measurements were taken between August and September of 2017.

4.2.2 Surface soil gas flux measurements

Surface gas fluxes of CH₄, CO₂, and N₂O were measured using a modified field chamber method as previously described in Molodovskaya et al. (2011) and Fernández-Baca et al., (2018b). Ten-ml samples were stored in pre-sealed 9-ml vials which were flushed twice with N₂ to remove residual atmospheric gases and evacuated to approximately -0.74 atm. Gas samples were measured every 10 minutes for 30 minutes from the flux chambers and analyzed via gas chromatograph equipped with a flame ionization detector for CH₄ and CO₂, a thermal conductivity detector for O₂, and an electron capture detector for N₂O (Shimadzu, Model Number GC2010). Gas fluxes were calculated by fitting a linear regression to chamber gas concentrations and taking the slope of the line divided by the chamber soil surface area.

4.2.3 Subsurface soil gas probe installation and measurements

Four stainless steel soil gas vapor probes (AMS Part No. 211.00) were installed in each leach field and control lawns for a total of 8 probes. Probes were installed using a 1 in diameter soil corer to create a hole; after the probe was placed at the desired depth the hole was backfilled with native soil. Probes were spaced a

minimum of 6 m apart and installed at two depths (0.2 m and 0.5 m) below the surface with the 0.5 m depth representing the location closer to the leach field laterals (which were sited approximately 1 m below the surface) and the 0.2 m depth representing ‘near-surface’ soils (**Error! Reference source not found.**). Tubing cut to the exact length for each depth was used to connect probes to a 3-way stopcock with luer lock connectors used for sampling. Stopcocks were kept in the closed position until sampling. Prior to taking a gas sample, the tubing was evacuated by using a syringe to pull the holdup volume of gas contained in the tubing and discarding it. The sample was then taken by pulling a 35 ml gas volume using a sterile syringe. Samples were stored in 20 ml pre-sealed, evacuated vials. Samples were analyzed for CH₄, CO₂, and N₂O using the same gas chromatograph method described above for flux measurements (Fernández-Baca et al., 2018b; Molodovskaya et al., 2011).

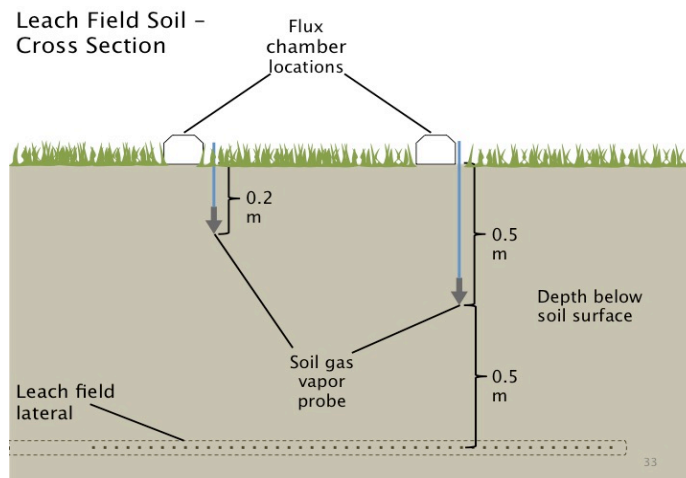


Figure 4.1. Cross-sectional view of soil gas vapor probe subsurface locations with respect to existing location of leach field laterals (not shown to scale). Flux measurements were taken immediately adjacent to subsurface measurements. The experimental setup was identical in control soils.

4.2.4 Baseline gas flux and depth measurements

Background gas flux and subsurface gas measurements were taken for the 4

weeks prior to the simulated rain event to establish ‘baseline’ GHG emissions and subsurface production at the site. Surface gas flux measurements were taken adjacent to each of the soil gas vapor probe locations for 4 measurements per leach field and control on each sampling date. Subsurface gas concentrations were measured through each of the installed soil gas vapor probes for 2 measurements at 0.2 m and 2 measurements at 0.5 m per treatment for each sampling date.

4.2.5 Rain event study

The simulated rain event took place over 6 hours in one afternoon. Six infiltration rings made of 0.3 m diameter PVC pipe with beveled edges were installed approximately 3 m apart to a depth of 5 cm in soils (Figure 4.1). Surface gas fluxes and depth measurements were taken immediately prior to the rain event in triplicate in each leach field and control soils (Figure 4.1). Following these ‘dry’ measurements, a rain event was simulated at two of the infiltration rings in each leach field and control soils, while one infiltration ring, situated between the two wetted sites, remained dry. The precipitation event was created by adding 3.75 l of well water to two of the infiltration rings per treatment (leach field or control), the approximate equivalent of a 5 cm rain event, resulting in a brief period of pooled water at the soil surface, before water percolated down into soil.

Flux and subsurface gas measurements were taken within the infiltration ring immediately after pooled water permeated the soil (e.g. no visible pooled water on the soil surface) approximately 30 minutes after the rain event and twice more at 1.5 h and 3 h after the wetting event.

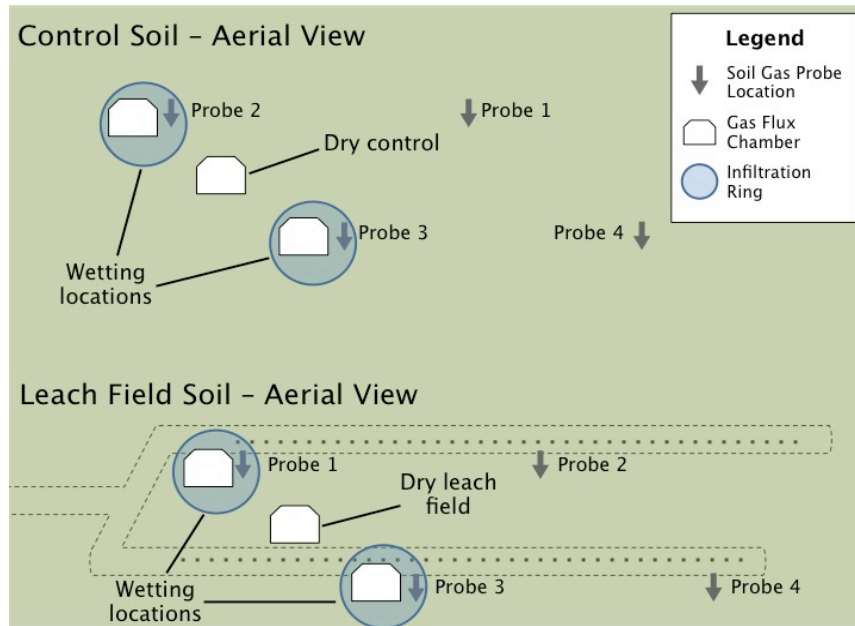


Figure 4.1. Experimental set-up for rain event with three flux chamber locations per treatment and all 8-soil gas vapor probe locations shown (not drawn to scale). Subsurface leach field lateral locations are shown with dotted outlines. Soil gas vapor probe depths are the same for leach field and control: Probe 1 – 0.2 m; Probe 2 – 0.5 m, Probe 3 – 0.2 m, and Probe 4 – 0.5 m.

4.2.6 Soil temperature and volumetric water content measurements

Soil temperature and volumetric water content (VWC) were measured periodically throughout the experiment within the infiltration ring area. Soil temperature was monitored using a 10 cm digital temperature probe, immediately adjacent to flux chambers within the infiltration rings. VWC was measured using two EC-5 Soil Moisture Sensors (Decagon Devices, Cat. No. 40593) inserted vertically into soil. Data was logged using the Em-50 5-channel data logger (Decagon Devices, Cat. No. 40800).

4.2.7 Soil Sampling

Soils were sampled immediately adjacent to the flux chamber within the infiltration ring prior to the rain event and twice more at 1.5 h and 3 h after the rain

event. One soil sample was taken per treatment and time point to avoid significantly altering the soil environment. Samples were taken using a 2.54-cm diameter soil corer that was rinsed with deionized water and ethanol and flame sterilized between samples. Soil samples were taken at a 0 to 10 cm depth and stored in 50 ml centrifuge tubes which were placed on ice before returning to lab where soils were flash-frozen in liquid N₂ and stored at -80°C until extraction. Soil from adjacent lawn was used to refill core holes to reduce gas exchange between subsurface soils and the atmosphere. Previously sampled soils were avoided for the next sampling time point.

4.2.8 Nucleic acid extractions and qPCR assays

Soil samples were homogenized using a sterile spatula prior to subsampling for duplicate extractions and gravimetric dry weight determination. Gravimetric dry weight determination was done using a pre-weighed tin with approximately 2 g soil, subsampled from each soil core. Soils were placed on a pre-weighed tin and reweighed. Samples were dried in an oven at 105°C ($\pm 1^\circ\text{C}$) for 24 h. Soil was removed from the oven and cooled in a desiccator to room temperature before weighing. The ratio of soil dry weight to wet weight was used to estimate the dry weight of soil samples used for DNA and RNA extractions.

DNA and RNA were extracted from approximately 2 g soil samples using the RNeasy PowerSoil Total RNA kit and the RNeasy PowerSoil DNA Elution kit (Qiagen) following manufacturer instructions. DNA concentrations were quantified using the Quant-iT PicoGreen dsDNA assay (Molecular Probes, Eugene, OR) and quality checked using a NanoDrop spectrophotometer (NanoDrop ND-1000, Thermo Scientific, Waltham, MA).

RNA was DNase treated to remove contaminating DNA using the RQ1 RNase-free DNase kit (Promega) following manufacturer's instructions. RNA was quantified using the Quant-it RNA assay kit (Invitrogen). The Advanced iScript cDNA synthesis kit (Bio-Rad) was used to synthesize cDNA from the DNase treated RNA, according to manufacturer's instructions.

Quantitative PCR assays were performed for all 4 biomarkers (*mcrA*, *pmoA*, *cnorB*, and *nosZ*) in triplicate for both DNA and cDNA using degenerate primers as previously reported in Fernández-Baca et al. (2018b) (Bourne et al., 2001; Braker and Tiedje, 2003; Ferris et al., 1996; Henry et al., 2006; Steinberg and Regan, 2008) The qPCR reaction mixture was composed of 1X SsoAdvanced Universal SYBR Green Supermix, 17.5 pmol of each primer, and 3 μ l of diluted template DNA (to achieve concentrations of approximately 10 ng μ l⁻¹) to a total reaction volume of 25 μ l. Thermal cycling and quantification were done using the iCycler IQ (Bio-Rad) with standard dilution curves as previously described in Fernández-Baca et al. (2018). Published thermal cycling protocols were used for selected primer sets (Bourne et al., 2001; Braker and Tiedje, 2003; Ferris et al., 1996; Henry et al., 2006; Steinberg and Regan, 2008). Ct values calculated in the iCycler IQ software were used for quantification. Melt curve analyses were conducted on all reactions to ensure specificity and confirmation of a subset of samples by Sanger sequencing at the Cornell University Biotechnology Resource Center showed amplification of target genes.

4.3 Results

4.3.2 Baseline greenhouse gas flux measurements

Prior to the rain event study, surface gas flux and subsurface concentrations were measured to determine baseline greenhouse gas levels in both control and leach field soils. Baseline measurements were taken once a week for 4 weeks prior to the simulated rain event study. CH₄, CO₂, and N₂O fluxes varied over the 4-week measurement period prior to the rain event study (Figure 4.2). CH₄ fluxes were similar between leach field (mean -0.0013 ± 0.0018 g CH₄ m⁻² d⁻¹) and control soils (mean -0.012 ± 0.025 g CH₄ m⁻² d⁻¹), with net emissions for both close to zero over the 4-week period. In contrast, net production of N₂O was observed in both treatments (mean 0.006 ± 0.001 g N₂O m⁻² d⁻¹ and 0.0003 ± 0.0002 g N₂O m⁻² d⁻¹ over the 4 weeks) with the exception of week 4 in which control and leach field soils were marginally net consuming (-0.002 g N₂O m⁻² d⁻¹ and -0.00003 g N₂O m⁻² d⁻¹ for control and leach field soils, respectively). As expected, CO₂ fluxes were net positive in both control and leach field soils for all dates, ranging from a maximum average flux of 39.4 g CO₂ m⁻² d⁻¹ and 22.4 g CO₂ m⁻² d⁻¹ in week 1 leach field and control soils, respectively, down to a minimum average flux of 14.7 g CO₂ m⁻² d⁻¹ and 13.4 g CO₂ m⁻² d⁻¹ in week 4 leach field and control soils, respectively. These results show a clear decrease in CO₂ emissions over time from week 1 to week 4 in both control and leach field soils ($p = 0.004$ and 0.0067 for control and leach field soils, respectively) indicating a decrease in net primary production as summer ends. Leach field fluxes were not significantly different from control soil fluxes for any of the gases during the 4-week period.

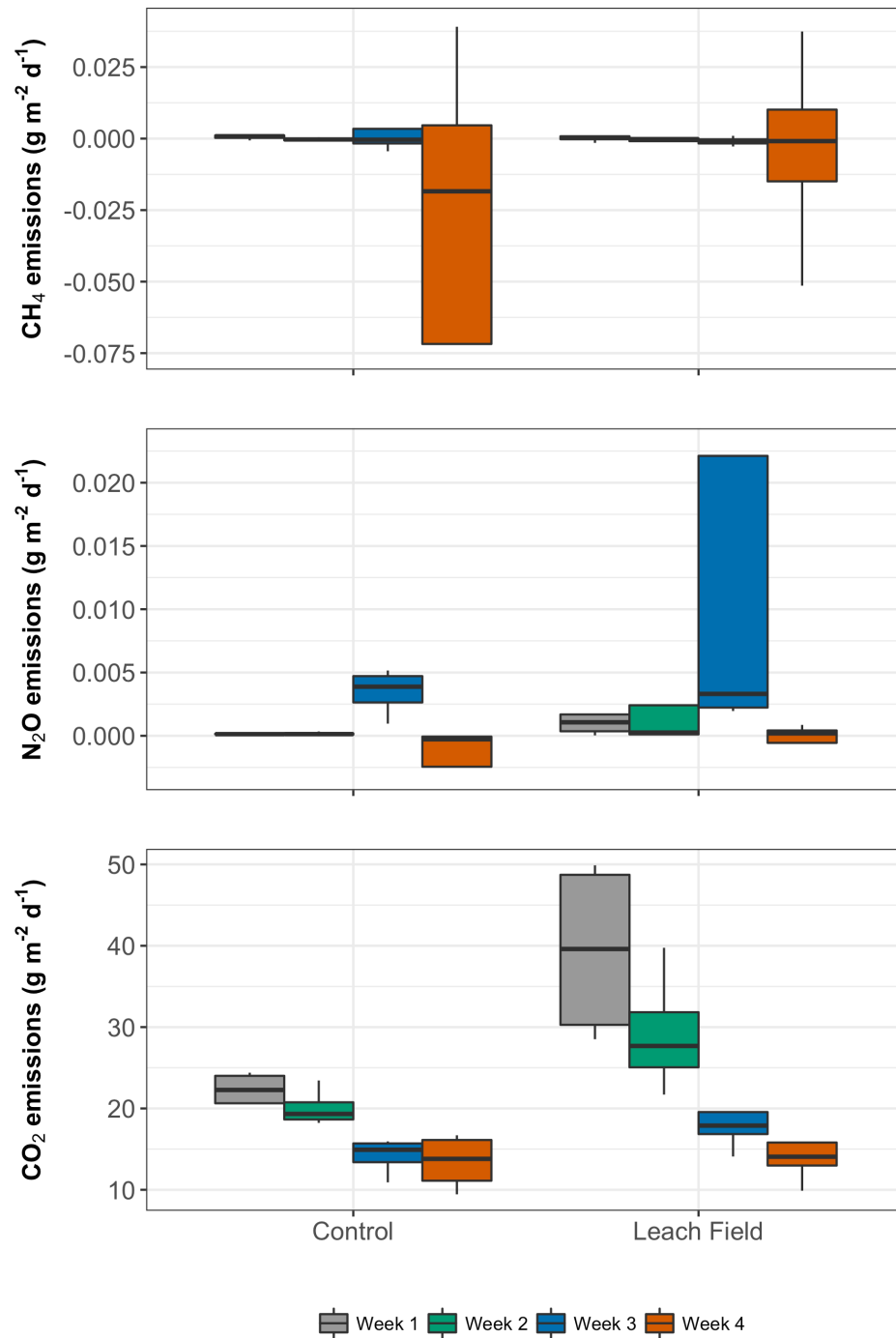


Figure 4.2. Surface CH₄, N₂O, and CO₂ gas fluxes in g m⁻² d⁻¹ for the 4-week baseline measurement period prior to the simulated rain event in both control and leach field soils ($n = 4$ for each treatment and week). Boxplots show the inter-quartile range (IQR) from quartile 1 at 25% to quartile 3 at 75%. The horizontal black line within the box indicates the median. Upper and lower whiskers indicate the highest and lowest data point within 1.5 times the IQR.

4.3.3 Baseline subsurface gas measurements

Subsurface soil gas concentrations of CH₄, CO₂, and N₂O were measured over a 4-week baseline period leading up to the rain event study at depths of 0.2 m and 0.5 m (Figure 4.3). In both leach field and control soils the 0.2 m deep CH₄ concentrations were close to atmospheric (mean concentrations over the 4-week period were 1.72 and 2.17 ppm, respectively) while deeper samples were generally below atmospheric (mean CH₄ concentrations of 1.39 and 1.29 ppm, respectively). However, differences between the two depths were not significant for CH₄ in any of the individual weeks at a 95% confidence interval, likely due to the low sample size ($n = 2$ for each depth, treatment, and sample date) and spread in the replicate samples. O₂ and N₂ had similar depth profiles to CH₄ with atmospheric concentrations in the shallower samples and lower mean concentrations (below atmospheric) in deeper samples (SI Figure 4.1). In contrast, N₂O had higher mean concentrations in the deeper 0.5 m samples (means, 1.58 and 1.06 ppm for control and leach field soils, respectively) as compared to the shallower 0.2 m samples (means, 0.88 ppm for control and 0.67 ppm for leach field). However, the observed difference in N₂O concentrations between the 0.2 m and 0.5 m depths was only significant in week 3 leach field soils ($p = 0.0037$). CO₂ had a similar pattern to N₂O, with 0.5 m samples having mean concentrations of 36,920 ppm and 20,004 ppm in control and leach field soils, respectively, as compared to the shallower samples with mean concentrations of 8,324 and 9,477 for control and leach field soils, respectively. Differences in CO₂ concentrations at depth were only significant for week 2 ($p = 0.023$) and week 3 ($p = 0.045$) in the control soils and week 3 ($p = 0.039$) in leach field soils.

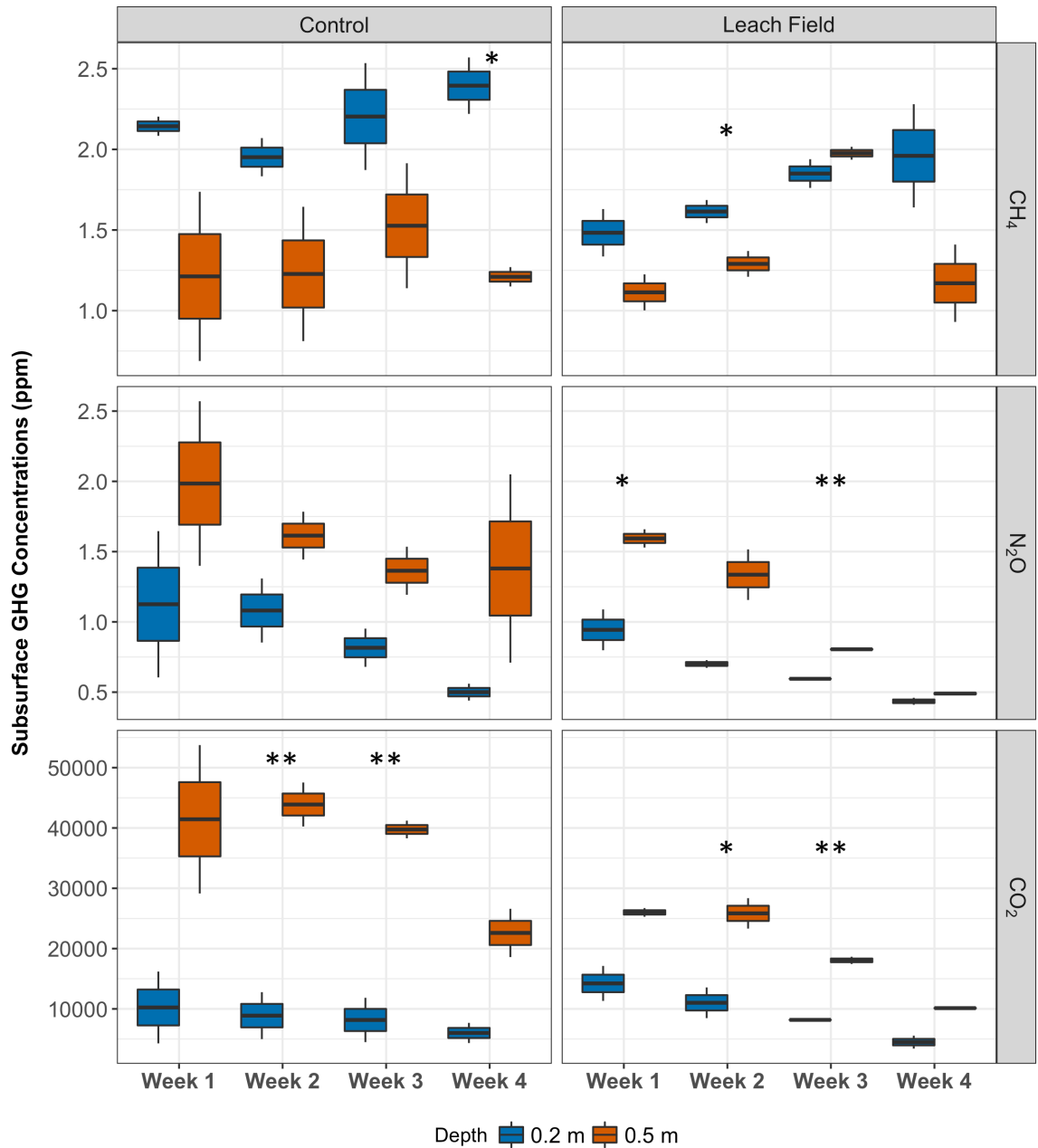


Figure 4.3. Subsurface concentrations of CH₄, N₂O, and CO₂ at 0.2 m and 0.5 m below the soil surface for both leach field and control soils over four weeks prior to simulated rain event ($n = 2$ for each sample date, treatment, and depth). Significant differences between depths at a 95% confidence interval are indicated with double asterisks (**), significance at a 90% confidence interval are shown with one asterisk (*). Boxplots show the inter-quartile range (IQR) from quartile 1 at 25% to quartile 3 at 75%. The horizontal black line within the box indicates the median. Upper and lower whiskers indicate the highest and lowest data point within 1.5 times the IQR.

4.3.4 Preliminary rain event data (2016)

A trial simulated rain event was conducted a year prior to this study to determine the optimal rainfall volume to stimulate CH₄ fluxes. The same experimental set-up described previously, using installed infiltration rings and gas flux chambers, was used for the trial run, however no subsurface soil gas vapor probes were installed. Three different simulated rainfall events of increasing intensity were created in three infiltration rings installed over the leach field. Rain events of approximately 1.25, 5, and 10 cm of rain were tested. One location representing ‘dry’ soil conditions received 0 in of rain and had an average soil VWC of 0.06 m³ m⁻³. Gas fluxes were measured 40 minutes after the rain event and again 1.5 hour after the rain event at each of three wetted locations as well as the dry site.

Elevated CH₄ emissions were observed at both the 40-min and 1.5 h measurements for each of the wetted locations as compared to the dry site. Soil VWC likewise increased with increasing rainfall volumes with averages of 0.272, 0.268, and 0.202 m³ m⁻³ for 1.25, 5, and 10 cm of rain, respectively. A linear relationship was observed between inches of rain and measured gas fluxes at both 40 minutes and 1.5 hours ($R^2 = 0.994$ and 0.999 , respectively) (SI Figure 4.2 and 4.3). Based on these preliminary data we chose to use a rain event of approximately 5 cm, which is within the range of heavy rainfall events observed in central New York.

4.3.5 Rain event simulation

4.3.5.1 Soil volumetric water content and temperature

Soil VWC and temperature changed over the course of the rain event study (Figure 4.4). Soil VWC was highest in the wetted soils and dried over time but did not

return to 'dry' leach field soil conditions (approximately $0.065 \text{ m}^3 \text{ m}^{-3}$) before the end of the experiment. Mean soil VWC for wetted sites over the course of the experiment were similar for control ($0.228 \pm 0.04 \text{ m}^3 \text{ m}^{-3}$) and leach field ($0.204 \pm 0.09 \text{ m}^3 \text{ m}^{-3}$) soils. Leach field soils had slightly higher VWC than control soils in the non-wetted soils $0.065 \pm 0.003 \text{ m}^3 \text{ m}^{-3}$ and $0.045 \pm 0.002 \text{ m}^3 \text{ m}^{-3}$, respectively.

Soil temperatures ranged from 23.9 to 26.6°C throughout the experiment (Figure 4.4). Wetted plots were slightly cooler than the corresponding dry plots with mean temperatures of 24.3°C and 24.8°C for wetted leach field and control soils respectively; whereas dry plots had on average warmer soils with means of 25.2°C and 25.9°C for leach field and control soils, respectively.

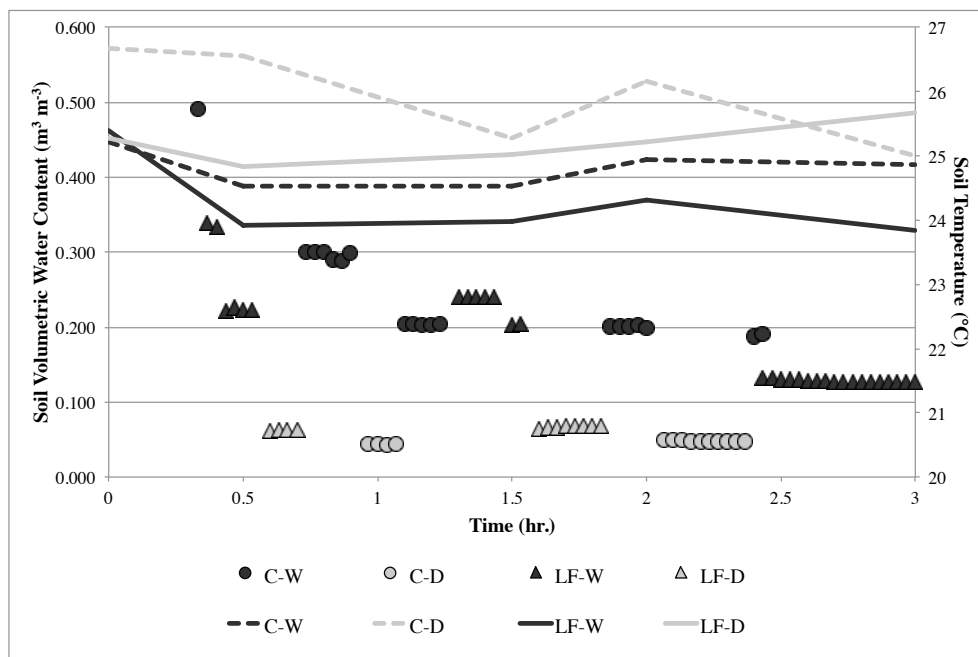


Figure 4.4. Soil volumetric water content (VWC) (leach field: triangles, control: circles) and temperature (leach field: solid lines, control: dotted lines) measured within the infiltration ring immediately following the rain event, approximately 10 cm below ground. Legend indicates treatment and wet or dry conditions: control soils wet (C-W), control soils dry (C-D), leach field wet (LF-W), and leach field dry (LF-D); triplicate measurements were taken at each time point.

4.3.5.2 Rain event gas flux measurements

Surface CH_4 , N_2O and CO_2 gas flux measurements were taken immediately prior to the rain event and were taken again 0.5, 1.5 and 3 h after the rain event (Figure 4.5). An initial increase in soil CH_4 emissions was observed from both leach field (mean, $0.017 \text{ g m}^{-2} \text{ d}^{-1}$) and control (mean, $0.014 \text{ g m}^{-2} \text{ d}^{-1}$) treatments as compared to the dry soils (means, 0.00059 and $-0.00076 \text{ g m}^{-2} \text{ d}^{-1}$ for leach field and control soils, respectively) but the pulse subsided by the 1.5 h mark. This emissions increase was significant in the leach field soils ($p = 0.026$) but not in control soils ($p = 0.095$). N_2O emissions spiked at the 0.5 h mark in wet leach field soils compared to dry soils ($p = 0.0006$) and continued to rise over time after the rain event. Control soils saw a

delayed increase in N₂O emissions, which were comparable to dry control soil emissions until 3 h after the rain event when they increased significantly ($p = 0.038$). An immediate, significant increase in CO₂ emissions was measured in both control and leach field soils ($p < 0.0001$ for both at the 0.5 h mark), with higher emissions observed in leach field soils. CO₂ emissions decreased slowly after the 0.5 h post rain time point in both treatments, but were still higher in the leach field as compared to the control soils at the 3 h mark (control soil mean of 17.2 g m⁻² d⁻¹ compared to a mean of 24.9 g m⁻² d⁻¹ for leach field soils).

In general, leach field and control soils had comparable emissions before and after the rain event. N₂O fluxes were higher from leach field soils as compared to control soils at the 0.5 h and 1.5 h measurements with p -values of 0.035 and 0.036, respectively. The only other measurement that was significantly higher in leach field soils as compared to control soils was CO₂ 3 h post rain ($p = 0.017$).

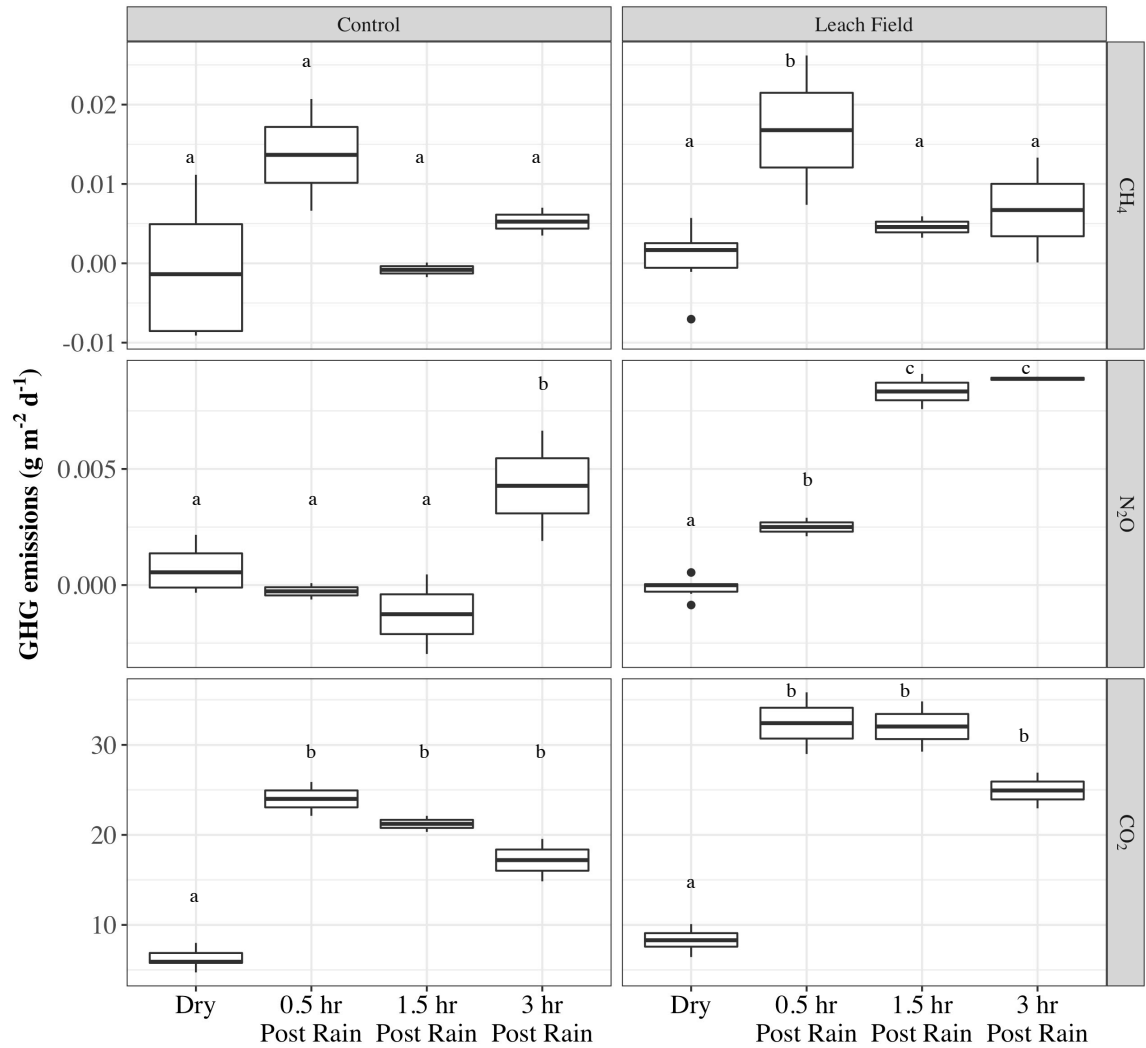


Figure 4.5. Boxplots of CH₄, N₂O, and CO₂ flux measurements before and after the rain event in leach field and control soils. Dry ($n = 3$), 0.5 h 1.5 h, and 3 h Post Rain ($n = 2$). Lowercase letters represent significant differences ($p < 0.05$) between sampling times. Boxplots show the inter-quartile range (IQR) from quartile 1 at 25% to quartile 3 at 75%. The horizontal black line within the box indicates the median. Upper and lower whiskers indicate the highest and lowest data point within 1.5 times the IQR.

4.3.5.3 Rain event subsurface gas concentrations

Subsurface CH₄, N₂O and CO₂ concentrations were taken immediately before the rain event and were measured again 0.5, 1.5 and 3 h post rain in both control and leach field soils (Figure 4.6). Only wetted soils were measure at the 0.5 h and 1.5 h

time point, in leach field soils this corresponded to probes 1 (0.2 m) and 3 (0.2 m) and in control soils probes 2 (0.5 m) and 3 (0.2 m) (Figure 4.1). All eight probes were sampled before rain and 3 h after rain.

Prior to rain, the subsurface measurements from control and leach field soils showed similar CH₄ patterns with ‘hot moment’ of high CH₄ concentrations observed in samples from probe 3 at the 0.2 m depth (approximately 150 ppm in both treatments). CH₄ concentrations in these ‘hot moment’ (probe 3 in both leach field and control) were uncharacteristically high compared to baseline measurements (highest observed measurement during baseline monitoring, in Figure 4.3 was approximately 2.5 ppm). Due to these measurement discrepancies, results described hereafter exclude probe 3 in leach field and control soils which both showed atypical CH₄ concentrations (SI Figure 4.4 shows subsurface GHG measurements removing “hot moments” observed in leach field and control probe 3). At the 0.5 h mark, all measured probes in both leach field and control soils showed an increase in subsurface CH₄ concentrations (greater than 20 ppm in all probes) as compared to before rain soils which were less than 5 ppm in all probes. Subsurface CH₄ concentrations dropped over time after the initial increase at 0.5 h post rain, and fell below 7 ppm in leach field soils and below 5 ppm in control soils at both depths.

Subsurface N₂O concentrations also showed a ‘hot moment’ in leach field probe 3 in the before rain measurement. Excluding this atypical probe, we observed a drop in below ground N₂O concentrations in both treatments at all depths (less than 0.378 ppm in all probes) 0.5 h after rain as compared to before rain measurements. N₂O concentrations increased again at the 3 h post rain sample in leach field (1.49

ppm in wetted 0.2 m probe and mean of 2.7 ppm in 0.5 m dry probes) and control (0.26 and 0.46 ppm for dry and wet 0.2 m depths, and 3.82 ppm and 2.46 ppm for dry and wet 0.5 m depths) soils. In general, higher N₂O concentrations were observed in deeper samples across all time points, regardless of wetting, as was seen with baseline measurements.

CO₂ subsurface concentrations at 0.2 m did not appear to vary over time with wetting. The subsurface concentrations were similar to baseline measurements in terms of magnitude for both control and leach field. In samples taken prior to the rain event, CO₂ subsurface concentrations were higher in the 0.5 m samples in control (mean, 28,561 ppm) and leach field (mean, 10,366 ppm) as compared to the 0.2 m control (mean, 5,374 ppm) and leach field (mean, 5,625 ppm) samples. A similar trend was observed 3 h post rain, where 0.5 m samples had higher CO₂ concentrations in control soils (24,255 ppm for dry soils and 34,433 ppm for wet soils) and leach field soils (mean, 10,450 ppm for dry soils) as compared to the 0.2 m control (mean, 8,101 ppm) and leach field (mean, 7,682 ppm) samples. Thirty minutes after rain, the 0.5 m depth concentration appeared to drop (to below 10,000 ppm) in control soils, however due to lack of replication in subsurface (0.5 m) samples, statistical analyses could not be carried out to determine significance of this pattern.

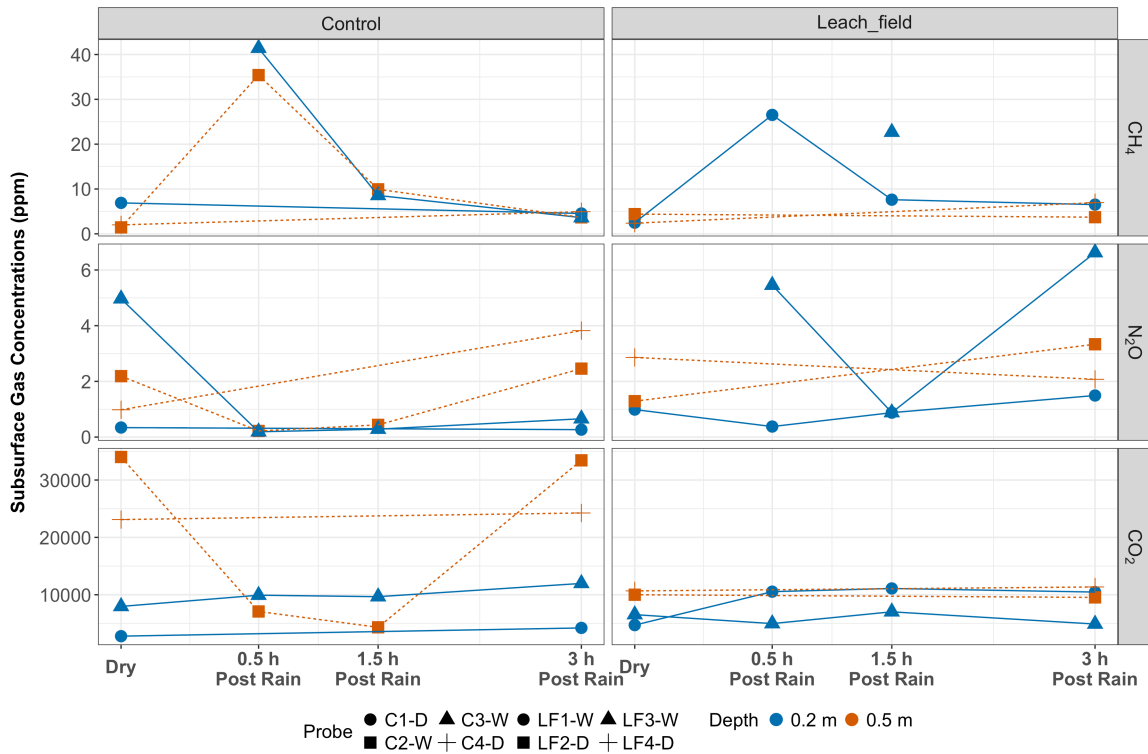


Figure 4.6. Subsurface CH₄, N₂O and CO₂ concentrations before rain, 0.5 h, 1.5 h, and 3 h post rain event at 0.2 m (solid line) and 0.5 m (dotted line) in control (C) and leach field (LF) soils. Wetted (W) and dry (D) probes are shown for each treatment.

4.3.5.4 CH₄ and N₂O cycling genes and transcript abundances

Gene abundances for key biomarker genes involved in CH₄ cycling (*mcrA* and *pmoA*) and N₂O cycling (*cnorB* and *nosZ*) as well as general Bacterial populations were similar across both treatments (Figure 4.7). Small variations were seen over time but were not significant for any individual biomarker between treatments or sampling times ($p > 0.05$ for all). Any variations observed likely reflect the inherent heterogeneity of soils as well as variability in extraction and qPCR efficiencies.

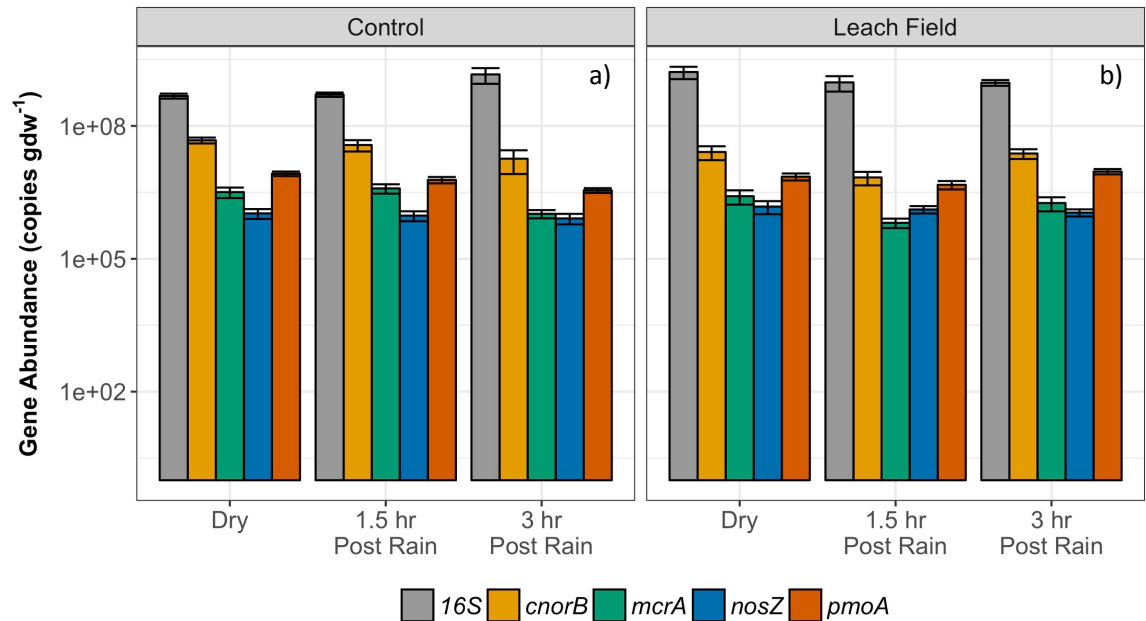


Figure 4.7. Gene abundances in a) control and b) leach field sites in dry soils, 1.5 h and 3 h after rain event for general bacterial 16S rRNA, *mcrA*, *pmoA*, *cnorB*, and “typical” *nosZ*. Error bars represent errors associated with duplicate DNA extractions and triplicate qPCR reactions.

Transcript ratios of production to consumption genes for CH₄ and N₂O showed variation with time (Figure 4.8). *mcrA:pmoA* transcript ratios increased in both control and leach field soils 1.5 h post rain compared to the dry soils ($p = 0.025$ for control and $p = 0.055$ for leach field soils). This *mcrA:pmoA* ratio increase lagged behind the elevated CH₄ fluxes we observed at 30 min. However soil samples were not taken at 30 min post rain thus elevated transcript ratios may have also occurred at this time point but were not captured in this study. *mcrA:pmoA* transcript ratios decreased again at 3 h post rain and were similar to those observed in the dry soils. Soil samples were not taken 0.5 h post rain, thus any relationship between the elevated CH₄ emissions observed and transcript abundance ratios of CH₄ cycling genes at the 30 min mark could not be examined. Transcript abundances for individual biomarkers and ratios of

transcript to gene abundances showed no clear patterns over time (SI Figure 4.5 for absolute transcript abundances per gram dry soil and SI Figure 4.6 for ratios of transcript to gene abundances).

cnorB:nosZ transcript ratios decreased from the dry soils to the 1.5 and 3 h post rain samples in both leach field and control, though not significant (Figure 4.8).

Surprisingly, a decrease of *cnorB* transcripts (the biomarker for N₂O production) relative to *nosZ* corresponded to elevated N₂O emissions in both the control and leach field soils at 1.5 and 3 h post wetting event.

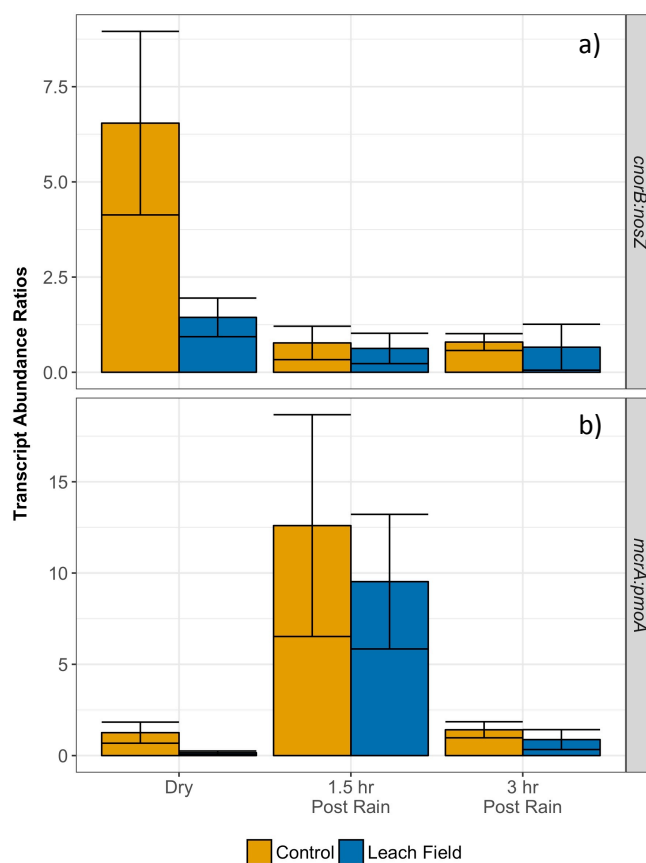


Figure 4.8. Ratios of transcript abundances for a) CH₄ cycling genes (*mcrA:pmoA*) and N₂O cycling genes (*cnorB:nosZ*) for dry soils and 1.5 and 3 h after rain event. Error bars represent errors associated with duplicate DNA and RNA extractions and triplicate qPCR reactions for each extract.

4.4 Discussion

Studying the surface greenhouse gas flux and subsurface depth profiles of leach field systems is important to understanding how these soil-based wastewater treatment systems respond to an instantaneous increase in soil VWC in terms of GHG production and cycling. Additionally, quantifying the microbial populations responsible for greenhouse gas cycling is key to a better understanding of their role in greenhouse gas mitigation. The temporal link between a precipitation event, GHG emissions, and the expression of functional genes responsible for GHG cycling is poorly understood, and has not been studied in leach field soils.

4.4.1 Baseline gas flux and subsurface concentrations

Surface gas flux and subsurface concentrations of greenhouse gases vary over time in both leach field and control lawn soils. Truhlar et al. (2016) previously found that N₂O emissions were significantly higher in leach field as compared to control soils ($p < 0.001$), however, in this study, over the course of the 4-week baseline measurements we did not find significant differences between leach field and control soils for N₂O for any given week. Likewise, no significant differences were observed for either CH₄ or CO₂ between leach field and control soils for any given week. However, when all dates were considered together, CO₂ was significantly greater in leach field soils compared to control soils ($p = 0.023$) but again there were no significant differences observed for CH₄ ($p = 0.77$) and N₂O ($p = 0.33$). Additionally, all values we observed for average fluxes from the leach field (CH₄: -0.0013 g m⁻² d⁻¹, CO₂: 25.5 g m⁻² d⁻¹, and N₂O: 0.0059 g m⁻² d⁻¹) were comparable to those previously reported by Truhlar et al. (2016) for this site in summer of 2014 (CH₄: -0.0031 g m⁻² d⁻¹

¹, CO₂: 9.1 g m⁻² d⁻¹; and N₂O: 0.00096 g m⁻² d⁻¹) which were all taken during typically ‘dry’ days (average VWC of 14.3 m³ m⁻³ for leach field and 10.6 m³ m⁻³ for control soils for summer 2014). Control soils likewise had similar flux measurements between the two studies.

We expected leach field soils to have higher subsurface concentrations of CH₄, N₂O, and CO₂ at the 0.5 m depth as compared to control soils due to subsurface inputs of septic effluent in the leach field. We measured dissolved gases in the liquid of the septic tank and found high dissolved gas concentrations for CH₄ (87.3 ± 24 mg l⁻¹), N₂O (0.21 ± 0.02 mg l⁻¹), and CO₂ (277 ± 89 mg l⁻¹). Thus, we expected to see higher subsurface GHG concentrations *in situ* at the 0.5 m depth than at the 0.2 m depth in the leach field, and higher subsurface GHG concentrations in the leach field compared to control soils. However, only one week showed significant differences in subsurface gas concentrations between leach field and control soils at the 0.5 m depth where the control had CO₂ concentrations higher than the leach field ($p = 0.022$). When all weeks were considered together, control soils had higher subsurface concentrations of CH₄ at the 0.2 m depth than at the 0.5 m depth ($p = 0.034$) and higher subsurface concentrations of N₂O and CO₂ at the 0.5 m depth than at the 0.2 m depth ($p = 0.014$ and $p < 0.0001$, respectively). These results were counter to our hypothesis that subsurface concentrations would be higher in leach field soils. It is possible that elevated subsurface concentrations of these GHG may be found even deeper than 0.5 m depth we sampled in this study, closer to the leach field laterals where wastewater is percolating into the soil. (Fernández-Baca et al., under review, 2018a) used lab-scale leach field soil columns to examine CH₄ concentrations and CH₄ cycling populations

with depth. Their results indicate that peak CH₄ emissions were observed in the area immediately surrounding the leach field laterals, and decreased in near-surface soils to down to atmospheric concentrations. It is likely we are seeing a similar pattern with our *in situ* measurements of subsurface CH₄.

Furthermore, any dissolved gases released subsurface in the leach field may be consumed quickly by the soil microbial communities found above the leach field laterals which are likely primed for leachate inputs. Fernández-Baca et al. (under review, 2018a) found that CH₄ cycling communities were present throughout the soil depth profile in leach field soil columns, including methanotrophic populations who can readily consume any CH₄ introduced subsurface. Additionally, evidence for the presence of anaerobic methanotrophs of the NC10 phylum and ANME-2D, thought to couple methane oxidation to nitrite and nitrate reduction, respectively, was found via Illumina sequencing of 16S rRNA in both leach field and control soils (Ettwig et al., 2010; Fernández-Baca et al., 2018b; Haroon et al., 2013). Thus, CH₄ consuming populations, both aerobic and anaerobic, likely have the potential to actively mitigate subsurface inputs of CH₄ in leach field soils. Overall, the baseline measurements revealed that under typical ‘dry’ soil conditions, these leach field and lawn covered soils are net consumers of atmospheric CH₄ and net producers of N₂O and CO₂ and any subsurface inputs of dissolved GHGs can be cycled by existing soil microbial communities.

4.4.2 Precipitation driven trends in greenhouse gas emissions and subsurface concentrations from leach field and lawn-covered soils

4.4.2.1 CH₄ emissions

Previous studies have shown that CH₄ emissions are driven by sustained high soil VWC in leach field and subtropical pasture soils (Chamberlain et al., 2016; Fernández-Baca et al., 2018b). In this study, CH₄ emissions from an instantaneous increase in soil VWC were examined. CH₄ emissions resulting from the simulated precipitation event were immediate in both control and leach field soils. We observed this same trend with previous tests of precipitation events on leach field soils (SI Figure 4.2 and 4.3) which showed linear increases in CH₄ fluxes with increasing amounts of rainfall both 30 min and 1.5 h after precipitation. Significant increases in CH₄ emissions were observed from the leach field at the 30 min mark ($p = 0.026$) but not from control soils ($p = 0.095$). After 30 minutes, neither treatment had CH₄ emissions distinguishable from ‘dry’ soils. Mean CH₄ emissions from the leach field increased almost 30-fold in the 30 minutes after rain compared to ‘dry’ soils.

Gas push-pull tests (GPPT) conducted *in situ* in these soils (both control lawn and leach field) revealed that CH₄ cycling populations have a limited capacity for CH₄ oxidation (SI Figure 4.7, experimental description in Appendix). Under typical ‘dry’ conditions, methanotroph populations are able to keep pace with methanogen activity, resulting in net methane sinks in the soils examined herein. However, a sudden pulse of high CH₄ concentrations overwhelms the native methanotroph populations, who are unable to consume these substantial subsurface CH₄ inputs. Thus, although there appears to be significant CH₄ mitigation in leach field and control soils, methanotroph

populations are not infinitely capable of consuming CH₄, likely resulting in the significant pulse of CH₄ measured after the simulated rain event.

Before rain measurements of subsurface concentrations of CH₄ were much higher in two of the 0.2 m probes, probe 3 in both leach field control soil, as compared to the replicate 0.2 m probes and the 0.5 m samples. Thirty minutes post rain, concentrations of CH₄ increased in three of the measured probes compared to the same probes pre-rain, however this increase in subsurface CH₄ production subsided by the 1.5 h mark and continued to decrease at the 3 h time point. These results suggest that CH₄ production is occurring even at relatively shallow depths in the soil profile. Chamberlain et al. (2016) found that CH₄ was produced subsurface in flooded pasture soils at 0 to 0.1 m below the surface, even shallower depths than examined in this study. They found that an increase in subsurface CH₄ concentrations due to flooding occurred concomitantly with an increase in surface CH₄ emissions and suggested that near-surface production of CH₄, not deeper CH₄ production, was responsible for CH₄ emissions observed at the surface. Our results support this finding, while subsurface concentrations of CH₄ were relatively low, we did observe increases in subsurface CH₄ concentrations as well as increased CH₄ emissions from both leach field and control soils 30 min after wetting. These observed increases in CH₄ surface emissions and subsurface production may be explained by enhanced soil microbial activity of methanogens, which thrive under anaerobic conditions caused by high soil VWC which in turn can suppress aerobic methanotrophy (Kim et al., 2012; Thauer, 1998).

4.4.2.2 N₂O emissions

Davidson (1992) found that there was an immediate response of N₂O

production (within minutes) in rewetted grass-covered soils. They found N₂O emission rates after a wetting event were two to five times greater than those observed from dry soil and emissions increased immediately after wetting then remained elevated up to 25 hours post wetting event. Likewise, we observed an immediate increase in N₂O emissions from leach field soils which had a mean value of -0.0001 g m⁻² d⁻¹ before wetting that increased to a mean of 0.0025 g m⁻² d⁻¹ 30 minutes after the rain event. In contrast, control soils saw a delayed increase in N₂O emissions with fluxes indistinguishable from dry soils until 3 hours post rain event.

The immediate pulse of N₂O seen from leach field may be explained by physical displacement of subsurface N₂O. However, concentrations of subsurface N₂O decreased, in both leach field and control soils at the 30 min mark but surface fluxes only increased in leach field soils. Delay in N₂O emissions from control soils may be due to the lag time associated with the microbial processes of reducing NO₃⁻ to N₂O. However, mechanisms controlling N₂O emissions in soils, likely a combination of physical mechanisms and microbial activity, are poorly understood and should be further studied in soil systems (Kim et al., 2012).

4.4.2.3 CO₂ emissions

Before wetting, CO₂ emissions from dry soils in this study (means, 6.24 g m⁻² d⁻¹ for control and 8.30 g m⁻² d⁻¹ for leach field) were higher than those observed in other lawn soils in central New York (2.42 g m⁻² d⁻¹) and Boston, MA (3.1 g m⁻² d⁻¹) (Decina et al., 2016; McPhillips et al., 2016). However, they were comparable to observed CO₂ fluxes from lawns in Melbourne, Australia, which ranged from 4 g m⁻² d⁻¹ for unfertilized lawns up to 12.8 g m⁻² d⁻¹ for fertilized lawns. Our CO₂ flux

measurements of 'dry' leach field soils were also comparable to previous measurements by Truhlar et al. (2016) for leach field soils, which ranged from 4.26 g m⁻² d⁻¹ up to 18.3 g m⁻² d⁻¹. They also found control soils to have higher mean CO₂ emissions compared to leach field soils (mean, 11.6 g m⁻² d⁻¹ for controls and 17.7 g m⁻² d⁻¹ for leach field).

In soil microcosms, increased CO₂ fluxes have previously been correlated to increases in soil VWC due to a precipitation event (Smart and Peñuelas, 2005). In this study, there was an immediate and sustained increase in CO₂ emissions from both control and leach field soils following the simulated rain event. Smart and Peñuelas (2005) found that this sustained increase in CO₂ emissions after a significant rain event (approximately 2 in) lasted 36 hours but decreased over time. Although in this study measurements were only taken up to 3 hours post rain event, we did observe CO₂ emissions decreasing over time from means of 24.0 and 32.4 g m⁻² d⁻¹ for control and leach field soils at 30 minutes post rain decreasing to means of 17.2 g m⁻² d⁻¹ for control and 24.9 g m⁻² d⁻¹ for leach field 3 hours post rain. Both temperature and soil moisture have previously been shown to be controlling factors for soil respiration, in our study temperature did not change significantly over the course of the experiment, thus we suggest soil VWC is driving the increase in CO₂ emissions (Kim et al., 2012; Livesley et al., 2010).

A portion of the observed CO₂ fluxes 30 min after wetting may also be caused by physical displacement of subsurface gases. Subsurface measurements of CO₂ before the rain event were consistent with baseline measurements, where deeper 0.5 m samples had higher CO₂ concentrations than the 0.2 m samples in both control and

leach field soils. CO₂ concentrations before the rain event were higher in control soils (mean >28,000 ppm) compared to leach field soils (mean, 10,336 ppm) at the 0.5 m depth, but were similar at the 0.2 m depth (means, 5,374 ppm and 5,626 ppm for control and leach field soils, respectively). This pattern was again observed 3 h after the rain event, however the 0.2 m depth had elevated concentrations of CO₂ compared to before rain control soils regardless of wetting. In leach field soils, probe 1 (0.2 m depth) CO₂ concentrations increased 3 h post rain compared to before rain; however, leach field probe 3 (0.2 m depth) in the leach field soils decreased 3 h post rain.

Observed increases in belowground concentrations of CO₂ at the 0.2 m depth may be due to a combination of increased microbial activity creating higher soil respiration *in situ* and/or increases in water filled pore space that consequently slows CO₂ diffusion through the soil matrix (Liu et al., 2017; Smart and Peñuelas, 2005). Smart and Peñuelas (2005) suggested observed delays in CO₂ diffusion in their wetted soil microcosms were caused by increased water filled pore space, leading to a build-up of subsurface CO₂ after a wetting event. However, it is also well known that increases in soil VWC can directly impact soil microbial respiration increasing microbial activity, particularly in characteristically dry soils (Kim et al., 2012; Liu et al., 2017). Thus, we suggest the increases in subsurface CO₂ observed in this study may be due to diffusion limitations caused by increases in soil VWC, an increase in near-surface respiration, or a combination of the two.

4.4.2.4 Presence and activity of greenhouse gas cycling organisms

Biomarker gene abundances for CH₄ and N₂O cycling organisms did not change over the course of the simulated rain event. Gene abundances of *mcrA* and

pmoA, biomarkers for CH₄ production and consumption, respectively, and *nosZ* and *cnorB*, production and consumption biomarkers for N₂O, were not significantly different between the two treatments or between sampling time points. Gene abundances of *mcrA* (mean, $1.68 \times 10^6 \pm 9.77 \times 10^5$ copies gdw⁻¹ for leach field and $2.71 \times 10^6 \pm 1.49 \times 10^6$ copies gdw⁻¹ for control) and *pmoA* (mean, $7.06 \times 10^6 \pm 3.47 \times 10^6$ copies gdw⁻¹ for leach field and $5.96 \times 10^6 \pm 2.42 \times 10^6$ copies gdw⁻¹ for control) were similar to those observed at this site in Fernández-Baca et al. (2018b) in surface soils (0 to 10 cm) with means of 3.55×10^6 and 5.94×10^5 *mcrA* copies g⁻¹ soil for control and leach field soils and 5.18×10^6 and 2.85×10^6 *pmoA* copies g⁻¹ soil for control and leach field soils, respectively. In both studies, *pmoA* gene abundances were always higher than *mcrA* gene abundances within every sample. In general, *cnorB* gene abundances were higher than the other GHG cycling biomarker genes (*mcrA*, *pmoA*, and *nosZ*) quantified in this study and were similar to previously reported *cnorB* abundances in leach field soils (Fernández-Baca et al., 2018b). *nosZ* gene abundances were the lowest with means of $1.31 \times 10^6 \pm 2.03 \times 10^5$ copies gdw⁻¹ in leach field soils and $9.39 \times 10^5 \pm 1.21 \times 10^5$ copies gdw⁻¹ in control soils. The presence of these biomarker genes in the 0 to 10 cm depth of soils indicates that considerable GHG cycling can occur at shallow depths in lawn soils, whether or not they are associated with a leach field system.

Transcript ratios of production to consumption biomarker genes for CH₄ (*mcrA:pmoA*) and N₂O (*cnorB:nosZ*) were examined under the hypothesis that after a wetting event, increased soil VWC would lead to anaerobic conditions in soil ultimately resulting in elevated transcript levels for CH₄ and N₂O production genes.

Prior to the precipitation event, the transcript ratios of *mcrA:pmoA* were below 2 for both control and leach field soils. Post rain event, this ratio increased to greater than 9 for both treatments. This increase was significant for control soils ($p = 0.025$) and marginally significant for leach field soils ($p = 0.055$) at the 1.5 h mark, however the *mcrA* to *pmoA* transcript ratio dropped below 2 again at the 3 h mark. Because soils were not sampled at the 0.5 h mark when a significant pulse of CH₄ occurred in the leach field, an even greater increase in the transcript ratios of *mcrA* to *pmoA* may have been missed. Future studies attempting to capture the dynamic relationship between soil VWC, GHG emissions, and transcript abundances of key functional genes, will require more immediate and frequent sampling post wetting event.

Transcript ratios for *cnorB:nosZ* were greater than 1 prior to the rain event and decreased to 0.77 and 0.63 for control and leach field soils, respectively. The ratio remained below 1 even 3 h post rain. Significant differences were not found for the N₂O cycling genes ($p > 0.05$) for the different sampling times. In contrast to the methane cycling biomarkers (*mcrA* and *pmoA*), the complexity of the N₂O cycle makes it difficult to capture all of the denitrification genes that are involved in N₂O production and consumption. There are many atypical versions of the *nosZ* gene which are not captured by the primers used in this study (Sanford et al., 2012). Additionally, cNor (which uses cytochrome c as the electron donor) and qNor (quinol electron donor) are two different forms of the Nor enzyme that could both contribute to N₂O production (Braker and Tiedje, 2003). In this study we chose to quantify *cnorB* as our biomarker for N₂O production because it is specific to denitrifying strains while *qnorB* has been found in non-denitrifying bacteria. However, excluding *qnorB* may have led

to an underestimation of the denitrifying population capable of producing N₂O and thus an incomplete picture of the denitrifying community in leach field soils. Further studies attempting to elucidate the activity of key microbial populations involved in N₂O cycling would benefit from targeting a more diverse set of functional genes for the N₂O cycle.

The heterogeneity of soils adds another complication in capturing the response of soil microorganisms to a rain event. In this study, one core was taken per treatment and time point to avoid substantially disturbing the soil system. The infiltration area was relatively small (less than 1 m²) and was mostly covered by the gas flux chambers, thus leaving a small area from which to take soil cores. Additionally, although core holes were replaced with soil from adjacent lawn, the sampling likely introduced air into the soil environment and allowed for some gas exchange between the subsurface soils and the atmosphere. Future studies would benefit from sampling multiple cores over a larger infiltration area to get a more representative soil sample as well as to avoid disturbing the activity of soil microbes by introducing air to the subsurface environment.

4.5 Conclusions

This study provides the first surface fluxes and coupled subsurface measurements of methane, carbon dioxide, and nitrous oxide from leach field soils after a significant simulated rain event. We found that both leach field and control lawns were either weak sinks or weak sources of CH₄ during baseline measurements, but became net sources by the first time point (30 min) post rain event. Likewise, leach field lawns were weak net emitters of N₂O but became strong net producers immediately after a

rain event, whereas the control soil N₂O pulse was not seen until 3 hours post rain event. All lawns were net emitters of CO₂, which increased in both treatments after wetting. Subsurface GHG trends for leach field and control soils were similar during baseline measurements. Thirty minutes after the wetting event, an increase in subsurface CH₄ production at both depths was observed which decreased over time. In contrast, N₂O subsurface concentrations decreased after wetting and returned to pre-rain concentrations by the 3 h post rain time point. Subsurface CO₂ concentrations were likewise similar before rain and 3 h post rain. Biomarker abundances for CH₄ and N₂O cycling genes were consistent over the course of the precipitation experiment. Transcript abundance ratios of production to consumption genes were higher in the wetted soils 1.5 h post rain as compared to dry soils ($p < 0.05$) for CH₄, however the opposite trend was observed for N₂O cycling genes. Three hours after the rain event, both *mcrA:pmoA* and *cnorB:nosZ* transcript ratios were below 2 in leach field and control soils. Our results suggest further studies on the link between instantaneous increases in soil VWC, atmospheric GHG fluxes, subsurface production of GHG, and activation of GHG cycling microbial communities are needed to understand the dynamic response of soil systems to precipitation events. These results suggest that under typical ‘dry’ conditions, microbial communities are capable of mitigating GHGs entering through, or produced near, subsurface leach field laterals. In contrast, during rain events leach field soils, and control lawn soils alike, become net greenhouse gas producers; however timing and subsurface trends of produced greenhouse gases differ by the compound.

References

- Bourne, D.G., McDonald, I.R., Murrell, J.C., 2001. Comparison of pmoA PCR primer sets as tools for investigating methanotroph diversity in three Danish soils. *Appl. Environ. Microbiol.* 67, 3802–9.
- Braker, G., Tiedje, J.M., 2003. Nitric oxide reductase (norB) genes from pure cultures and environmental samples. *Appl. Environ. Microbiol.* 69, 3476–83.
- Chamberlain, S.D., Gomez-Casanovas, N., Walter, M.T., Boughton, E.H., Bernacchi, C.J., DeLucia, E.H., Groffman, P.M., Keel, E.W., Sparks, J.P., 2016. Influence of transient flooding on methane fluxes from subtropical pastures. *J. Geophys. Res. Biogeosciences* 121, 965–977. <https://doi.org/10.1002/2015JG003283>
- Christiansen, J.R., Levy-Booth, D., Prescott, C.E., Grayston, S.J., 2016. Microbial and Environmental Controls of Methane Fluxes Along a Soil Moisture Gradient in a Pacific Coastal Temperate Rainforest. *Ecosystems* 19, 1255–1270. <https://doi.org/10.1007/s10021-016-0003-1>
- Colin Murrell, J., Radajewski, S., 2000. Cultivation-independent techniques for studying methanotroph ecology. *Res. Microbiol.* 151, 807–814. [https://doi.org/10.1016/S0923-2508\(00\)01146-3](https://doi.org/10.1016/S0923-2508(00)01146-3)
- Cooper, J.A., Loomis, G.W., Kalen, D. V., Amador, J.A., 2015. Evaluation of Water Quality Functions of Conventional and Advanced Soil-Based Onsite Wastewater Treatment Systems. *J. Environ. Qual.* 44, 953. <https://doi.org/10.2134/jeq2014.06.0277>
- Dandie, C.E., Burton, D.L., Zebarth, B.J., Henderson, S.L., Trevors, J.T., Goyer, C.,

2008. Changes in bacterial denitrifier community abundance over time in an agricultural field and their relationship with denitrification activity. *Appl. Environ. Microbiol.* 74, 5997–6005. <https://doi.org/10.1128/AEM.00441-08>
- Davidson, E.A., 1992. Sources of Nitric Oxide and Nitrous Oxide following Wetting of Dry Soil. *Soil Sci. Soc. Am. J.* 56, 95.
<https://doi.org/10.2136/sssaj1992.03615995005600010015x>
- Decina, S.M., Hutyra, L.R., Gately, C.K., Getson, J.M., Reinmann, A.B., Short Gianotti, A.G., Templer, P.H., 2016. Soil respiration contributes substantially to urban carbon fluxes in the greater Boston area. *Environ. Pollut.* 212, 433–439.
<https://doi.org/10.1016/J.ENVPOL.2016.01.012>
- Diaz-Valbuena, L.R., Leverenz, H.L., Cappa, C.D., Tchobanoglous, G., Horwath, W.R., Darby, J.L., 2011. Methane, carbon dioxide, and nitrous oxide emissions from septic tank systems. *Environ. Sci. Technol.* 45, 2741–7.
<https://doi.org/10.1021/es1036095>
- Ettwig, K.F., Butler, M.K., Le Paslier, D., Pelletier, E., Mangenot, S., Kuypers, M.M.M., Schreiber, F., Dutilh, B.E., Zedelius, J., de Beer, D., Gloerich, J., Wessels, H.J.C.T., van Alen, T., Luesken, F., Wu, M.L., van de Pas-Schoonen, K.T., Op den Camp, H.J.M., Janssen-Megens, E.M., Francoijs, K.-J., Stunnenberg, H., Weissenbach, J., Jetten, M.S.M., Strous, M., 2010. Nitrite-driven anaerobic methane oxidation by oxygenic bacteria. *Nature* 464, 543–8.
<https://doi.org/10.1038/nature08883>
- Fernández-Baca, C.P., Omar, A.-E.H., Pollard, J.T., Richardson, R.E., 2018a. Microbial communities controlling methane and nutrient cycling in leach field

soils. Manusc. Submitt. Publ.

- Fernández-Baca, C.P., Truhlar, A.M., Omar, A.-E.H., Rahm, B.G., Walter, M.T., Richardson, R.E., 2018b. Methane and nitrous oxide cycling microbial communities in soils above septic leach fields: Abundances with depth and correlations with net surface emissions. *Sci. Total Environ.* 640–641, 429–441. <https://doi.org/10.1016/J.SCITOTENV.2018.05.303>
- Ferris, M.J., Muyzer, G., Ward, D.M., 1996. Denaturing gradient gel electrophoresis profiles of 16S rRNA-defined populations inhabiting a hot spring microbial mat community. *Appl. Environ. Microbiol.* 62, 340–6.
- Haroon, M.F., Hu, S., Shi, Y., Imelfort, M., Keller, J., Hugenholtz, P., Yuan, Z., Tyson, G.W., 2013. Anaerobic oxidation of methane coupled to nitrate reduction in a novel archaeal lineage. *Nature* 500, 567–70. <https://doi.org/10.1038/nature12375>
- Henry, S., Bru, D., Stres, B., Hallet, S., Philippot, L., 2006. Quantitative detection of the *nosZ* gene, encoding nitrous oxide reductase, and comparison of the abundances of 16S rRNA, *narG*, *nirK*, and *nosZ* genes in soils. *Appl. Environ. Microbiol.* 72, 5181–9. <https://doi.org/10.1128/AEM.00231-06>
- Kim, D.-G., Vargas, R., Bond-Lamberty, B., Turetsky, M.R., 2012. Effects of soil rewetting and thawing on soil gas fluxes: a review of current literature and suggestions for future research. *Biogeosciences* 9, 2459–2483. <https://doi.org/10.5194/bg-9-2459-2012>
- Kotiaho, M., Fritze, H., Merilä, P., Juottonen, H., Leppälä, M., Laine, J., Laiho, R., Yrjälä, K., Tuittila, E.-S., 2010. Methanogen activity in relation to water table

- level in two boreal fens. *Biol. Fertil. Soils* 46, 567–575.
<https://doi.org/10.1007/s00374-010-0461-0>
- Lee, H.J., Kim, S.Y., Kim, P.J., Madsen, E.L., Jeon, C.O., 2014. Methane emission and dynamics of methanotrophic and methanogenic communities in a flooded rice field ecosystem. *FEMS Microbiol. Ecol.* 88, 195–212.
<https://doi.org/10.1111/1574-6941.12282>
- Liu, Z., Zhang, Y., Fa, K., Qin, S., She, W., 2017. Rainfall pulses modify soil carbon emission in a semiarid desert. *CATENA* 155, 147–155.
<https://doi.org/10.1016/J.CATENA.2017.03.011>
- Livesley, S.J., Dougherty, B.J., Smith, A.J., Navaud, D., Wylie, L.J., Arndt, S.K., 2010. Soil-atmosphere exchange of carbon dioxide, methane and nitrous oxide in urban garden systems: impact of irrigation, fertiliser and mulch. *Urban Ecosyst.* 13, 273–293. <https://doi.org/10.1007/s11252-009-0119-6>
- McPhillips, L.E., Groffman, P.M., Schneider, R.L., Walter, M.T., 2016. Nutrient Cycling in Grassed Roadside Ditches and Lawns in a Suburban Watershed. *J. Environ. Qual.* 45, 1901. <https://doi.org/10.2134/jeq2016.05.0178>
- Molodovskaya, M., Warland, J., Richards, B.K., Öberg, G., Steenhuis, T.S., 2011. Nitrous Oxide from Heterogeneous Agricultural Landscapes: Source Contribution Analysis by Eddy Covariance and Chambers. *Soil Sci. Soc. Am. J.* 75, 1829. <https://doi.org/10.2136/sssaj2010.0415>
- S. C. Whalen, W.S.R., 2010. Methane Oxidation, Production, and Emission at Contrasting Sites in a Boreal Bog. *Geomicrobiol. J.* 17, 237–251.
<https://doi.org/10.1080/01490450050121198>

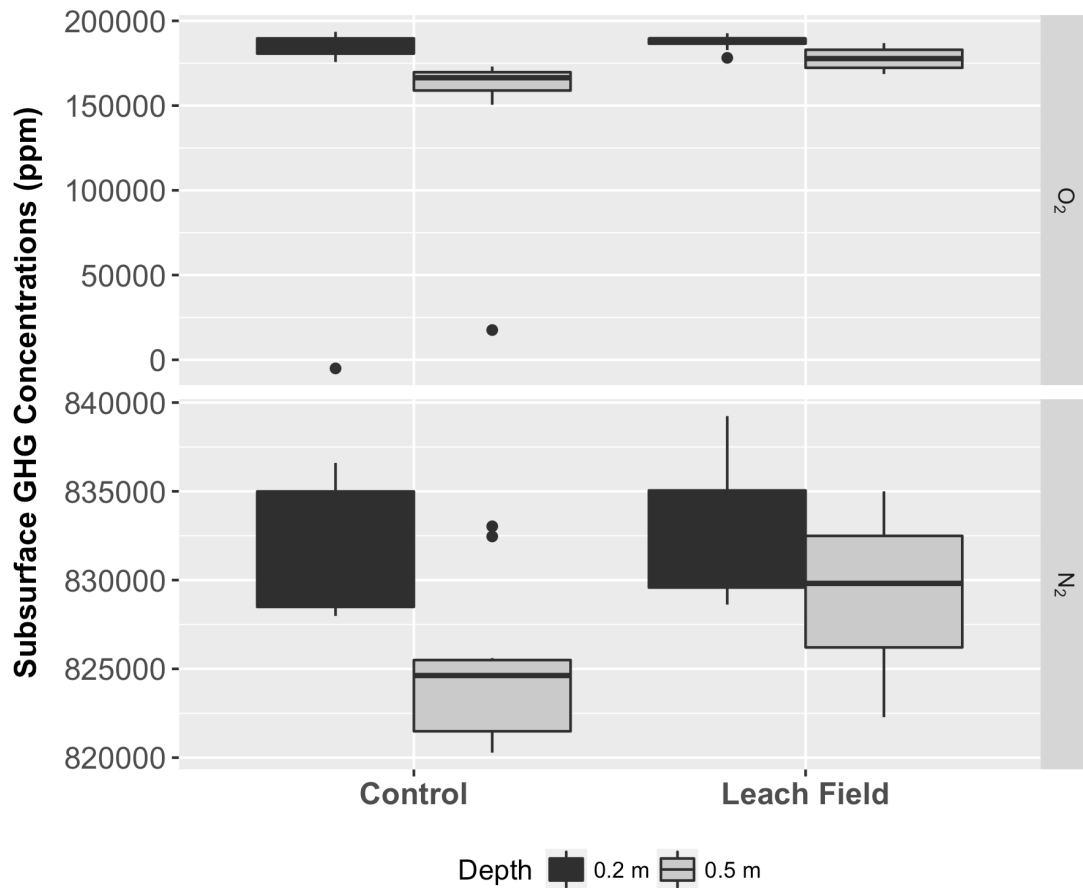
- Sanford, R.A., Wagner, D.D., Wu, Q., Chee-Sanford, J.C., Thomas, S.H., Cruz-García, C., Rodríguez, G., Massol-Deyá, A., Krishnani, K.K., Ritalahti, K.M., Nissen, S., Konstantinidis, K.T., Löffler, F.E., 2012. Unexpected nondenitrifier nitrous oxide reductase gene diversity and abundance in soils. *Proc. Natl. Acad. Sci. U. S. A.* 109, 19709–14. <https://doi.org/10.1073/pnas.1211238109>
- Smart, D.R., Peñuelas, J., 2005. Short-term CO₂ emissions from planted soil subject to elevated CO₂ and simulated precipitation. *Appl. Soil Ecol.* 28, 247–257. <https://doi.org/10.1016/J.APSOIL.2004.07.011>
- Smith, K.A., Ball, T., Conen, F., Dobbie, K.E., Massheder, J., Rey, A., 2003. Exchange of greenhouse gases between soil and atmosphere: interactions of soil physical factors and biological processes. *Eur. J. Soil Sci.* 54, 779–791. <https://doi.org/10.1046/j.1351-0754.2003.0567.x>
- Steinberg, L.M., Regan, J.M., 2009. mcrA-targeted real-time quantitative PCR method to examine methanogen communities. *Appl. Environ. Microbiol.* 75, 4435–42. <https://doi.org/10.1128/AEM.02858-08>
- Steinberg, L.M., Regan, J.M., 2008. Phylogenetic comparison of the methanogenic communities from an acidic, oligotrophic fen and an anaerobic digester treating municipal wastewater sludge. *Appl. Environ. Microbiol.* 74, 6663–71. <https://doi.org/10.1128/AEM.00553-08>
- Thauer, R.K., 1998. Biochemistry of methanogenesis: a tribute to Marjory Stephenson. 1998 Marjory Stephenson Prize Lecture. *Microbiology* 144 (Pt 9, 2377–406.
- Truhlar, A.M., Rahm, B.G., Brooks, R.A., Nadeau, S.A., Makarsky, E.T., Walter,

M.T., 2016. Greenhouse Gas Emissions from Septic Systems in New York State. *J. Environ. Qual.* 45, 1153. <https://doi.org/10.2134/jeq2015.09.0478>

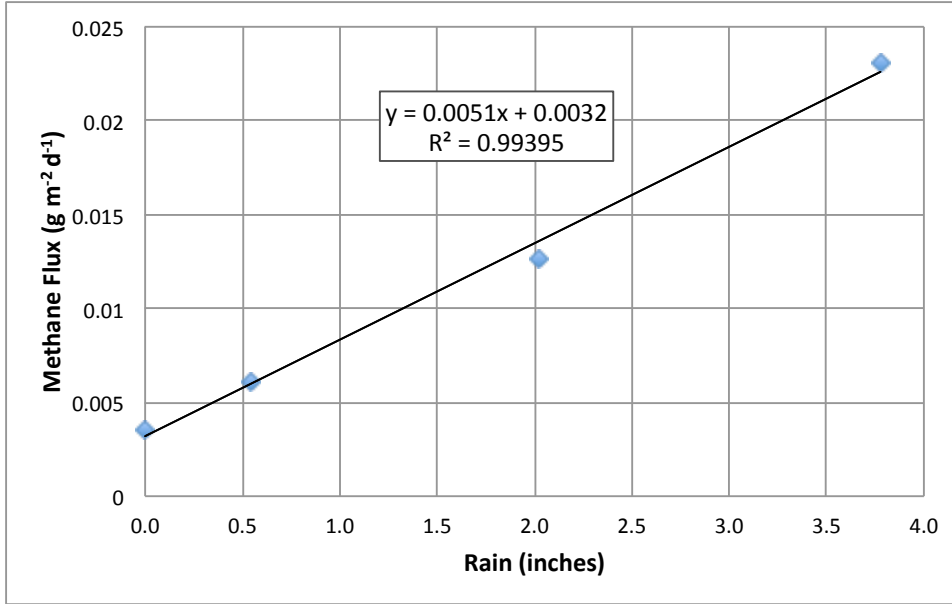
US EPA, 2012. Global Anthropogenic Non-CO2 Greenhouse Gas Emissions: 1990-2030 [WWW Document]. URL http://www.epa.gov/climatechange/Downloads/EPAactivities/EPA_Global_Non_CO2_Projections_Dec2012.pdf (accessed 4.13.15).

Wilson, D., Blain, D., Couwenberg, J., Evans, C.D., Murdiyarso, D., Page, S.E., Renou-Wilson, F., Rieley, J.O., Sirin, A., Strack, M., Tuittila, E.-S., 2016. Greenhouse gas emission factors associated with rewetting of organic soils. *Mires Peat* 17. <https://doi.org/10.19189/map.2016.omb.222>

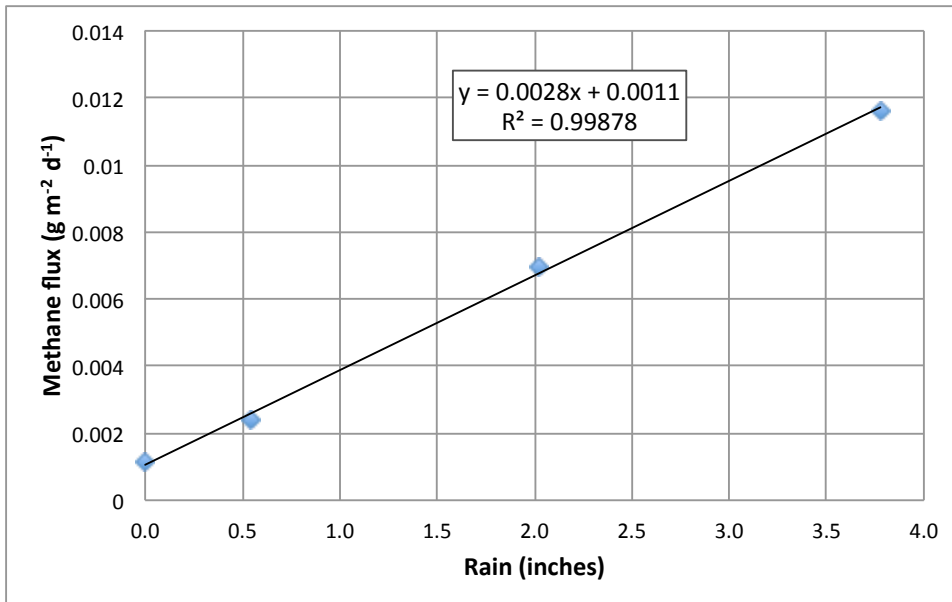
Chapter 4: Supplemental Information



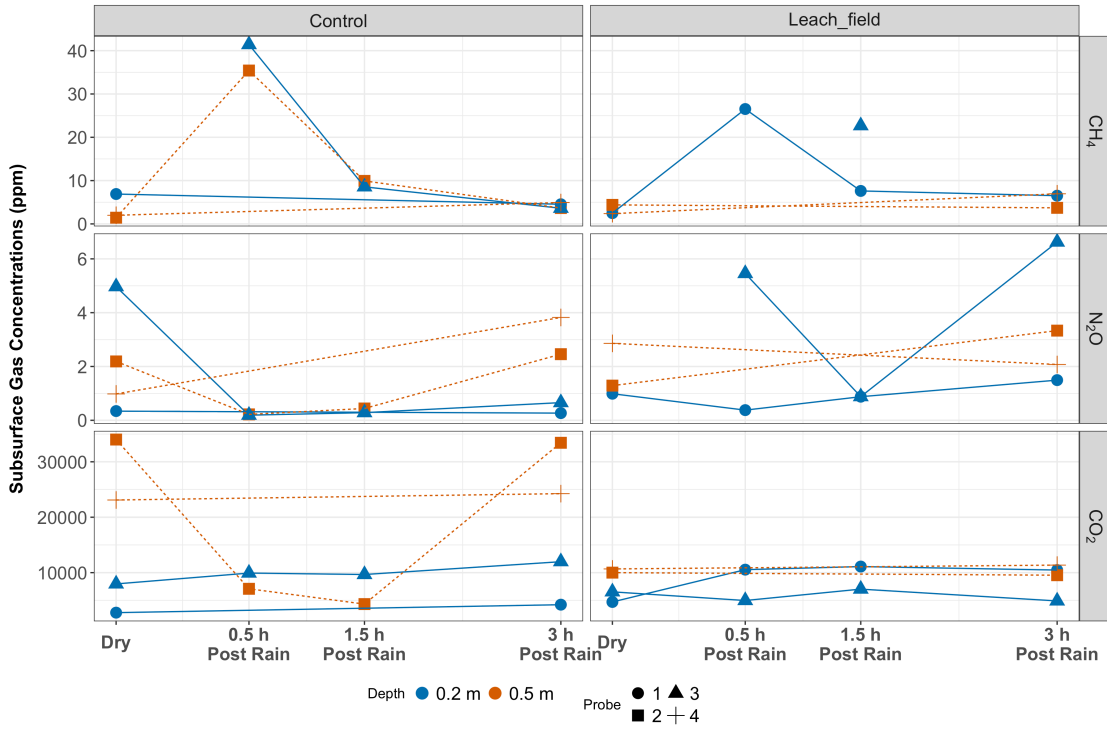
SI Figure 4.6. Baseline (4-week) O₂ (top) and N₂ (bottom) subsurface measurements at 0.2 m and 0.5 m below surface for control and leach field soils ($n = 2$ per treatment and depth per week). Boxplots show the inter-quartile range (IQR) from quartile 1 at 25% to quartile 3 at 75%. The horizontal black line within the box indicates the median. Upper and lower whiskers indicate the highest and lowest data point within 1.5 times the IQR.



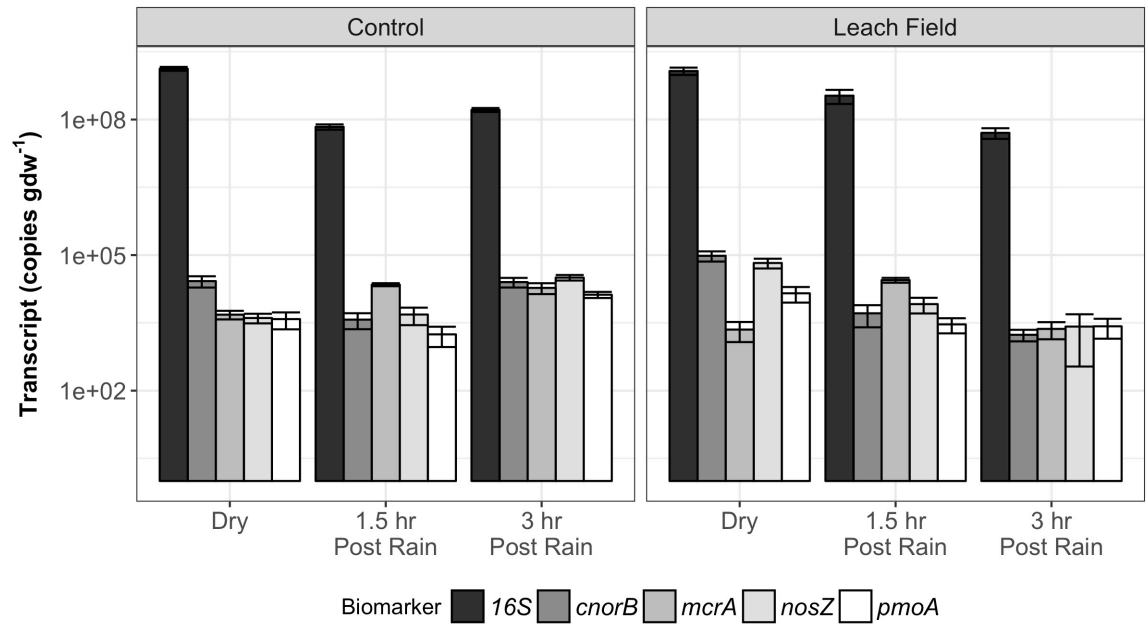
SI Figure 4.2. Preliminary study of CH_4 flux measure 40 minutes after rain event versus inches of rain.



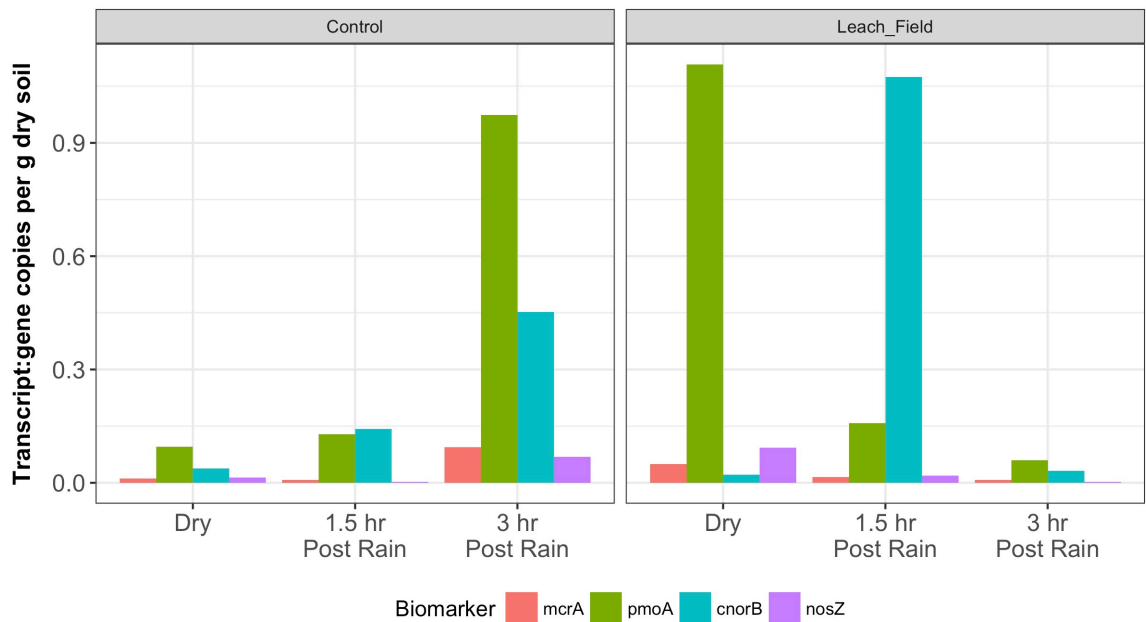
SI Figure 4.3. Preliminary study of CH_4 flux measure 1.5 hours after rain event versus inches of rain.



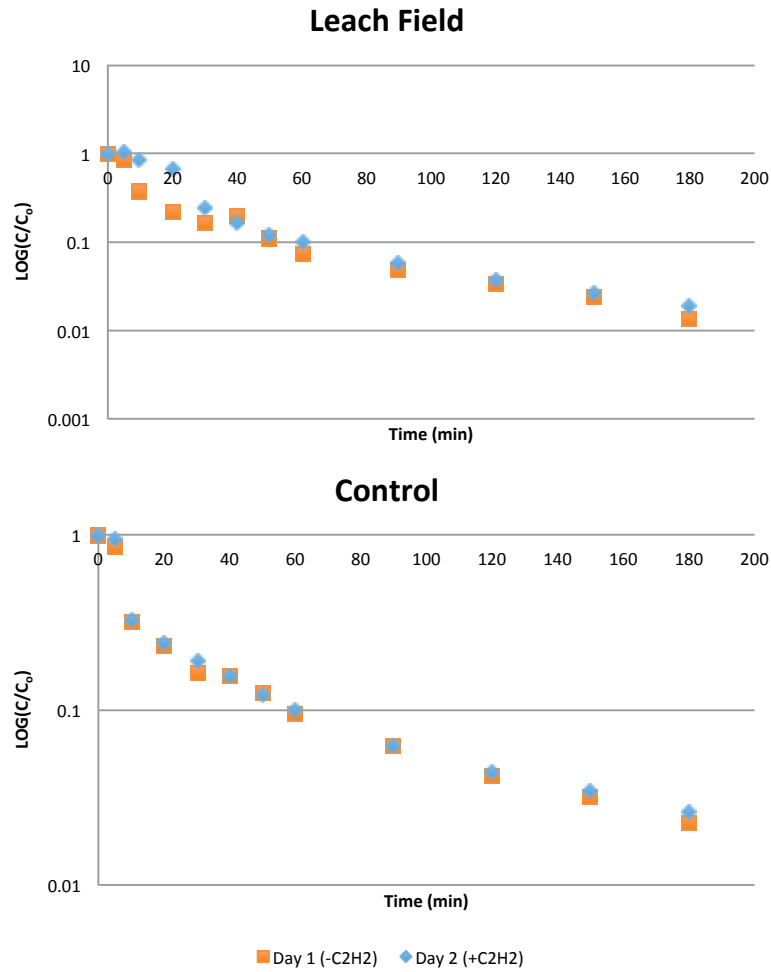
SI Figure 4.4. Subsurface greenhouse gas measurements in leach field and control soils at 0.2 m and 0.5 m below ground, removing ‘hot moment’ samples of methane and nitrous oxide for probe 3 in both leach field and control soils.



SI Figure 4.5. Transcript abundances of key functional genes involved in CH_4 and N_2O cycling recovered from control and leach field soils before and after a rain event.



SI Figure 4.6. Transcript to gene abundance ratios for biomarker genes involved in CH_4 (*mcrA* and *pmoA*) and N_2O (*cnorB* and *nosZ*) cycling.



SI Figure 4.7. Gas push-pull test (GPPT) results from leach field (top) and control (bottom) soils for 0.5 m depth showing \log_{10} concentrations of “pulled” CH₄ concentrations (C) over injected CH₄ concentration (C₀) over time. Day 1 gas mix included CH₄ and Day 2 gas mix included CH₄ and methane oxidation inhibitor acetylene (C₂H₂). No difference was observed in CH₄ oxidation between Day 1 and Day 2 in either treatment, likely due to overwhelming the system with high concentrations of CH₄.

CHAPTER 5

CONCLUSIONS

This dissertation examined the relationship between greenhouse gas (GHG) emissions and the soil microbial communities controlling their cycling in grass-covered leach field soils and corresponding control soils. This work expands on the growing literature studying controls on greenhouse gas cycling and associated microbial communities in soil systems. The results found herein have implications for furthering our knowledge of not just septic leach field soil microbial communities and greenhouse gas dynamics but for lawn and urban soils in general, which are understudied systems.

5.1 Quantifying greenhouse gas emissions from lawn and leach field soils

This work includes some of the first measurements of greenhouse gas emissions from leach field and lawn soils. Specifically, measurements of greenhouse gas fluxes from leach field and control lawns *in situ* over a summer (Chapter 2) and before and after a rain event (Chapter 4), as well as lab studies of methane emissions from leach field soil columns, operated in the lab under different volumetric water content regimes (Chapter 3). The goal of these studies was to understand the production and consumption of greenhouse gas emissions, namely CH₄, N₂O, and CO₂, from leach field soils impacted by subsurface septic effluent inputs, and the dynamics of abundance and activity of CH₄ and N₂O cycling organisms.

The field measurements presented here suggest leach field soils do not differ from control soils in terms of greenhouse gas emissions under normal operating conditions, with the exception of N₂O, which had higher emissions from leach field

soils as compared to control lawns. Under high soil VWC conditions, elevated GHG emissions were observed regardless of whether the VWC increase was due to sustained flooding or a rain event. Chapter 2 results indicated that sustained flooding in one site (Site 9) strongly drove higher CH₄ emissions in that system. In contrast, the other 8 sites, which were not flooded, were either low rate net emitters or net consumers of CH₄. Accounting for VWC differences, no difference in CH₄ emissions was observed between treatments. The results from this first chapter led us to explore the relationship between sustained failure by flooding in leach field systems and their potential net GHG impacts, which may be higher than previously quantified in well-maintained systems.

In Chapter 3 we studied the relationship between soil VWC and CH₄ subsurface production and surface emissions using lab-scale leach field soil columns. Two leach field soil column systems were operated in either a failing-by-flooding mode or a well-maintained mode (i.e. not flooded, where the water table was maintained well below the leach field lateral). As hypothesized, the leach field soil column operated under continuously flooded conditions had higher CH₄ surface emissions as compared to the column under proper operating conditions. Subsurface production of CH₄ was likewise higher in the flooded systems. Peak subsurface CH₄ concentrations, under both flooded and non-flooded conditions, occurred near the wastewater inlet and decreased above and below the inlet. Surprisingly, both well-maintained and flooded leach field soil conditions resulted in high removals of nutrients (e.g. nitrogen and phosphorus). In contrast, COD removal was variable and was negatively impacted by flooding. Thus, the impact of flooded leach field systems may be greater for air quality than water quality. Nevertheless, flooding is likely negatively impacting ground water due to low COD removals.

In the final chapter, we further explored the dynamic relationship between an

increase in soil VWC and both surface and subsurface GHG production in leach field soils *in situ* by simulating a heavy rain event to rapidly increase soil VWC. The study consisted of two parts: first, baseline GHG surface flux and subsurface measurements during a one-month period and second, a simulated 2-in precipitation event with subsequent monitoring of surface and subsurface GHG production coupled to quantification of GHG cycling microbial populations' presence and activity. In the first part, careful monitoring of leach field and control lawn soils for both subsurface and surface GHG production was done to understand conditions prior to a precipitation event. Baseline monitoring of both surface and subsurface GHG profiles confirmed there was no significant difference between leach field and control soils. After the simulated rain event, differences were observed in GHG flux patterns with emissions of CH₄ and CO₂ increasing immediately in both control and leach field soils while N₂O pulsed immediately in leach field soils but was delayed in control soils. Subsurface concentrations between leach field and control soils were similar before and after the precipitation event. Before wetting, subsurface trends were similar to baseline measurements, with higher concentrations of CH₄ measured in near-surface soils (0.2 m) as compared to deeper soils (0.5 m), and CO₂ and N₂O having opposite trends. Thirty minutes after rain, CH₄ subsurface concentrations appeared to increase, before dropping down to pre-rain concentrations 3 hours post rain. In contrast, subsurface N₂O concentrations appeared to decrease immediately after rain. CO₂ trends post rain showed the deeper samples decrease in concentration while shallow (0.2 m) concentrations increase.

Together these three studies indicate that sustained flooding (i.e. continuous high soil VWC) is different from instantaneous 'flooding' from a rain event, in terms of GHG emissions to the atmosphere. The CH₄, CO₂, and N₂O flux measurements herein reveal that the three greenhouse gases studied have differential temporal

responses to changes in soil VWC. Sustained flooding resulted in elevated CH₄ emissions, but did not necessarily result in elevated N₂O or CO₂ emissions. In contrast, an instantaneous increase in soil VWC, due to a rain event, resulted in elevated emissions of all greenhouse gases measured, albeit with different temporal trends post-precipitation. The findings from these studies suggest previous measurements of GHG emissions from leach field and control lawn systems may underestimate the net GHG production from these soils, particularly if systems have high soil VWC due to flooding or experiencing heavy rain events.

5.3 Advancing the understanding of soil microbial communities controlling CH₄ and N₂O cycling in soils

Microbial communities are complex and heterogeneous in soils. They encompass a large number of genera that carry out diverse processes including cycling of greenhouse gases and nutrients. Notwithstanding their importance in GHG cycling, soil microbial communities have not previously been examined in leach field soil systems. This dissertation aimed to increase knowledge of GHG cycling microbial populations in soils with a particular focus on those soils above leach field systems. In Chapters 2 and 4, we provide the first measurements of biomarker gene abundances for microbial populations involved in GHG cycling in leach field soils. Chapters 2 and 3, explored depth distributions of key GHG cycling microbial populations, and employed high-throughput sequencing techniques to analyze microbial community structure in leach field and lawn soils. Transcript abundances of key populations involved in GHG cycling were quantified in Chapters 3 and 4 in an effort to develop a correlation between activity of these key populations and measured GHG emissions and/or subsurface concentrations. The objective of these three chapters was to expand our current knowledge of soil microbial communities involved in GHG cycling with a

particular focus on how these communities respond to changes in soil volumetric water content.

Although previous literature has shown that soil VWC can be a major driver of CH₄ emissions and activity of methanogens and methanotrophs in peat bogs and rice paddy systems, the impact of flooding on microbial communities in leach field soils had not previously been studied (Freitag et al., 2010; Ma et al., 2013, 2012). Chapter 2 aimed to address this using Illumina sequencing of 16S rRNA and functional gene amplicon libraries of *mcrA* and *pmoA*. High-throughput sequencing allowed us to explore microbial community diversity in soils under different treatments (i.e. leach field, control, and sand filter soils). 16S rRNA amplicon libraries revealed that soil VWC was a strong driver of microbial community diversity in leach field soils. Soil microbial community composition was also driven by CH₄ emissions and N₂O emissions to a lesser extent. qPCR quantification of microbial populations using functional genes involved in CH₄ cycling (*mcrA* and *pmoA*, respectively) and N₂O cycling (*cnorB* and *nosZ*, respectively) revealed that abundances of all GHG cycling genes were higher *in situ* in near-surface soils. Additionally, soil VWC was strongly correlated with higher gene abundances of both methane cycle biomarkers (*mcrA* and *pmoA*) but not the N₂O cycling genes (*cnorB* or *nosZ*). This result suggests much of the GHG cycling, and therefore measured GHG emissions from soils, is a result of activation of microbial populations residing in near-surface soils. Furthermore, sustained high soil VWC was found to be a driver of CH₄ emissions and CH₄ cycling gene abundances but not of N₂O emissions or N₂O cycling genes.

In Chapter 3, we explored GHG cycling microbial communities in-depth using leach field soil columns constructed in the lab. Quantification of CH₄ cycling populations with depth revealed that methanogens and methanotrophs reside throughout the profile but have maximum populations in distinct niches within the soil

profile. Methanogens were found in greater abundance near the wastewater inlet where septic effluent enters the soil column subsurface. In contrast, methanotrophs were found in greater abundance near the soil surface. Transcript abundances for *mcrA* and *pmoA* did not reveal a strong association with measured CH₄ concentrations in the soil profile, but did follow a similar pattern to gene abundances with depth. High-throughput sequencing of 16S rRNA, *mcrA*, and *pmoA* libraries indicated that significant shifts in microbial community diversity occurred due to prolonged increases in soil VWC. Additionally, long term flooding significantly reduced microbial community diversity in the failing leach field soil column in contrast to the well-maintained column. Sequencing of cDNA samples revealed that active soil microbial populations were distinct from those at the DNA level. These results expand our limited knowledge of soil microbial communities in leach field soils and the distinct depth profiles of different microbial populations involved in CH₄ cycling.

In the third chapter, we again quantified abundances of key functional genes involved in CH₄ and N₂O cycling from leach field soils. In addition to gene quantification, we also measured transcript abundances of these biomarker genes to capture the relationship between a precipitation event, measured GHG emissions, and activity of populations controlling GHG cycling. As in Chapter 2, gene abundances of biomarkers for GHG cycling microorganisms did not vary between leach field and control lawns. Moreover, abundances did not change before and after a simulated rain event. However, we did see changes in transcript abundance ratios for production to consumption genes of CH₄ (*mcrA:pmoA*) and N₂O (*cnorB:nosZ*) cycling before and after rain. While the production-to-consumption gene transcript abundance ratio for CH₄ increased after rain, the ratio decreased for N₂O. These seemingly contradictory results for N₂O may be due to primer selection. We quantified *cnorB* as opposed to, and excluding, *qnorB*, thus the findings reported here may underestimate the

denitrifier population capable of N₂O production. To clarify results, either more primer sets could be used for qPCR to capture the diversity found in N₂O cycling genes, or metatranscriptomes could be used to reduce bias from functional gene specific primer sets.

This dissertation as a whole aimed to understand the relationship between microbial communities responsible for GHG cycling of CH₄ and N₂O and measured GHG emissions in response to different soil VWC conditions. Ultimately, we found the soil microbial community structure and diversity was driven by soil VWC particularly under prolonged saturated conditions. In addition, we found that gene abundances of microbial populations involved in greenhouse gas cycling were higher in surface soils, but were found throughout the soil depth in column studies. Furthermore, this work revealed that microbial activity, as measured via gene transcript abundance, although ultimately not predictive of GHG production or consumption, was impacted by instantaneous changes in soil VWC.

5.3 Limitations

Key findings in the presented studies are not without their limitations, which are discussed here to describe obstacles encountered that may provide insight for future work. Limitations included primer selection biases, workflow issues for RNA extractions and amplification, and lack of adequate number of replicates for soil samples particularly for soil nucleic acid analyses.

Primer biases are inherent in any PCR based method, and our studies relied on primers for both quantification and creation of amplicon libraries. For qPCR-based quantification we chose to use degenerate primers to target functional genes involved in CH₄ and N₂O cycling. While the *mcrA* and *pmoA* primers chosen targeted the well-conserved genes of MCR in methanogens and pMMO in aerobic methanotrophs, the

primers also captured anaerobic methanotroph sequences. Thus, results of *mcrA* amplification were not necessarily limited to methanogens but may also include ANME-2D type reverse-methanogenesis organisms. Likewise for *pmoA*, non-specific amplification of the homologous *amoA* gene found in ammonia-oxidizing bacteria, and/or amplification of anaerobic nitrite-utilizing methanotrophs could lead to overestimation of the aerobic methanotroph population found in soils (Bourne et al., 2001; Luesken et al., 2011). Similarly, the chosen primers for *nosZ* and *cnorB* amplification were not all encompassing. *nosZ* in particular has many relatively recently discovered atypical forms that cannot be captured with one set of primers (Sanford et al., 2012). Indeed, almost a dozen primer sets would be needed to capture the full diversity of *nosZ* (Hegarty, 2013). For the nitric oxide reductase enzyme, the two forms, qNor and cNor, complicate the ability to quantify this step accurately. Our studies focused on measuring the latter because of its specificity to denitrifier strains, however this also could lead to underestimation of nitric oxide reducing populations (Braker and Tiedje, 2003). Lastly, the 16S rRNA sequencing primers we selected resulted in biased amplification. The chosen primers were partial to Bacterial sequences and biased against Archaeal sequences, thus microbial community analyses based on the 16S rRNA amplicon libraries were weighted heavily to Bacterial sequences (Klindworth et al., 2013). Future work focused on recovering accurate relative abundances of Bacterial and Archaeal populations would require selecting and/or designing primers that are likely to capture greater diversity in the soil microbial community.

The second major obstacle for these studies was the workflow for mRNA extraction, reverse transcription, and quantification. This challenge also relates to the third main limitation, which was the limited size and number of soil samples that could be collected and processed for nucleic acids. This finite number of samples,

combined with the inherent variability across replicate measurements, may have obscured relationships between observed GHG emissions and presence and activity of GHG cycling populations. One of the main challenges in the mRNA workflow was the amount of soil required to be able to quantify the relatively low abundance of transcripts for key functional genes of interest in our studies. In lab, we tested multiple extraction methods to recover high quality mRNA from soils while at the same time attempting to minimize the amount of soil required for duplicate extractions of DNA and RNA to avoid substantially disrupting the study system. Reverse transcription and quantification steps were also complicated by the low abundance of gene transcripts we were targeting, thus requiring larger soil samples for extraction. Moreover, there is inherent difficulty in achieving representative soil samples, even with multiple, sizeable samples, due to the heterogeneity of soils, which can lead to small niches of high activity and other areas of relatively low activity. Thus, future work would benefit from increasing the number and size of samples taken per treatment or time point to better capture a complete picture of the soil microbial community. Another potential solution to this obstacle of soil heterogeneity would be to increase the number of samples extracted and subsequently pool the extracts to achieve an overall more representative sample. Additionally, batch studies where soils can be incubated under controlled conditions in replicates would create a simpler study system in which the full soil sample could be extracted for DNA and RNA analyses, thus avoiding the issue of soil heterogeneity all-together.

Future studies should work to further resolve the vertical and temporal responses of soil microbial communities responsible for GHG cycling to changes in soil VWC. Specifically, quantifying the vertical distribution and activity of these key GHG cycling populations coupled to measurements of GHG depth profiles would lead to a more complete understanding of net GHG movement and ultimately emissions to

the atmosphere. Elucidating the differential responses of microbial populations responsible for producing and consuming greenhouse gases to changes in soil VWC is key to a better overall understanding of greenhouse gas production from soil systems.

5.4 Future Directions

These studies provide original conclusions about greenhouse gas fluxes from leach field and lawn soils as well as insights into microbial community structure and diversity in near-surface soils in general. Nevertheless, further studies in this study area can be done to add to the growing body of work on soil microbiomes, in particular those controlling greenhouse gas emissions in soil systems. Future work in this vein can take a variety of different avenues including quantification of pathogen removal efficiency in leach field systems, GHG emissions modeling in leach field and lawn soils, controlled batch incubation studies of leach field soils and metatranscriptomics of leach field and lawn soil microbial communities.

Our leach field column study did not address the question of efficiency of pathogen removal in leach field systems. Limitations due to the difficulty and safety-risk of using real domestic wastewater in the lab deterred us from exploring this area of study, however it is important to understand the ability of leach field systems to effectively treat and remove potential pathogens before effluent comes into contact with ground and/or surface water. Thus, we suggest future work to quantify leach field systems' efficacy in removing fecal indicator bacteria as well as viral, bacterial, and protozoal pathogens is a key research area that has not been well studied and should be further explored. In particular, elucidating how failing systems fair in terms of pathogen treatment as compared to well-maintained systems is essential to understanding septic systems' overall impact on public health.

Modeling GHG emissions and microbial activity in leach field and other lawn

systems could build on findings in this body of work. In these studies, we report data for presence and activity of key microbial populations involved in greenhouse gas cycling. These values, along with other measured soil properties (e.g. soil VWC), could be used to generate models for GHG emissions from lawn-covered soil systems. Additionally, batch studies aimed at exploring the relationship between soil VWC and microbial presence and activity of key populations involved in GHG cycling would be valuable for informing GHG flux models of lawn-covered soil systems. Climate models would benefit from a clearer understanding of the link between presence and abundance of GHG cycling populations and measured GHG fluxes from these soil systems. In our studies, we observed a correlation between elevated CH₄ emissions and abundance of CH₄ cycling biomarker genes, however there was no clear relationship between transcripts of the same biomarker genes and CH₄ fluxes. Therefore, exploring the presence and activity of soil microbial populations in soils and their net GHG fluxes would help to improve GHG emission estimates from soil systems. Developing these correlations between microbial presence and activity and measured GHG fluxes to the atmosphere is essential for informing future global GHG models.

Soil metatranscriptomics would be an interesting next step in these studies and would lead to a better fundamental understanding of GHG cycling microbial community dynamics. While we were able to quantify the presence and activity of a portion of the GHG cycling community, metatranscriptomes would help elucidate the activity of populations we were not able to target with our limited primer sets. Populations that we did not quantify in our studies (e.g. atypical *nosZ* and *qnorB* for N₂O or *pmoA* and *mcrA* of anaerobic methanotroph populations for CH₄) could be revealed through metatranscriptomes and indeed could help to link activity of GHG cycling microbial communities to measured GHG production in soils.

This work has set the foundation for exploring leach field and lawn-covered soil microbial community responses to changes in soil volumetric water content and how these changes are ultimately reflected in greenhouse gas production in soils. Our studies focused on increasing the body of work in leach field and lawn-covered soils, however future studies in other soil environments (e.g. landfill soils, urban landscapes, etc.) would allow for a more complete picture of soil GHG cycling. Ultimately, changes in global climate patterns may increase precipitation and flooding events, which would impact the activity of GHG and nutrient cycling microbial populations. Therefore, studying how these soil microbial communities are affected by changing environmental conditions is critical to our understanding of dynamic GHG cycling in soils.

References

- Bourne, D.G., McDonald, I.R., Murrell, J.C., 2001. Comparison of pmoA PCR primer sets as tools for investigating methanotroph diversity in three Danish soils. *Appl. Environ. Microbiol.* 67, 3802–9.
- Braker, G., Tiedje, J.M., 2003. Nitric oxide reductase (norB) genes from pure cultures and environmental samples. *Appl. Environ. Microbiol.* 69, 3476–83.
- Freitag, T.E., Toet, S., Ineson, P., Prosser, J.I., 2010. Links between methane flux and transcriptional activities of methanogens and methane oxidizers in a blanket peat bog. *FEMS Microbiol. Ecol.* 73, 157–65. <https://doi.org/10.1111/j.1574-6941.2010.00871.x>
- Hegarty, B., 2013. QUANTITATIVE DETECTION OF DENITRIFICATION GENES – WITH A PARTICULAR FOCUS ON ATYPICAL NITROUS OXIDE REDUCTASE DIVERSITY. Cornell University.
- Klindworth, A., Pruesse, E., Schweer, T., Peplies, J., Quast, C., Horn, M., Glöckner, F.O., 2013. Evaluation of general 16S ribosomal RNA gene PCR primers for classical and next-generation sequencing-based diversity studies. *Nucleic Acids Res.* 41, e1. <https://doi.org/10.1093/nar/gks808>
- Luesken, F.A., Zhu, B., van Alen, T.A., Butler, M.K., Diaz, M.R., Song, B., Op den Camp, H.J.M., Jetten, M.S.M., Ettwig, K.F., 2011. pmoA Primers for detection of anaerobic methanotrophs. *Appl. Environ. Microbiol.* 77, 3877–80. <https://doi.org/10.1128/AEM.02960-10>
- Ma, K., Conrad, R., Lu, Y., 2013. Dry/Wet cycles change the activity and population dynamics of methanotrophs in rice field soil. *Appl. Environ. Microbiol.* 79, 4932–9. <https://doi.org/10.1128/AEM.00850-13>

- Ma, K., Conrad, R., Lu, Y., 2012. Responses of methanogen *mcrA* genes and their transcripts to an alternate dry/wet cycle of paddy field soil. *Appl. Environ. Microbiol.* 78, 445–54. <https://doi.org/10.1128/AEM.06934-11>
- Sanford, R.A., Wagner, D.D., Wu, Q., Chee-Sanford, J.C., Thomas, S.H., Cruz-García, C., Rodríguez, G., Massol-Deyá, A., Krishnani, K.K., Ritalahti, K.M., Nissen, S., Konstantinidis, K.T., Löffler, F.E., 2012. Unexpected nondenitrifier nitrous oxide reductase gene diversity and abundance in soils. *Proc. Natl. Acad. Sci. U. S. A.* 109, 19709–14. <https://doi.org/10.1073/pnas.1211238109>

APPENDIX

A gas push-pull test (GPPT) was conducted in leach field and control soils to quantify microbial methane oxidation *in situ* using the soil gas vapor probes described in Chapter 4. The following is a brief description of the experiment and data not presented in Chapter 4 Supplemental Information.

Experimental set-up

The gas-push-pull tests consisted of a two-day back-to-back experiment using one soil gas vapor probe in each the leach field and control soils. On the first day, a mix of gases (including CH₄ and tracer gases SF₆ and He) was pumped subsurface into soil via the soil gas vapor probes in both leach field and control soils at a depth of 0.5 m. Immediately after the full volume of gas mixture was delivered, the pump was turned off and discrete samples were pulled and via the soil gas vapor probe stored in pre-sealed, evacuated vials for next-day GC analyses (using the same GC method as described in Chapter 4). On the second day, the same gas mixture was pumped into the soil again via the soil gas vapor probes, however the gas mixture additionally contained acetylene (C₂H₂), a methanotrophic inhibitor. Samples were again pulled and stored in vials for analysis via GC. Differences between the day 1 and day 2 CH₄ concentrations over time indicate if any changes occurred in CH₄ oxidation rates (presented in Chapter 4 Supplemental Information).